ELECTROCATALYTICALLY INDUCED LIBERATION OF MINERAL MATTER FROM COAL

by

Anton Dilojaan Paul

Dissertation submitted to the Faculty of the

Virginia Polytechnic Institute and State University

in partial fulfillment of the requirements for the degree of

Doctor of Philosophy

in

Materials Engineering Science

APPROVED:

Roe-Hoan Yoon, Committee Chairman	Gregory T. Adel
Gerald H. Luttrell	James R. Craig
John G. Dillard	Kenneth L. Reifsnider, Dept. Chairman

June 24, 1988

Blacksburg, Virginia

ELECTROCATALYTICALLY INDUCED LIBERATION OF MINERAL MATTER FROM COAL

by

Anton Dilojaan Paul

Roe-Hoan Yoon, Committee Chairman

Materials Engineering Science

(ABSTRACT)

A new method for demineralizing coal has been developed which is based on the osmotic pressures that occur when electrical double layers overlap. In this technique, coal is exposed to ferric ions in an acidic medium which causes the coal to lose electrons and become positively charged, thereby establishing ionic double layers in the vicinity of its surface. Inside the pores and crevices in which mineral matter is entrapped, the ionic double layers overlap and reduce the chemical potential of water, creating an osmotic pressure. The build-up of such pressure pushes the mineral matter out of the crevices, resulting in mineral liberation. Since the process, which is termed electrocatalytically induced liberation (EIL), relies on surface-chemical reactions, the energy consumption is substantially lower than in conventional liberation processes based on comminution.

Tests on several different seams of coal from varying geological locations have indicated that the process may be used to remove over 70% of the mineral matter present in coal. Mass balance studies conducted on a Wyodak coal indicate that approximately 90% of the ash removed is by the EIL mechanism, while the balance may be attributed to acid dissolution and the loss of material during handling. Scanning electron micrographs of the coal samples taken before and after treatment show morphological changes consistent with the proposed EIL mechanism. The technique

has been used successfully to clean bituminous coals, low-rank coals and preparation plant refuse, and to further reduce the ash content of coals pre-cleaned by other means.

A theoretical model has been developed to calculate the osmotic pressure that occurs inside a typical coal crevice during the EIL treatment. The changes in the aqueous chemical potential are calculated using semi-empirical equations derived from solution theory, while partial molar volume changes are accounted for in the final calculation of the osmotic pressure. The model indicates that pressures on the order of 4-7 atmospheres can develop inside crevices with walls 100-1000Å apart. These values are numerically consistent with those predicted by other models developed using different approaches.

Acknowledgements

The author wishes to express his appreciation to Professor Roe-Hoan Yoon for his guidance, support and useful suggestions throughout the course of this study. Special thanks are given to Professor G. H. Luttrell and to Professor J. R. Craig for their invaluable help and cooperation at all times.

Special thanks are given to all fellow graduate students in the department, particularly Courtney Young, Cesar Basilio, Mike Mankosa, Ricky Honaker, and Zhenghe Xu for their friendship, support and willing assistance at all times.

Sincere gratitude is also expressed to Beth Howell, Wayne Slusser and Jim Overfelt for their technical support and to Roy Hill for his assistance in conducting some of the X-Ray and SEM work.

The author also wishes to acknowledge the financial support from the Amvest Coal Co., VA., and the Dept. of Energy needed for funding this project.

Finally, the author is thankful to God for helping him complete this project despite several major obstacles. Deep appreciation is expressed to all non-departmental friends for their love and support and specially to his wife, Naomi, for her continuing love,

patience and support in typing and reading the manuscript and for keeping all else working smoothly during the writing of this thesis.

Table of Contents

List of Illustrations

List of Tables

1.0 INTRODUCTION

1.1 Preamble

The bright future for coal seen in the light of the 1973 oil embargo has almost faded as petroleum conservation measures led to a modest oversupply condition of gasoline and related fuels in the 1980's. The cost of highly refined coal or its derivatives as alternate fuels at present has by far exceeded the cost of imported petroleum. However, the petroleum route to energy is not only chancy in terms of the capricious nature of oil prices, but may also put the U.S. back in position of dangerous dependence on foreign oil. Furthermore, temporary easings of the petroleum supply divert attention from the reality that the world oil supply *is* limited and will be severely depleted in a few decades as compared to the hundreds of years for coal. The world has over 845 billion metric tons of recoverable coal reserves (Wilson, 1980), and the development of alternate coal fuels would provide a hedge against future uncertainties in price and availability of oil. A clean coal fuel is the first and most difficult step towards meeting this objective.

Long experience, both in research and industrial operations, has identified the mineral impurities in coal as the source of the more significant problems of coal utilization. Fortunately, coal cleaning research has been increasingly attentive to these requirements and numerous coal cleaning techniques have been developed for preparing *"superclean coals"* containing less than 2% ash.

Methods of preparing these superclean coals may be classified into two general categories, *i.e.*, Chemical Coal Cleaning (CCC) and Physical Coal Cleaning (PCC). While CCC processes can be very efficient, their high operating costs have given way to the development of advanced PCC processes which may not be as efficient, but are intrinsically cheaper. The prerequisite for any PCC technique is sufficient liberation of mineral matter from coal, usually achieved by pulverizing the coal to sizes of 5 microns or less. Unfortunately, pulverization can be a significant part of the expense in a PCC process, even with efficient grinding techniques utilizing stirred-ball milling (Herbst and Sepulveda, 1978) or ultrasonic techniques (Heinz, 1985). Furthermore, several problems are encountered when processing a micronized coal. Due to the small sizes of the particulates involved, separation of the liberated mineral matter from the coal by conventional flotation processes becomes increasingly difficult.

This dissertation presents a detailed study of a process that achieves mineral liberation from coal by utilizing surface-chemical forces induced by electrocatalysts, referred to as the ***Electrocatalytically Induced Liberation*** process or as the EIL process. This process utilizes surface forces to cause partial fracture of the coal, presumably along its grain boundaries, to liberate the mineral matter entrapped inside it. Energy consumption, therefore, is substantially lower than conventional liberation processes which are based on random size reduction. The feed coals need not undergo any significant size reduction and only the ash-forming minerals, which are usually attached to the coal, are liberated by the process. However, some of the ash may be removed

by chemical dissolution because the process employs a mild acid-treatment. Futhermore, the process is capable of removing pyritic sulfur by chemical or electrochemical dissolution and the spent catalyst can be easily regenerated for reuse.

1.2 Description of the EIL Process

1.2.1 Working Principles

Beall et al. (1983) have shown that the reaction of anhydrous ferric chloride with coal at 230°C under a stream of nitrogen gas for 45-90 minutes increases the surface area of the coal from 3.25 to 116 m^2/gm. Examination of the processed coal samples by a scanning electron microscope (SEM) revealed that cracks had developed on the coal particles; some of the cracks were perpendicular to the surface of the platelets while the others were parallel. Although Beall et al. had not speculated on the reaction mechanism, their work showed that ferric ions caused cracks in coal by the intercalation of the ferric iron in the coal. It is possible that the reaction mechanism involved a reduction of ferric to ferrous ions, coupled by a concomitant oxidation of the coal surface.

Parks (1984) showed that the adsorption of OH^- or H_3O^+ on a quartz surface reduced the surface energy of quartz by tens of mJ/m^2. These energy changes were qualitatively consistent with the observed fracture properties and crack-propagation velocities of quartz under the same conditions. This prompted him to speculate that such minerals could be cracked by means of a surface-chemical force in an aqueous medium

(Parks, 1986). He suggested that the ionic imbalance across the electrical double layer can enhance the propagation of cracks present in a quartz particle. However, his conjecture was based on theoretical speculations alone, and has not been substantiated experimentally.

It is well established that a hydrostatic repulsive pressure exists between two charged surfaces in aqueous solutions when the surfaces are close enough to cause their respective double layers to overlap. Most coals are porous with irregular surfaces and attain positive or negative charge in aqueous solutions, depending on the pH. This in turn would cause a double layer of counter-ions to build up inside the pores and crevices. If the average pore diameter is small enough to cause these double layers to overlap, the walls of the pores would experience the hydrostatic repulsive pressure. When the pressure is large enough, the pores will crack open and release any mineral matter entrapped inside them. The repulsive pressure may be increased by enhancing the charge on the coal surface and this is achieved by using ferric ions. The coal is oxidized by the ferric ion catalysts to form surface oxides (Dhooge and Park, 1983a). These surface oxides increase the positive charge on the coal by undergoing a surface charging mechanism, similar to that of mineral oxides (Parks, 1965).

1.2.2 Operating Principles

In the EIL process, a feed coal is exposed to a solution containing a small amount of ferric ions ($\simeq 10^{-3}$M/ℓ). The EIL process is different from conventional ferric-ion leaching processes in that the ferric ion is used as a catalyst and not as a reagent. Any excess iron remaining in the treated coal will help in keeping the ash-fusion temperature high. This is important in the utilization of ultraclean coal for gas turbines.

An acidic solution below approximately pH 2 or 3, is used to keep ferric ions from precipitating as ferric hydroxide. During the EIL process, ferric ions are reduced to ferrous ions on the coal surface and the ferrous ions are converted back to ferric by an electrolytic method for reuse. After the desired length of contact time, the processed coal is removed from the reactor and separated from the liberated mineral matter by one of many methods such as screening, filtration, froth flotation, etc. The clean coal may be repeatedly treated for further removal of mineral matter. Since most coals contain pyrite (FeS_2), ferric ions are self-generated in the acidic media provided that the redox potential (Eh) of the system is kept above the reversible potential for pyrite oxidation. Inorganic sulfur is removed from the coal by dissolution and/or the liberation mechanism.

1.2.3 The Mechanism

The mechanism of mineral liberation by this process may be explained as follows. Ferric ions are continuously reduced by the coal to form ferrous ions in solution and surface oxides on the coal surface (Dhooge and Park, 1983a).

$$Fe^{3+} + e \rightarrow Fe^{2+} \qquad [1.1]$$

$$\tfrac{1}{4}C + \tfrac{1}{2}H_2O \rightarrow \tfrac{1}{4}CO_2 + H^+ + e \qquad [1.2]$$

or

$$\tfrac{1}{2}C + \tfrac{1}{2}H_2O \rightarrow \tfrac{1}{2}CO + H^+ + e \qquad [1.3]$$

in which the carbon (C) is a simplistic representation of coal. This is followed by the re-oxidation of the reduced ions at the electrode.

$$Fe^{2+} \rightarrow e + Fe^{3+} \qquad [1.4]$$

The proton is reduced at the cathode to produce hydrogen, which along with reactions [1.2] and [1.3] constitute the basis of the electrochemical gasification process (Coughlin and Farooque, 1979a). It is suspected that the oxidation occurs preferentially on the sessile bonds of the coal molecules, which may help break up part of the cross-linked coal structure. Evidence for this is that a coal subjected to this mechanism shows an increased solubility in pyridine (Paul, 1984). The electrolytic coal oxidation reaction should most surely proceed by a multi-step mechanism, since it is highly unlikely for reactions involving single step, multi-electron transfer to occur.

The reaction of coal with ferric ions seems to be limited to a few reactive carbon sites, probably associated with peripheral carbon heteroatoms. When the coal surface is superficially oxidized via reaction [1.2] or [1.3], it is likely that the coal surface becomes positively charged because it loses electrons to the ferric ions (Dhooge et al., 1982, 1983). Anthony and Linge (1983) noted that the positive charge acquired during the electron transfer process is retained on the coal and increases the oxidation state of the residual carbon to approximately zero. Based on the elemental analyses of their coal sample, these investigators showed that the average oxidation state of carbon is -0.3 initially. Thus, the charging mechanism involving reactions [1.2] and [1.3] may be a transient phenomenon, which eventually leads to the formation of oxygen-containing groups such as carboxylates. Similarly, Kreysa and Kochanek (1985) suggested that the hydroquinone groups in coal are oxidized to quinone groups by Fe^{3+} via positively charged intermediates. The chemical oxidation of coal also occurs via the formation of positively charged radicals (Berkowitz, 1979).

However, the electrostatic repulsion forces between the minerals and the coal may not by itself be sufficient to widen the crevices containing the mineral matter and cause liberation. The proposed mechanism is that the osmotic pressure caused by the overlap of ionic double layers builds up inside the pores of the coal and ejects the mineral matter

out of the pores. Alternatively, the pressure can cause the pores to fracture and subsequently liberate the mineral matter. This is similar to the osmotic pressure differential created by the Donnan equilibrium of macromolecules on one side of a semi-permiable membrane (Chang and Kaplan, 1977). The positively charged surfaces of coal and mineral matter cause negatively charged ions to migrate into the crevices or pores in which the mineral matter is contained, setting up a diffuse electrical double layer. As a result of the high concentration of ions inside the crevices, the chemical potential of water inside the pores or crevices is reduced below that of the bulk water outside. This chemical potential difference forces the water molecules to migrate into the crevice, creating an osmotic pressure. The pressure will continue to build up slowly inside the crevice as long as reactions [1.1], [1.2] and/or [1.3] continue to take place. When the pressure is large enough, the mineral matter will be ejected out or the crevice will eventually break open and the trapped mineral matter will be released into the aqueous phase. Scanning electron photomicrographs of the processed coal show the opening of cracks and crevices, and the liberated mineral matter is visible by the naked eye in many cases.

Thus, the ferric ions are converted to ferrous during the process, and by regenerating the spent ions via reaction [1.4], the process may theoretically be continued indefinitely. There are several methods of regenerating the spent catalyst ions. The first is simply to aerate or oxygenate the coal slurry. This technique is commonly used in the ferric ion leaching of sulfides and uranium oxides. Secondly, the bacterium, *Thiobacillus Ferrooxidans* and/or *Sulfolobus Acidocaldarius* may be used to oxidize the ferrous ions to ferric (Myserson and Kline, 1984; Beyer et al., 1986). At present, 10-15% of the total U.S. copper production relies on a ferric ion leaching process using *Thiobacillus Ferrooxidans.* The third technique is to use an inert anode to oxidize the

ferrous ions and the work described here employed this technique. Other oxidizing agents may also be used as long as it is economically feasible.

Evidently, the role of the Fe^{3+}/Fe^{2+} couple in this liberation process is that of an electocatalyst. It may be possible to use other redox couples such as Ce^{4+}/Ce^{3+}, Cu^{2+}/Cu^{+} and Sn^{4+}/Sn^{2+} as electrocatalysts. Thermodynamically, both Fe^{3+}/Fe^{2+} and Ce^{4+}/Ce^{3+} have been found to possess the necessary characteristics for electrocatalytic agents in the coal oxidation reaction (Dhooge and Park, 1983a). These couples are sufficiently electropositive to react with oxidizable sites on the coal, are sufficiently soluble in the acid solution and oxidize rapidly at the electrode surface. However, it is convenient to use Fe^{3+}/Fe^{2+}, since it may be derived from pyrite and other ferruginous impurities present in the coal. Furthermore, by controlling the population of these ions in solution, it is possible to optimize the removal of pyrite, which would reflect a reduction in the inorganic sulfur content of the coal as well.

Finally, since the organic groups of coal are affected by the ferric ion oxidation mechanism, the oxidation of sulfur-containing groups such as dibenzothiophene may be possible which would result in the removal of organic sulfur from the coal.

1.3 Research Objectives

The objectives of this study may be broadly classified as follows

1. To test or explore the EIL process as a means of producing superclean coals having an ash content of less than 2%.

2. To study the effect of the following process variables on the deashing and desulfurization efficiency of the EIL process.
   a. Coal type and particle size
   b. Synergistic effects from acid types, concentrations and combinations of acids
   c. Reaction time and temperature
   d. Electrode type
   e. The effect of externally added ferric ions
   f. Reactor configuration

3. To investigate the EIL process in conjunction with an advanced PCC technique such as microbubble flotation.

4. To compare the efficiency of the EIL process with the well-known ferric-ion leaching process for coal pyrite.

5. To determine the proportion of mineral matter removed by dissolution and by liberation during the EIL process.

6. To examine by means of scanning electron microscopy, the feed and product coals for morphological changes that may occur during the EIL process.

7. To develop a quantitative model to estimate numerical values for the osmotic pressures that can develop inside the pores and crevices of coal during the EIL process. These values are to be compared with the tensile strengths of coal to determine if they are sufficient to cause fracturing of coal along the pores and crevices in which mineral matter is trapped.

1.3.1 Chapter Outline

The results of this study are reported in a series of relatively dependent chapters and sections. Owing to the very recent development of the EIL process, pertinent research papers are naturally scant. Chapter 2 nevertheless provides a comprehensive review of all the literature that contributed towards the development of the EIL process. Chapter 3 details experimental equipment and operations and summarizes the procedures adopted to use the EIL process to demineralize coal. The first part of Chapter 4 presents the coal-cleaning results obtained from several coals under different experimental conditions. The remaining sections focus on some fundamental aspects of the EIL process and address various key issues pertaining to alternate mechanisms that could explain the removal of mineral matter from coal by the EIL process. Chapter 5 presents a theoretical model which calculates the osmotic pressure developed inside a coal pore during the EIL process. Chapter 6 summarizes the work with conclusions and detailed suggestions for future work.

2.0 LITERATURE REVIEW

2.1 Electrochemical Treatment of Coal

2.1.1 Introduction

The electrolysis of coal was initially investigated as an alternative method of obtaining chemicals from coal. Prior to World War II, the chemical industry was based primarily on coal and its by-products and this provided incentives for investigating new ways to convert coal into useful chemicals. However, with the development of the petrochemical industry, the interest in coal diminished until it was somewhat rekindled with the oil embargo of 1973. One of the new, but commercially untried methods for coal conversion that resulted from this renewed interest was the electrochemical treatment of coal. Coal was originally investigated as an anodic depolariser for the economic production of hydrogen and oxygen from water by electrolysis. Later on, the emphasis changed to the electrochemical oxidation or

reduction of the coal to different products without expending large amounts of energy. Two main areas are discussed in the literature: (i) The electrochemical gasification of coal with the formation of hydrogen and carbon dioxide and (ii) the modification of the coal structure and its elemental composition by the electrochemical oxidation or reduction process. Most of the research efforts in these two areas met with purely theoretical interest and were not commercially implemented. The consequent investigations of other pertinent areas from these research efforts contributed towards the development of the EIL process.

2.1.2 Electrochemical Reduction of Coal

Probably the first reported investigation of the electrochemical reduction of coal was carried out by Belcher (1948) who worked with Meltonfield vitrain and a copper cathode. Only a small increase in the hydrogen content of the vitrain was observed and no water-soluble products were detected in the electrolyte. Given and Schoen (1958), in electrolysing extracts of coal in dimethlyformamide with n-tetraethyl ammonium iodide, showed that electrolysis at controlled potentials in the region -0.4 to 0.7V NHE reduced the carbonyl groups in the coal, in particular, the quinones. Further work by the same authors at -2.2V NHE led to the conclusion that up to 17 atoms of hydrogen could be added to 100 atoms of carbon in addition to the hydrogen atoms added to other carbonyl groups in the coal. Given (1958) studied the behaviour of model compounds as related to the structures present in coal under applied negative potentials.

Further work by Fuchs et al. (1959) with lead electrodes and slurries of coal in 0.1N lithium hydroxide indicated that coal could be reduced to water and alkali soluble materials with 65% conversion. A special cell and stirrer design ensured close contact

between the coal and cathode and avoided mass transport effects, thus enabling the authors to isolate aromatic and aliphatic acids from the electrolysed coal. Their work however, did not lend itself to any postulations of reaction mechanisms as the amount of hydrogen atoms added to the coal by electrolysis was not measured.

An alternative method to electrolytically reduce coal using lithium amine was proposed by Sternberg and Wender (1962) and by Reggel et al. (1958). With the usual electrolytic methods, coal must be brought into intimate contact with the electrons for reduction to take place: *i.e.* at the surface of the electrode. In the work described by Fuchs et al. (1959), even with the use of special techniques, close contact was only partially achieved. The use of lithium amine however, provided solvated electrons in the form of ion pairs $Li^{+}.....e^{-}$ which had excellent migratory properties and were powerful reducing agents. Utilizing this principle, Markby et al. (1963) reduced coal in an electrolyte consisting of ethylenediamine and lithium chloride at ambient temperature and claimed to have added as much as 44 atoms of hydrogen per 100 atoms of carbon. Their current efficiencies were 46% at the beginning of the electrolysis, but dropped to 10% after 10-15 hours of treatment. Following these observations, Sternburg et al. (1966) postulated a detailed mechanism for the reduction of coal during electrolysis and studied the effect of the electrochemical treatment on the solubility of coal in pyridine and benzene. The increased solubility indicated that structural changes may have taken place within the coal matrix as a result of the electrolysis. The sulfur content of the coal had decreased as well.

Later, Sternburg (1967) used structure analysis on the electrochemically reduced coal and concluded that electrochemical reduction was not only achieved by close contact between the coal and the generated electrons, but by the production of solvated electrons. Hydrogen added at the beginning of the reaction had a significantly greater effect on the solubility of coal in pyridine than hydrogen added at a later

stage. A similar effect was seen by Whitehurst et al. (1977) with respect to an increase in the evolution of volatile matter from the coal during thermogravimetric analysis of the electrolyzed coal. The authors cautioned, however, that these results were quite sensitive to the exact conditions of the electrolysis. Vaseen (1979) proposed a method to produce hydrogen from coal dust and water using electrochemical reduction. The drawbacks in his method were the very high temperatures and pressures required, although power requirements were only 9.5 kcals/mole of hydrogen. Research interest in the electrochemical reduction of coal somewhat decreased after this and the technique has not been revived since.

2.1.3 Electrochemical Oxidation of Coal in Alkaline Media

The earliest recorded attempt of electrochemically oxidizing coal in alkaline media was by Bartoli and Papasogli (1881) who used wood charcoal and graphite with aqueous potassium hydroxide as electrolyte. They observed that the electrolysis disintegrated part of the carbonaceous material to a fine powder and turned the electrolyte dark in color. When carbon electrodes were used, the oxygen evolved during the process was lower than when metallic electrodes were used. This led the authors to conclude that the liberated oxygen combined with the carbon from the electrodes to form soluble, colored products in the electrolyte. Beersohne (1923) utilized this principle in a German patent to produce colloidal products of an acidic nature. Lynch and Collett (1932) worked with fine coal in 6N sodium hydroxide with lead electrodes and produced an important oxidized form of coal called humic acid. They determined that the anode and cathode compartments needed to be separated by a porous diaphragm and reasoned that the electrode material was a factor in determining the

nature of the oxidation of the coal. Most of their work was confirmed by Eddinger and Demorset (1947) who used catalysts such as vanadium pentoxide, molybdenum oxide and cobalt chloride to obtain very much higher coal conversion rates. Belcher (1948) confirmed that the humic acids produced during alkaline coal electrolysis were similar to the products obtained by the oxidation of coal in alkaline potassium permanganate. He proposed two theories to explain that coal initially oxidized to form humic acids which further oxidized to yield water-soluble acids. A temperature of about 60°C optimized the production of humic acids and a maximum yield was obtained in about 12 hours.

Work in this area slowed down until Sentle et al. (1981) working with anthracite proposed an oxidation mechanism according to which OH^- ions were first discharged at the electrode surface to form OH• radicals and possibly other similar radicals as well. The OH• radicals were similar to those observed by Tomat and Rigo (1979) in their studies on the oxidation of polymethylated benzenes. These radicals attacked the coal molecules by hydrogen abstraction and/or addition to the aromatic rings to form aldehydes, ethers and other oxygenated compounds. The oxidation continued to yield humic acids as end products. Lalvani et al. (1986) working with lignite slurries in 1N sodium hydroxide solution examined the effect of various parameters such as coal concentration, temperature and reaction time on the oxidation of coal and the production of humic acids. An optimum potential of 2.7V SCE was established for the production of humic acids above which these acids degraded by a Kolbe-type reaction. A later report (Lalvani, 1987) indicated that the oxidation of the coal did not proceed via a single reaction step, but through many complex pathways. Some possible reaction pathways were postulated following analysis using FTIR, GC mass spectrometry, SEM and elemental analysis on the reaction products. Wapner and Lalvani (1988) reported on the removal of organic sulfur from coal

following electrochemical oxidation in alkaline media. Their work indicated that at potentials between 1.2-1.6V SCE, the removal of pyritic sulfur was highest while the removal of organic sulfur was greatest at potentials ranging from 1.8-2.0V SCE.

2.1.4 Electrochemical Oxidation of Coal in Acidic Media

Coal was initially used as an anodic depolariser in the production of hydrogen from water, as it reduced the potential required for the decomposition of water by about 66%. Significant studies on the electrochemical oxidation of coal in acidic media have only recently appeared in the literature. Farooque and Coughlin published a series of papers on the anodic oxidation of coal in both sulfuric acid and hydrochloric acid solutions (1979a, 1979b, 1979c). They studied the effect of various parameters such as coal particle size, slurry concentration, reaction temperature, supporting electrolyte etc., on the rate of oxidation. It was proposed that coal slurries oxidized at the platinum anode to produce carbon oxides as anodic products and hydrogen as a cathodic product according to the following reaction.

$$C + 2H_2O \rightarrow CO_2 + 4H^+ + 4e \qquad [2.1]$$

or

$$C + H_2O \rightarrow CO + 2H^+ + 2e \qquad [2.2]$$

at the anode and

$$4H^+ + 4e \rightarrow 2H_2 \qquad [2.3]$$

at the cathode. The cleaning of coal by electrolysis was first observed by Farooque and Coughlin (1979c). Their studies showed that the specific surface area of the coal increased by 164 m^2/kg when 16.36% of the coal was electrochemically consumed. However, the theoretical increase calculated by assuming a uniformity in size and

sphericity of the coal particles was only 86.4m^2/kg. The difference between the calculated and observed surface areas was attributed to (a) the removal of ash from the coal particles during the reaction and (b) the non-uniformity and non-sphericity of the particles as well as non-uniform consumption of material from the particle surfaces. Scanning electron photomicrographs of the particles before and after electrolysis showed evidence of these phenomena. As the applied potential was about a third of the potential required to electrolytically decompose water into hydrogen and oxygen, the authors suggested the process as an attractive prospect for the economical production of hydrogen. In a later report, Coughlin and Farooque (1980) evaluated the economics of hydrogen production by electrolysis in aqueous slurries. They concluded that with off-peak hour electric power rates and anticipated developments in solid polymer electrodes, the electrolysis of coal-water mixtures could compete with conventional processes for the production of hydrogen. However, their analysis did not take into consideration the possible production of organic chemicals and the cleaning of the coal by the process.

A study on the electrolysis of Kentucky coals in aqueous 0.1M lithium chlorate was carried out by Baldwin et al. (1981). Using voltammetry they observed that freshly-prepared coal slurries invariably yielded smaller currents than identical slurries that had been allowed to stand for a period of time prior to the voltammetric analysis. The length of time required for the currents to stabilize ranged from several hours to several days, depending on the coal. Since equilibration periods were necessary to obtain consistent currents, it was suspected that the electroactive species undergoing oxidation at the electrode surface was an extracted solute species and not the coal matrix itself. Atomic absorption analysis on the electrolyte solution showed iron as a major component. By comparing the voltammetric behavior of the extracted

electrolyte solution with that of the Fe^{3+}/Fe^{2+} redox couple, the authors identified the ferric ion as the active species in the electrochemical oxidation of coals.

Okada et al. (1981) repeated most of the work done by Coughlin and co-workers and confirmed their observations. They determined that the oxidation of ferrous iron to ferric played an important role in the electrochemical conversion of coal. This led to the important conclusion that ferrous ions oxidized to ferric during the first few hours of the electrolysis and caused the large current densities at the beginning. As the electrolysis continued, the ferrous ions depleted and the limiting current density fell to around 0.1 mA/cm^2. The authors confirmed their reasonings by electrolysing coal that had been washed to remove the iron present in it. They found that on electrolysis the initial current densities were as low as the final limiting current densities of the unwashed coal. Since coal electrolysis could not produce sustained high-current densities, it could no longer be considered as an economic alternative to produce hydrogen which required current densities of 100-500 mA/cm^2.

Extending the work of Okada et al.(1981), Coughlin et al. (1981) used cyclic voltammetry at different scan rates to confirm the role of the Fe^{3+}/Fe^{2+} redox couple in the electrolysis. They suggested that ferrous ions oxidized at the anode could continuously react with the coal in a non-electrode process. The electrochemical behaviour of the acid electrolyte after filtration showed remarkable similarity with that displayed by the coal slurry itself. Hence, they suggested that coal pyrite, which is normally insoluble in acid became soluble during the course of the electrochemical oxidation and played a major part in the reaction.

Guruswamy and Alexander (1982) determined that electrolysis removed 80-85% of the ash from the coal and that a number of elements like Al, Mg, Ca, Rb, Fe, Zn, Ni, Sn, and Na were leached from the coal into the electrolyte. They observed an increase in the solubility of coal in pyridine from 10% to 35% and attributed this

to the removal of inorganics and the breaking of sessile bonds in the coal as a result of the electrolysis.

Dhooge et al. (1982), in an attempt to further confirm the role of the Fe^{3+}/Fe^{2+} redox couple in the oxidation of coal slurries, conducted their electrochemical experiments with only ferrous ions in the electrolyte. The current-potential curves obtained were similar to those obtained with coal particles in the electrolyte. They determined the rate constant for the catalytic oxidation of coal by ferric ions and cerric ions to be 3.0×10^{-5}sec.$^{-1}$ and 1.1×10^{-4}sec.$^{-1}$, respectively, and recommended the use of the Ce^{4+}/Ce^{3+} redox couple as a superior oxidizing agent for the process. If the oxidation of ferrous to ferric were the only electrochemical process occuring, then the electrolysis current theoretically should decrease to zero when all the ferrous ions had been oxidized. Since Coughlin and Farooque had observed that the limiting currents could remain at non-zero values for as long as 450 hours, Dhooge et al. concluded that it was necessary to assume that other reactions were occurring that kept the current flowing. In their studies they found that practically no anodic currents were observed with coals thoroughly washed in 1.0M sulfuric acid. These coal particles were washed by stirring in sulfuric acid solution for more than 50 hours. However, when ferric ions were added to the washed, untreated coal and the anodic potential held high enough for ferrous ions to oxidize to ferric, anodic currents were observed for several hours, indicating that ferrous ions were generated by reaction of the ferric ions with the coal. This theory was substantiated by their subsequent work (1983a) which supported the catalytic oxidation of coal slurries by ferric ions in solution followed by the oxidation of the spent ferric ions at the electrode.

A study of the oxidation of coal slurries in acidified ferric sulfate solution indicated that the coal oxidation rate (R) by the ferric ions was of the form

$$R = k/t^n \qquad [2.4]$$

where k and n were empirical constants (Anthony and Linge, 1983). A value of 0.4 ± 0.1 was attributed to n for lignite and high rank bituminous coals. k measured intrinsic coal reactivity and increased with decreasing coal rank.

The anodic oxidation of coal slurries in flow-through, packed-bed electrodes was investigated by Morooka et al. (1984). The anode was a bed of platinum plated titanium pellets through which the coal slurries circulated. This design reduced the oxidation of coal by the electrodes, facilitating the study of the various oxidative reactions taking place during the electrolysis. From these studies, the authors concluded that the anodic reaction was not solely due to the oxidation of ferrous to ferric, but also due to the oxidation to CO or CO_2 of water-soluble organic compounds dissolved from the coal. With plate electrodes, the collisions between coal particles and the anode were so few that the anodic oxidation of the ferrous ions to ferric predominated as the main anodic reaction. However, when a packed-bed electrode was used, collisions between the coal and the electrode took place in sufficient numbers for the anodic reaction of coal to be enhanced. The contribution of each reaction to the current density was dependent on electrode geometry, coal type, materials and operating conditions.

Using cyclic voltammetry on the slurry and the unelectrolyzed filtrate, Lalvani et al. (1983) showed that both displayed the single electron oxidation of Fe^{2+} to Fe^{3+} as a major reaction. On the basis of these observations, they suggested that the electrochemical reactions may involve direct oxidation of the pyritic sulfur by coal particles striking the anode (with much lower currents) or by the dissolved Fe^{3+}/Fe^{2+} redox couple acting as an electron transfer agent between the anode and the solid pyrite minerals as well as the carbonaceous components of the coal. Their preliminary

experiments indicated that up to 40% of the total sulfur in coal could be removed by electrolysis while a later report (1985) indicated sulfur removals as high as 70%. Inorganic sulfur from pyrites and organic sulfur from thiophene groups in the coal were oxidized by the ferric ions to water-soluble sulfate forms. This was suggested to occur via a complex reaction whose rate-determining step was the formation of a complex S-O compound at the platinum electrode.

Voltammetric and mass spectrometric experiments conducted during coal slurry electrolysis further confirmed that the electrochemical activity resided in the conversion of leached ferrous ions to the ferric form (Taylor et al. 1985). The studies were done on a series of coals ranging from lignite to anthracite in 4M sulfuric acid. The authors attributed the currents below 1.3V NHE to the oxidation of inorganic ions and currents in the 1.4-1.7V NHE range to the oxidation of organic material leached from the coal. Inorganic ions leached from the coal were found to play no significant role in the oxidation of coal or electrolyte to *gaseous* products, but reduced the fraction of the current leading to gas evolution.

Park (1984) recognized that two types of coal oxidation occurred in the presence of the Fe^{3+}/Fe^{2+} redox couple. The first was the electrochemical oxidation of coal, given by Equation [2.1], whose rate was generally observed to be very slow. This reaction occurred at the surface of a coal-electrode and was potential dependent. The second was the chemical oxidation of coal through the chemical redox reaction between the ferric ions and the coal. This reaction occurred on the coal surface as follows;

$$4Fe^{3+} + C + 2H_2O \rightarrow CO_2 + 4H^+ + 4Fe^{2+} \qquad [2.5]$$

No current was generated by this reaction since the charges of the anodic and cathodic reactions are balanced. However, the ferrous ions produced by this reaction migrated to the anode and were oxidized to ferric, which produced an electric current in the circuit.

At high temperatures it was possible that some of the oxides generated on the coal surface were reduced by the ferrous ions themselves as follows (Dhar et al., 1986);

$$4Fe^{2+} + C_sO_x + 4H^+ \rightarrow 4Fe^{3+} + C_sO_{(x-2)} + 2H_2O \qquad [2.6]$$

where the subscript *s* refers to the surface carbon atoms. Since the above reaction produced no current, the net effect would be a lowered oxidation of the coal without a diminution of the oxidation current.

2.1.5 Surface Reactions of Coal During Electrolysis

The second area of research on the electrochemical treatment of coal was the modification of the coal structure and its composition. Previous work had by now confirmed that the primary electro-active species was not the coal, but the dissolved iron in the electrolyte.

Early work reported that the controlled oxidation of purer carbons, whether by electrochemical or chemical means resulted in the formation of surface oxides (Panzer and Elving, 1975). These oxides were often considered to consist of carbonyl, carboxyl and phenolic groups as well as cyclic peroxides, esters, lactones and carboxylic acids. Of these, the carboxylic groups usually predominated. Farooque and Coughlin (1979c) believed that similar oxides formed on the coal surface during the anodic oxidation of coal. This was suggested to explain the fall in the rate of electrochemical oxidation with time. The various surface oxides were suspected to adhere to the coal surface and render electron abstraction harder for the ferric ion as the reaction proceeded. It was not certain whether the adherence of the oxides to the coal surface was caused by a concentration effect. Their reasonings, however, were substantiated by the fact that

the original reactivity of the coal could be restored by washing off these oxides from the coal with acetone.

These authors further attributed the decrease in the oxidation current (*i.e.*, the reaction rate) in part with the accumulation of tar-like coatings on the coal particles during electrolysis. These coatings were composed of additional reaction products in the form of small aliphatic fragments which broke away from the larger coal molecules during the anodic oxidation.

FTIR studies on electrochemically oxidized coals from the San Juan basin of New Mexico and the Pittsburg #8 seam indicated that oxygen-containing compounds were formed on the coal surface during reaction with ferric ions (Dhooge and Park, 1983b). The treatment was carried out in 1.0M sulfuric acid in the presence of Fe^{3+} or Ce^{4+} with or without the application of a potential of 1.0V NHE. The spectra revealed the presence of aliphatic acids, ethers, alcohols, as well as evidence of conjugated C=O compounds (*i.e.*, quinoids). Combining FTIR with isotope experiments, the authors concluded that water was intimately involved in the electrochemical oxidation by supplying oxygen for the production of carbon oxides. The source of carbon dioxide was from a straightforward oxidation of carbon sites in the presence of an oxygen source (*i.e.*, water). This disputed the contention put forward by Okada et al. (1981) that the carbon dioxide produced during the electrochemical oxidation of coal was produced by reaction of carbonates with the acid or other oxygen compounds extant in the coal.

The kinetics and reaction mechanisms of the reaction of ferric ions with coal during electrolysis are not yet well understood. Kreysa and Kochanek (1985) investigated the electrolysis of a German coal in sulfuric acid using a platinum rotating disc electrode (RDE) at 1.25V SCE. These authors concluded that from the many coal structure models proposed (Given, 1960), the only group with sessile bonds capable of undergoing a redox reaction in the potential range of the Fe^{3+}/Fe^{2+} couple was the

quinone/hydroquinone system. Their conclusions were supported by a kinetic analysis using transient current methods, IR spectroscopy and elementary analysis. The experimentally observed increase of the C=O band ($\simeq$1600 cm^{-1}; 1100-1400 cm^{-1}) and the parallel reduction of the OH band ($\simeq$3400 cm^{-1}) after electrochemical coal oxidation was in accordance with a coal oxidation mechanism suggested by Vetter (1961).

2.2 *Coal Cleaning Techniques*

2.2.1 Mineral Matter in Coal

The primary reactions of coal electrolysis have by now been established as the oxidation of ferrous to ferric iron at the electrode coupled with a concomitant reduction of the ferric ions at the coal surface to the ferrous state. These ions have to be produced *in-situ* or be externally supplied for the electrochemical reaction to proceed. A possible supply of ferrous or ferric ions in solution could come from the dissolution of any of the iron-bearing minerals present in coal.

Minerals become associated with coal in various ways. They may develop in the coal basin either as the coal itself is forming (authigenic) or be transported into the coal basin from other regions (allogenic). Minerals may also be introduced into the coal depositional basin by wind or flowing water. Gluskoter (1977) compiled a comprehensive list of the mineral species observed in coal together with their chemical formulas. The most abundant mineral species are those of the clay group (Gluskoter, 1977; Raask, 1982), which on the average, constitute 60-80% of the mineral matter in

most of the world's coals. Kaolinite and illite are the most common clay minerals in coal and of these, kaolinite is the dominant species in the majority of the world's coals (Stach et al. 1982). However, as these minerals do not contain any iron (Appendix I), they cannot provide any ferrous or ferric ions by dissolution in the electrolyte.

Second in abundance are the minerals of the carbonate group. Huggins et al. (1982) indicated that calcite is the only carbonate which is an important constituent of coal, although Gluskoter (1977) stated that dolomite and ankerite are the dominant carbonates in most of the world's coals. Since certain coals produce carbon dioxide during the *initial* stages of reaction with an acid, it is likely that this is due to the action of the acid on certain exposed carbonate minerals in the coal matrix. The reaction of such iron-bearing mineral carbonates such as siderite and ankerite with acid would yield carbon dioxide and provide ferrous or ferric ions in solution.

Most of the non-clay silicate minerals contain various forms of iron (Appendix I), but quartz is the only common non-clay mineral reported in coals (Gluskoter, 1977; Stach, 1982). Thus, it is unlikely that the dissolution, if any, of non-clay silicate minerals could provide ferric or ferrous ions in solution, particularly if they are present only as minute fractions of the total coal body.

Among the sulfides, pyrite occurs most abundantly in coal (Brown et al., 1952; Gluskoter, 1977). Its polymorph, marcasite is as common, as well as sphalerite and galena. Pyrite ranges in size from microscopic single crystals and framboids to large inclusions clearly visible in hand specimens. It is present in nearly all of the world's coals and its importance is indicated by the large number of studies on pyrite available in the literature.

2.2.2 Pyrite Behavior in Ferric Solutions

From the chemical and electrochemical behaviour of pyrite, it is more than likely that a large part of the *in-situ* iron for the EIL process comes from the pyrite in coal since other ferrugenous minerals (such as siderite) are usually present in smaller amounts in coal. Under the experimental conditions of pH≤2.0 and electrode potential ≥0.4 NHE, pyrite is unstable and should dissolve to yield ferrous or ferric ions according to the Pourbaix diagram (Garrels and Christ, 1965). Peters and Majima (1968) investigated the anodic behaviour of pyrite in 1M $HClO_4$ and showed from product and coulometric analyses that pyrite could dissolve in an anodic environment as follows:

$$FeS_2 + 8H_2O \rightarrow Fe^{3+} + 2SO_4^{2-} + 16H^+ + 15e \qquad [2.7]$$

Further work (Biegler and Swift, 1979) showed that the overall anode reaction was a combination of the above reaction and

$$FeS_2 \rightarrow Fe^{3+} + 2S^\circ + 3e \qquad [2.8]$$

If x was the fraction of pyrite reacted, the overall process could be written as

$$FeS_2 + 8xH_2O \rightarrow Fe^{3+} + 2xSO_4^{2-} + 2(1-x)S + 16xH^+ + (12x+3)e \qquad [2.9]$$

The value of x (and thus the sulfate yield) increased linearly with potential between the range 0.5-1.5V SHE. The sulfate yield increased with potential while the yield of elemental sulfur decreased.

The rates of reaction between various pulverized (100-200 mesh) samples of marcasite and pyrite with ferric ion at pH 2.0 were first order (Wiersma and Rimstidt, 1984). The measured rate constants ranged from 1.0×10^{-4} to 2.7×10^{-4} sec^{-1} ±5%.

Further electrochemical studies (Lalvani and Shami, 1986) conducted with pyrite at electrode potentials of 0.8V SCE indicated that the reaction was autocatalytic. The

oxidation of pyrite resulted in the formation of dissolved iron, which catalyzed the oxidation according to the two reactions given below.

$$FeS_2 + 2Fe^{3+} + 2SO_4^{2-} \rightarrow 3Fe^{2+} + 3SO_4^{2-} + 2S \qquad [2.10]$$

$$6Fe^{3+} + 9SO_4^{2-} + S + 4H_2O \rightarrow 6Fe^{2+} + 6SO_4^{2-} + H_2SO_4 \qquad [2.11]$$

The ferrous ions produced were oxidized to ferric at the electrode according to [1.1] as evidenced by cyclic voltammetry.

2.2.3 Desulfurization of Coals by Ferric-Ion Leaching

The possibility of desulfurizing coal by oxidizing the pyrite present in it with ferric sulfate was investigated by several workers and is one of the more important methods for coal desulfurization (Yurovskii, 1974; Dutrizac and MacDonald, 1974; Meyers 1977). A 66% reduction in total sulfur was achieved using high sulfur Russian coals in 16% ferric sulfate solutions at 100°C for one hour (Yurovski, 1974). An inverse relationship existed between the ash content of the feed coal and the oxidizing power of the ferric sulfate as low-ash coals responded better than high-ash coals. Using comparative results of sulfur removal from natural low-ash coals and artificially created high-ash coals, it was concluded that aluminosilicates retarded the rate of desulfurization. A plausible explanation offered was that the aluminum sulfate formed by reaction adsorbed fairly extensively on the coal surface. This created a film on the surface of the coal particles, obstructing the diffusion of the oxidizing solution into the pyrite inclusions. Further, even a small amount of adsorbed, sparingly-soluble aluminium sulfate left on the coal adversly increased the sulfur content of the product

coal. Interestingly, coal pyrites that were free of aluminosilicates oxidized more intensively than the pure mineral pyrites.

In the Meyers process, aqueous ferric sulfate or chloride selectively oxidized the pyritic sulfur in coal at approximately 100°C to form elemental sulfur and ferrous sulfate (Meyers, 1977). The ferrous sulfate gradually oxidized to ferric with molecular oxygen while the elemental sulfur was removed from the coal matrix by steam or vacuum vaporization or solvent extraction with toluene. From tests conducted on 21 run-of-mine U.S. coals, the median pyritic sulfur removal was 53% in 0.5 hr. and 90-95% in 23 hours.

An attempt at quantifying the deashing and desulfurization of coal with ferric sulfate was carried out by Shimada et al. (1984). A high ash (31.3%) Brasilia Santacatarina coal was reacted with concentrated (up to 2.0M) ferric sulfate solution at 20 to 130°C from 1 to 19 hours at atmospheric pressure. The removal of ash and sulfur was modelled using a 1-dimensional shrinking-core model. The rate-determining step of the mineral removal was dependent upon the mass transfer rate of the dissolved ash through the pore filled with ferric sulfate solution. The removal of ash and sulfur was correlated with ferric sulfate concentration, mean particle diameter, reaction time and temperature.

The leaching properties of ferric sulfate are not limited to coal pyrite, but to several other base metal sulphides as well (Dutrizac and MacDonald, 1974). Although temperatures >100°C are usually required for the ferric-ion leaching process, a great advantage was the ease and variety of methods available for the generation of lixiviant. It may be prepared by oxidizing pyrite at high temperatures and pressures (Johnson, 1965) or by bacterial oxidation of pyrite (McReady and Zentilli, 1985). The spent lixiviant may be regenerated by anodic electrolysis or aeration. The rate of ferric formation from ferrous was enhanced if the aeration process was replaced by reacting

the ferrous solutions with molecular oxygen. An investigation by Mathews and Robins (1972) with solutions containing 0.01M to 1M ferrous sulfate indicated that the rate of formation of ferric iron from ferrous by molecular oxygen was dependent on the ferrous concentration, dissolved oxygen in the solution and the pH. Cupric ions were found to increase the rate of oxidation while the effects of other ions were negligible. The authors proposed a mechanism and a rate expression for the rate of oxidation.

An extensive review on pyrite oxidation discussed several of the mechanisms and associated kinetics of pyrite oxidation (Lowson, 1982). A model for the ionic equilibria of ferric sulfate-sulfuric acid solutions taking into account the effect of ionic strength provided a basis for optimizing the ferric-ion concentration in solution (Lee and Tavlarides, 1985).

The major types of organic acids that could be present in air-oxidized coals were itemized by Wen (1979). The effects of acid-oxidation on the electrochemical behavior of coal pyrite was examined using varying concentrations of oxalic and succinic acids as model substances (Ogunsola and Osseo-Asare, 1987). Using polarization analysis, the authors concluded that the formation of a strong non-porous film, probably β-$FeC_2O_4 \cdot 2H_2O$, on the pyrite surface reduced the surface reactivity of coal pyrite during a coal desulfurization process. This film was suspected to be caused by the reaction of pyrite and oxalic acid.

2.2.4 Coal Cleaning by Aqueous Leaching

The removal of mineral matter from coal by chemical leaching has been attempted by several workers and forms the basis for several important CCC techniques (Fan et al. 1984a; Chi et al. 1986; Markuszewski et al. 1986). Most of these processes have not

yet been commercially implemented due to the high temperatures and pressures necessary for the coal cleaning reaction to proceed. Essentially, these processes involve reacting coal with a hot alkaline solution to dissolve quartz and to convert other clay minerals and iron pyrites into acid-soluble compounds. These compounds are removed in a second step by acid treatment. When used for treating coal with non-liberated mineral matter, the rate of cleaning depended on the penetration of the solvent into the coal matrix or the migration of the dissolved mineral out of the coal matrix.

The penetration of the coal matrix as a means to liberate mineral matter was investigated over a decade ago (Datta et al. 1976; Howard et al. 1977). The solvent-treated coals showed selective breakage along bedding planes and mineral-maceral boundaries (Howard and Datta, 1977). The authors claimed that chemical comminution caused by solvent penetration liberated considerably more pyritic sulfur from Illinois #6, Redstone, Pittsburgh and Upper Freeport seam coals than mechanical crushing. Although a few chemicals were capable of comminuting coal, those that appeared to have the greatest effect were ammonia and methanol (Aldrich et al., 1974). These compounds contained a lone pair of electrons (*e.g.*, oxygen and nitrogen) which were suspected to cause swelling and breakage in the coal. It was therefore suggested that solvent swelling was the mechanism causing the breakage of the coal (Keller and Smith, 1976). However, the only support of this contention was a theoretical discussion, which became invalid when it was observed that even gaseous ammonia could comminute coal (Howard et al., 1977).

The heats of immersion of bituminous and sub-bituminous coals in alkanols reflected the accessibility of alcohols into the pore structure of coal (Widyani and Wightman, 1982). The size of the alkanol molecule affected its ability to penetrate the coal matrix as seen by the lower heats of immersion of the smaller alkanol molecules. Experiments indicated that the straight chain butanol molecules could penetrate coal,

but that secondary and tertiary isomers were progressively excluded as their molecular dimensions exceeded the nominal pore size of the coals examined. A mechanism suggested for the penetration of coal by alkanols was that the polar sites on the coal surface attracted the hydroxyl groups on the alkanol, provided there was no steric hindrance between the coal and the alkanol. The molecular size of the solvent was therefore an important parameter for chemical comminution, particularly if penetration of coal matrix was deemed a rate-determining factor.

Studies by a number of workers reported the possible formation of intercalation compounds in the aromatic planes of carbon atoms in coal with various metallic reagents and transition metal chlorides. Beall (1979, 1980) and Beall et al. (1983) observed the reaction of anhydrous ferric chloride with bituminous and sub-bituminous coals of different volatilities at 230°C. The x-ray and chemical analysis of the coals after reaction showed a considerable amount of ferric ions incorporated in the coal structure. However, no ferric salts could be determined in the coal by X-Ray Diffraction after the reaction, indicating that the ferric-ion did not exist in the reacted coal as crystalline entities. Scanning electron photomicrographs of the reacted coal samples showed that cracks had developed along the coal surface. This was consistent with an intercalation process in which ferric chloride molecules entered the layered carbon planes at their edges.

Waugh and Bowling (1984) investigated the demineralization of three Australian coals and a vitrinite using sodium hydroxide solutions at 200-300°C under pressure in an autoclave. The feed coals assayed 4-8% ash while the beneficiated products assayed 0.25-0.75% ash. The major minerals removed were silica and kaolin, which were converted into sodium alumino-silicates (sodalites) by reaction with the alkali. The sodalites were insoluble in water or alkalis, but were readily soluble in aqueous acids. The authors presumed that the penetration of the alkali into the coal occured via the

functional groups on the coal and was aided by the hydrothermal pressure exerted during leaching. Other similar attempts were carried out by Fan et al. (1984b) who treated several coals with 1M sodium carbonate at 250°C and 13.6 atm. and obtained a 56-86% reduction in the sulfur content of the coals examined.

Demineralizing coal with aqueous hydrogen peroxide/sulfuric acid was examined by Vasilakos and Clinton (1984) under a variety of experimental conditions. A near complete elimination of the pyritic sulfur and the sulfate in solution was claimed by the authors. An optimal sulfuric acid concentration was established above which the acid had an adverse effect on pyrite oxidation.

2.3 Osmotic Behavior of Porous Media

2.3.1 Introduction

The osmotic behavior of porous media is associated with the change in the surface free energy of the medium caused by the adsorption of foreign molecules or ions onto the surface. Adamson (1982) defines the surface free energy of a solid as the work required to produce a unit of new surface by a reversible process to yield an equilibrium surface. The surface free energy change is thermodynamically related to the osmotic pressure and this forms the basis for calculating the osmotic properties of porous media such as clays and soils described in sections 2.3.3 and 2.3.4. The pore structure of coal causes it to exhibit many of the properties of porous media and in particular, those discussed in the following sections.

2.3.2 Pore Structure of Coal

The EIL process is based on the development of osmotic pressures inside the cracks and crevices present on a coal surface. Coal is a highly heterogeneous substance and a complete determination of its actual structure is an elusive goal. Some reviews on the structure of coal (Krevelen, 1961; Lowry, 1963) described it as an organic chemical substance, a rock structure containing petrographic features, a solid colloid and a cross-linked polymer. Coal has an extensive pore structure (Renton, 1982) and can contain large amounts of absorbed water in its pores, ranging from 1 to 5% in bituminous coals to nearly 45% by weight in lignite. The pores in coals vary in size from cracks of micron dimensions to apertures impervious even to helium at room temperature. The IUPAC classified micropores as those pores ranging from 8 to 20Å. Spitzer et al. (1977) determined the pore volumes of 20 different coals of varying carbon content. The characteristic radii of pores found these coals varied between 5.5-6.8Å, classifying the pores in coal as micropores. Since most of the surface areas of coals and cokes are located in micropores, the overall rates of coal reactions are determined by the ease with which reactant molecules diffuse into and product molecules diffuse out of the pore structure of coal.

It is well accepted today that all coals contain microporosity with voids less than 20Å in size, (Walker 1981). Much of this porosity is in or behind voids that are around 5-6Å. The characterization of this microporosity was achieved by (a) absorption of carbon dioxide at 289K and nitrogen at 77K, (b) displacement of hydrogen or mercury at 298K and (c) uptake of liquids at 298K (Reucroft et al., 1984). Because of these ultra micropores, coals can behave as molecular materials.

2.3.3 Osmotic Flow Models

The ability of porous media to act as semi-permeable membranes has been conclusively demonstrated by field and experimental evidence (Coplen and Hanshaw, 1973; Kharaka and Berry, 1973). The osmotic flow of water through compacted clays acting as semi-permeable membranes was invoked to explain disparate phenomena in the subsurface such as anomalous hydraulic heads (Marine, 1974), overthrust faulting (Hanshaw and Zen, 1965) and breaching of clay liners in seepage ponds holding saline waste (Hudec, 1980).

Kharaka and Smalley (1976), using bentonite and kaolinite samples compacted up to 10,000 psi., studied the osmotic flow of water through these clays. The ability of these natural materials to behave as semi-permeable membranes was demonstrated at different temperatures, hydraulic pressures and compaction encountered in typical subsurface situations. Studies on the thermo-osmosis of water through kaolinite indicated that thermal gradients could cause or assist the osmotic flow of water through clays (Srivastava and Avasthi, 1975).

A mechanism for the osmotic flow of water through compacted clays was proposed by Marine and Fritz (1981). The negative charges on clay particles (Grim, 1968) attracted cations from an electrolyte solution and created a double layer on the surfaces of these particles. As a result of the high concentration of ions around these clay particles, the chemical potential of water between particles is smaller than that in the surrounding bulk solution. Driven by this chemical potential difference, uncharged water molecules pass through the clay membrane, whereas the dissolved ions are somewhat prevented from doing so by the double layer charge around each of the particles. If the more saline solution is in a tightly contained body of rock, the

water flow results in an increased hydrostatic pressure that raised the activity of water in the confined solutions. The osmotic flow will continue until the aqueous activity is the same for solutions on both sides of the clay "membrane". However, clays could only act as effective membranes when they were compacted sufficiently such that the ionic double layers surrounding the clay platelets effectively overlapped. If the interparticle spacings were sufficiently large such that the traversing ions were not influenced by the overlapping double layers, no osmotic pressure would develop.

In an ideal membrane, the predicted (theoretical) osmotic pressure $\Delta\Pi$, is equal to the observed, osmotically-induced, hydrostatic pressure ΔP. In non-ideal membranes, typical of most practical cases, the hydrostatic pressure generated by osmosis would be less than that predicted by the general osmotic equation. To account for the non-ideality of clay membranes, Kedem and Katchalsky (1962) defined three practical phenomenological coefficients (α, L_p and ω) whose values were empirically determined. The reflection coefficient, α, was by far the most informative because its value predicted the expected, osmotically-induced hydraulic pressure in a membrane system. The ratio of the observed osmotic pressure to the theoretical osmotic pressure was termed the reflection coefficient (Staverman, 1952.).

Marine and Fritz (1981) derived an equation for α. Their model related the value of the reflection coefficient to the porosity and surface charge density of the membrane and to the mean solute concentration on either side of the membrane. A comparison of the actual osmotic pressures developed in a buried Triassic basin near Aiken, South Carolina with those predicted by the model resulted in a discrepancy; the measured hydrostatic heads exceeded the calculated osmotic heads by 9-12%. This discrepancy was attributed to the water samples measured by the osmometer of being non-representative of the actual zone of highest pressure. A later attempt to verify the

model reported closer agreement between predicted and measured values for the reflection coefficient (Fritz and Marine, 1983).

The theoretical osmotic pressures calculated from solution properties were much larger than those observed in shale subsurfaces. It was suggested that although $\Delta\Pi$ values were large when concentration gradients across clay membranes were high, the low value of α due to the membrane's properties rendered $\alpha\Delta\Pi$ and thus the true osmotic pressure, ΔP, low. Alternatively, if the concentration difference was low, then $\alpha\Delta\Pi$ was low because $\Delta\Pi$ was already low (Fritz and Marine, 1983).

Fritz (1986) offered physical interpretations for the three phenomenological coefficients defined for clay membranes. The hydraulic permeability constant L_p was a measure of the system's sluggishness of response in transporting solution and solute through the membrane structure. Low values of L_p corresponded to highly compacted membranes and vice-versa. The solute permeability coefficient ω, controlled the rate at which the osmotic potential of the membrane cell was dissipated; *i.e.*, the rate at which the saline side of an osmotic cell diffused its salt across the membrane to the more dilute side. The reflection coefficient α, approached unity as the membrane approached ideality while ω values approached zero.

2.3.4 Calculation of Osmotic Pressures

Probably the earliest known calculation of the repulsive pressure between two charged surfaces containing an electrolyte was made by Schofield (1946). The electrostatic stress caused by double layer interaction was equated to the repulsive osmotic pressure to yield a fairly simple expression relating the osmotic pressure to the electrolyte concentration. Although the expression was valid only for very small

concentrations ($\simeq 10^{-4}$M), it nevertheless showed that an osmotic pressure $\simeq$0.01 atm. could develop between mica plates containing $\simeq$30Å thick water films. Low and Hemwall (1956) derived an expression relating the hydrostatic repulsive force that caused reversible clay swelling to the number of ions in solution, the partial molar volume of water and the potential energy of water which was attributed to the adsorptive forces between the material and water. Following this, equations were derived relating the partial molar free energy and the activity of soil water to the osmotic pressure of moist soils with or without dissolved salts (Low and Anderson, 1958). Low (1980) derived a semi-empirical equation to calculate the swelling pressure of montmorillonite which related two variables, α and β, to the osmotic swelling pressure Π by a simple exponential equation. α and β were empirically related to the specific surface area, cation exchange capacity and the mass ratio of the clay to water. The experimental data was further used to develop semi-empirical equations where the swelling pressure decreased exponentially with the surface charge density of the montmorillonite and the distance between the superimposed layers of the clay over the water layers. The calculations showed that a pressure of 1-6 atms. could develop inside two parallel montmorillonite layers 50-200 Å apart. Usui and Hachisu (1984) utilized the principles of double layer interaction to derive an equation for the osmotic pressure developed between two charged flat plates. The equation related the osmotic pressure to the potential at the center of the plane separating the two charged flat plates by a hyperbolic cosine function.

An expression relating the osmotic pressure to the surface separation, surface potential and bulk concentration was derived by Israelachvili (1985), who used the *center-value theorem* to calculate the potential variation across the double layer instead of the usual Debye-Huckel approximation. Since the osmotic pressure equations did not contain parameters dependent on the specific nature of the surface, it was suspected that

a common factor influenced the different properties of water and its osmotic pressure (Sun et al., 1986). This implies that a repulsive osmotic pressure would be experienced by ***any*** charged surface with overlapping double layers in an aqueous medium.

Alternatively, osmotic pressure, being a thermodynamic property, may be calculated from the aqueous activities of solutions on either side of an ideal semi-permiable medium. The activity of water is a unitless number whose magnitude is controlled by solute concentration, pressure and temperature. Since aqueous activities in solutions are dependent on the properties of the solute, a constant termed the osmotic coefficient was defined to describe osmotic systems. The osmotic coefficient Φ, unique for any particular solute, is temperature dependent and related to the water activity in solution by an exponential equation (Harned and Owen, 1958). Thus, equal molalities of different salt solutions will not yield the same osmotic pressure because each salt has a unique osmotic coefficient.

Two basic approaches were used in the literature to compute a value for this thermodynamic quantity; fundamental and statistical. Fundamental models were based on rigorous thermodynamic analyses of solution and solute properties. However, these models required values of several parameters pertaining to solutions and solute properties, not all of which were readily available nor were easily determined.

On the other hand, statistical models did not require any pre-determined values for any parameters other than the coefficients that defined the statistical model. However, their use was usually restricted to the experimental range in which they were developed.

Most fundamental models started from first principles or from the properties of ions and molecules determined from microscopic experiments. The calculation of any thermodynamic property of a solution required a knowledge of all interactions, solute-solute, solute-solvent and solvent-solvent. The nature of the system had to be well

understood; *i.e.*, the nature of the particles constituting the system and the interactions or intermolecular forces acting on these particles. Assuming these were available, it was theoretically possible to develop an algorithm based on statistical mechanics to compute any thermodynamic property of the solution. However, if all of the contributions were rigorously accounted for, the calculation of any thermodynamic property often became a mathematical nightmare. Hence, to simplify computations, several solution models and approximations were developed in the theory of ionic solutions over the last decade or so. The basic reference model was the primitive model, reviewed by Rasaiah (1973) and Outhwaite (1975). This early model was improved upon by modifications (Thomlinson and Outhwaite, 1982), corrections (Nordholm, 1983) and new models (Bratcko, 1983). Other models developed rapidly as direct Monte Carlo simulations provided a kind of ideal experimental test of the statistical mechanical methods applied. At present, theories such as the cluster expansion, hypernetted chain or mean spherical approximation can provide reasonable predictions from infinitely dilute to moderately concentrated solutions (Rasaiah and Friedman, 1969; Grigera and Blum, 1976).

A method based on the Gibbs-Duhem equation was proposed for the calculation of the activity of water in multicomponent electrolyte solutions (Zaitsev and Aseev, 1982). Although the model predictions correlated well with observed values for binary systems at 298.15K, it required extensive heat capacity data for its application. Cochran (1983) developed an equation to calculate the contribution to osmotic potential from separate solutes. The equation was based on a molecular model of osmosis that evaluated individual molecular osmotic pressures that existed in water solutions containing a mixture of ions. The validity of the equation was tested for six dilute sodium and potassium compounds in water at 20°C.

Pitzer and Kim (1979) discussed several methods of calculating osmotic and activity coefficients using the familiar theory of Debye and Huckel (1923) and several other

equations developed by himself and his co-workers. A subsequent publication challenged the accuracy of these equations when applied to mixtures (Ialenti and Caramazza, 1984), and asserted that Pitzer's equations did not relate the change in property of one component with that of another when present together in a mixture. Pitzer (1984) responded that all of his equations were derived from a single expression for the excess Gibbs free energy, from which equations for activity and osmotic coefficients were derived by appropriate differentiation. The Pitzer and the Debye-Huckel equations were utilized in an iterative procedure to calculate activity and osmotic coefficients (Goldberg, 1984). However, it required a knowledge of the equilibria in solution and assumed values for single-ion activity coefficients. Calculations were iteratively performed until the assumed values agreed with the calculated ones. Activity and osmotic coefficients calculated for three different acids and inorganic salt solutions provided good agreement between calculated and observed properties for solutions up to to molalities of around 1.0mol./Kg.

In the statistical approach, the thermodynamic properties of solutions were measured as accurately as possible by a variety of techniques and the data represented by least-squares equations. These equations may then be used to calculate other thermodynamic properties of the solution. The activities of several hundred single-salt solutions have been determined, the majority of which were measured by the isopiestic method. The popularity of this method was obvious as it was perfectly general and could be applied to any system comprising non-volatile solutes dissolved in a volatile solvent. Several methods of measuring solvent activities and osmotic coefficients are discussed by Pytkowicz (1979).

The osmotic coefficients of several salt solutions were isopiestically determined at 25°C by Rard and Miller (1981) and fitted into suitable least-squares equations. These

equations predicted the values of the osmotic coefficients within the limits of the experimental errors involved in their measurement.

2.3.4.1 Osmotic Coefficients of Sulfuric Acid

A short review on the osmotic coefficients of sulfuric acid is included because of its importance in the development of a thermodynamic model for the EIL process in Chapter 4. The determination of the osmotic coefficients of sulfuric acid has been unusually difficult because the dissociation constant of HSO_4^- lies in the most troublesome region where methods successful for weaker acids begin to fail. It is troublesome in view of the higher charge on the sulfate ion and the correspondingly large changes in its activity coefficient. Pitzer et al. (1977) fitted equations based on intermolecular forces and distributions with established thermodynamic data of sulfuric acid over the range 0 - 6M. Agreement between observed and predicted values was within the limits of experimental uncertainty up to 5M at 25°C. Rard et al. (1976) re-examined and updated the existing isopiestic data of the osmotic coefficients of sulfuric acid. A total of 174 data points of measured osmotic coefficients at 25°C ranging from 0.1 to 27.7mols./Kg. water were fitted into a semi-empirical equation coupled with a least-squares fit. The accuracy of this equation measured by the standard deviation was within the limits of experimental error. An assesment of all published data for the osmotic coefficients of aqueous sulfuric acid at 25°C was made by Rard (1983), with recommendations as to which data were more reliable and as to which should be given greater weight in future evalutions.

3.0 EXPERIMENTAL DETAILS

The essential feature of the EIL process is that an electrocatalytic oxidizing agent (such as Fe^{3+}) is contacted with coal, while it is continually regenerated from its reduced state (*e.g.*, Fe^{2+}). As mentioned earlier, there are several methods of regenerating the ferric ions. The method employed in this study has primarily been an electrochemical technique in which ferrous ions were anodically oxidized on the surface of an inert platinum or graphite electrode.

3.1 Materials

All chemicals used were of the analytical grade and were obtained from Fischer Scientific Co. Coal samples were obtained as run-of-mine or heavy-media float products from different coal mining companies. A list of these samples and their respective suppliers is provided in the Appendices. The coal was first ground in a roll

mill and/or ball mill and screened to the desired sizes using a mechanical Ro-tap screening machine.

3.2 Equipment

3.2.1 Electrochemical Reaction Vessels

Two different reaction vessels were developed for this study. The apparatus of Figure 1 comprised of a water- jacketed, stirred-tank reaction vessel. The temperature of the cell was maintained constant by circulating water through the water-jacket. A working electrode (platinum or graphite) was inserted through the top of the vessel into the slurry contained within the vessel. The reference electrode communicated via a Luggin capillary with the working electrode. The counter electrode was placed in a separate chamber with a glass frit attached to the bottom of this chamber. A thermometer passed through a stopper in the cover of the vessel into its interior. The coal slurry in the vessel was kept in suspension by a Teflon-coated magnetic stirring bar, specially designed so that its spinning action did not pulverize the coal. The reference electrode was a Saturated Calomel Electrode (SCE), which provided a reference against which potentials could be measured.

The reactor shown in Figure 2 was the preferred form for treating coarse coal. In this reactor, the coal particles did not contact the electrode surface, but the electrolyte flowed continuously around the coal particles. This design prevented the oxidation of

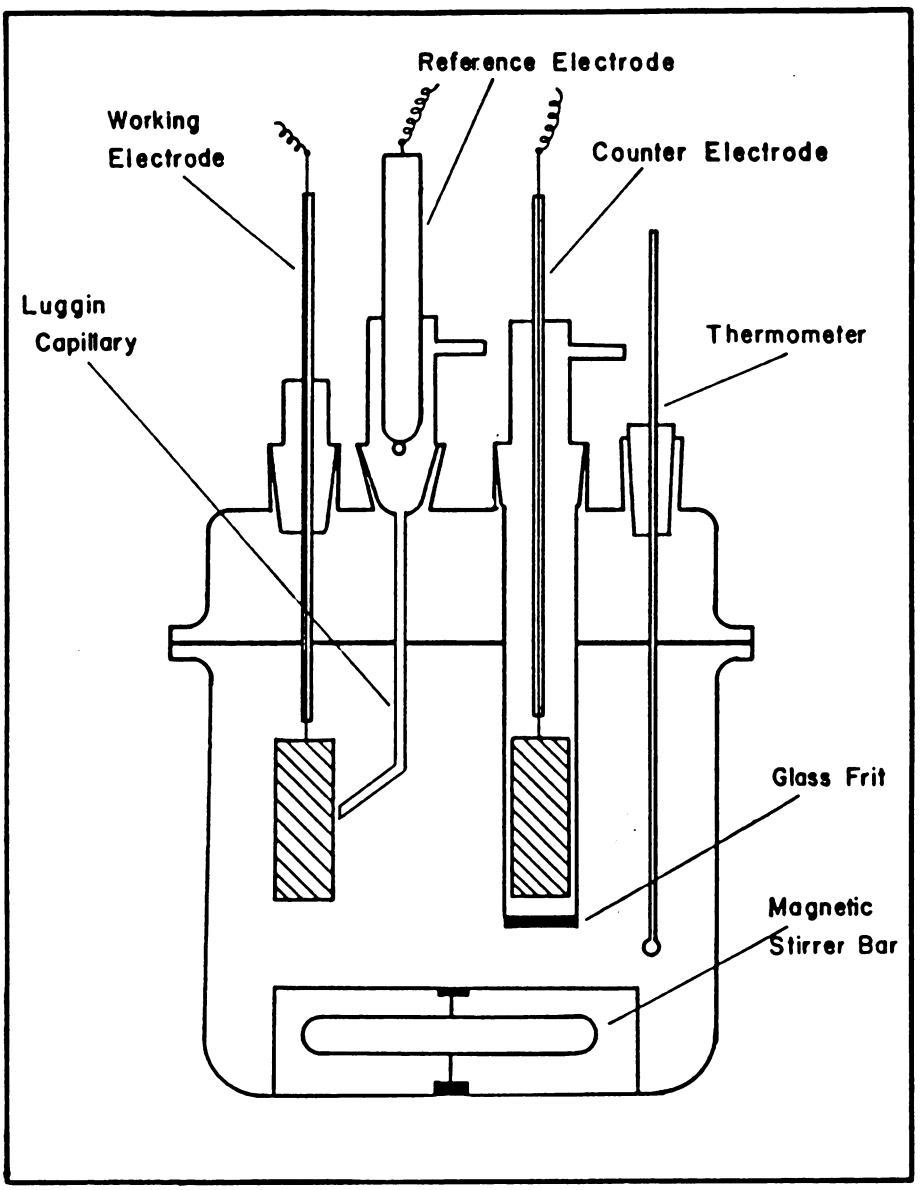

Figure 1. The Stirred-Tank Reaction Vessel

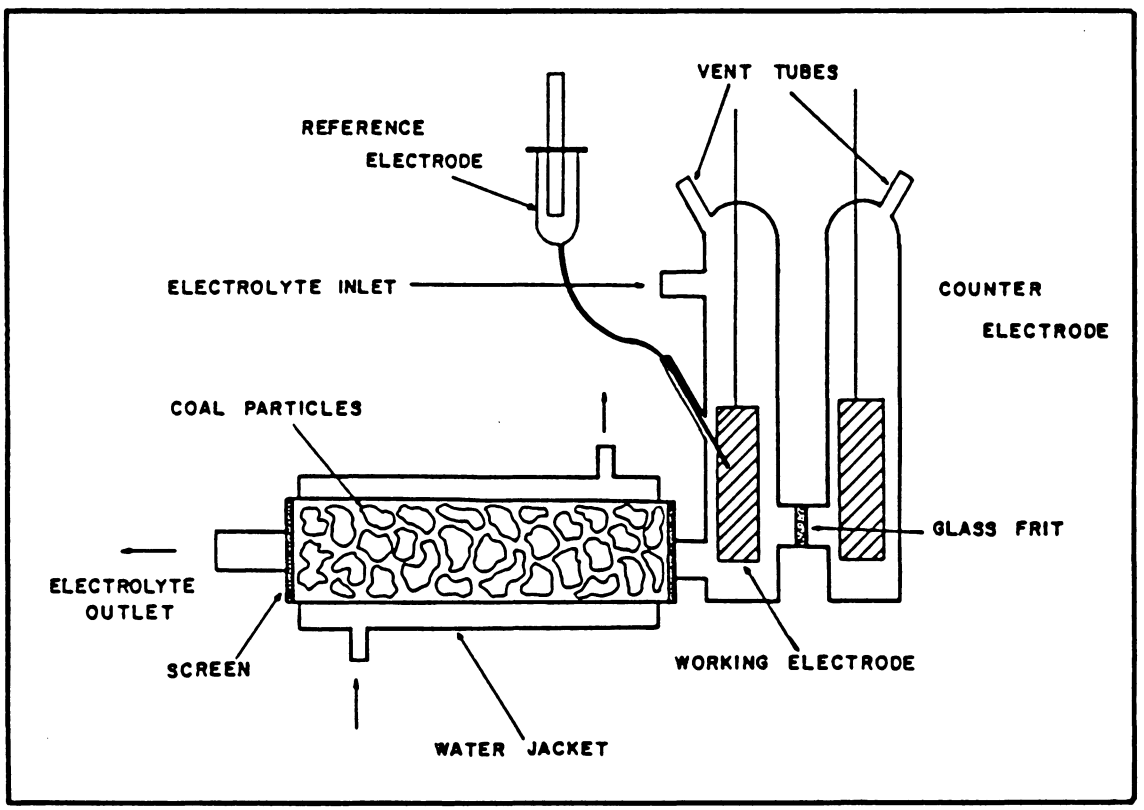

Figure 2. The Flow-through Reaction Vessel

the coal by contact with the electrodes, permitting only the ferric ions to oxidize the coal.

The reactor consisted of a container which had both of its ends closed off by porous polypropylene diaphragms. Coal particles were loosely packed to form a porous plug inside the reactor which was surrounded by a water jacket to maintain constant temperature.

At the first end of the container was the inlet chamber which included a fluid inlet, a working electrode and a reference electrode. The counter electrode was attached to the inlet chamber through a glass frit. A pump continuously circulated electrolyte from the outlet, past the working electrode and through the coal particles in the container.

Ferric ions, which were constantly regenerated at the working electrode, flowed through the coal bed and were reduced to ferrous iron by reaction with coal. The ferrous ions were pumped back into the electrochemical chamber where they were converted to ferric iron and the process continued throughout the duration of the experiment. The reactor was normally used for cleaning relatively coarse coal so that the particle bed formed was porous enough to pass the electrolyte without substantial pressure drop.

The ash removal stage comprised of a conventional wet-screening device for separating the ash particles from the coal particles. The treated coal was placed on a screen and sprayed with water until all the liberated matter had passed through the screen. If the coal particles were of a size 325 mesh or smaller, the liberated mineral matter was removed either by filtration using coarse filter paper (20-25μ pore size) or by a flotation technique.

3.2.2 Electronic Equipment

Potentials necessary for the oxidation of ferrous ions to ferric were supplied using an EG&G PARC model 362 potentiometer. A 3-electrode system was used to minimize "IR" drops and to control the potential of the working electrode versus a saturated calomel reference electrode. Currents were measured with the aid of another circuit consisting of the working electrode and a counter electrode. Current-time behavior was measured using a 4500 series strip-chart recorder manufactured by Houston Instruments.

Measurements of the current and charge passed during a given reaction were measured with an EG&G PARC model 379 digital coulometer.

3.2.3 Atomic Absorption Spectrometry

A Spectrospan IV plasma emission spectrometer from Spectrametrics Inc. was used to analyze the various elements in the spent acid from the EIL process. Argon was used as the plasma gas in the spectrometer. The instrument was calibrated using standards for the different elements manufactured by Fisher Scientific, Inc.

3.2.4 Ash and Sulfur Content

The ash content of various coals before and after treatment was obtained using a Fisher model 495 isotemp programmable ashing furnace. The ash analyses were carried out according to ASTM standards. Sulfur contents were determined using a Leco model

SC132 computer-controlled sulfur determinator. With some coal samples, the ash and sulfur determinations were performed by the Glamorgan Coal Company.

3.2.5 Low Temperature Ashing Oven

Isolation of mineral matter from coals was accomplished using a low temperature asher. This device passed oxygen from an external source into two Pyrex chambers where the coal samples were placed. A wire coil wrapped around each chamber carried a Radio Frequency (RF) signal and established an RF field in the chamber. In the RF field, the oxygen was excited vibrationally, rotationally and electronically, and a variety of atomic and molecular species were produced (Gleit, 1963). The temperature in the chamber during the process was 150°C or less, possibly as low as 80°C (Gluskoter, 1977). Thus, low temperature ashing left the mineral matter nearly unaltered, although the maximum temperature encountered during the process would probably dehydrate all hydrated mineral species. Clay minerals would therefore be expected to lose their interlayer water molecules. However, it was likely that these minerals would rehydrate in the laboratory atmosphere prior to analysis. Once the mineral matter was isolated from the coal, it was identified by X-ray diffraction and Energy Dispersive X-ray microanalysis.

3.2.6 Particle Size Analyzer

An Elzone 80XY particle size analyzer was used to determine the particle size distribution of the low temperature ash from a variety of coals. A software package

developed at Virginia Tech provided an interface between an IBM-PC and the Elzone 80XY to allow computer-controlled operation of the particle size analyzer as well as data logging and manipulation (Mankosa, 1986). The computer program blended all data from succesively smaller orifice tubes in the Elzone 80XY and determined the weight percent distribution of material in a particle size distribution finer than the lower detection limit of the analyzer.

3.2.7 Zeta Potential Measurement

Zeta potentials of coal particles in various solutions were determined using a model 500 Laser Zee Meter manufactured by PenKem, Inc. A rotating prism method was utilized to avoid the typical time-dependent errors associated with conventional instruments making microelectrophoretic measurements. The instrument provided zeta potential values directly as calculated internally from Smoluchowski's equation.

3.2.8 Scanning Electron Microscope

Scanning electron photomicrographs were obtained using a Stereoscan 120 scanning electron microscope from Cambridge Instruments Inc., equipped with a backscattered electron detector. A 30KV electron accelerating voltage was used with a working distance of around 15 mm for most of the operations. A Denton Vacuum Desk II cold sputter/etch unit was used for sputter-coating the coal samples. A Kevex Analyst 8000 Energy Dispersive X-ray analysis unit was interfaced with the microscope and provided auto-identification of elements present in a given sample.

3.2.9 X-Ray Diffraction

The instrument used in these analyses was a Picker Nuclear Diffractometer manufactured by Picker X-ray Corporation. Copper K-α radiation generated 35KV and 16 mA was used in all of the cases with a scan rate of 2°/min. Each XRD test was run from an initial diffraction angle, 2θ, of 5° to a final angle of 65°, corresponding to d-spacings in the range of 17.6723-1.4347Å. This range was sufficient to detect the low-angle maxima produced by the large interplaner spacings in clay minerals and also to collect enough diffraction data to identify major minerals likely to be encountered in the typical mineral matter found in coal.

Identification of the mineral phases from the XRD data was manually conducted by comparing the spectra with existing powder diffraction files. This was sometimes complicated by the interference of peaks for 2 or more phases.

3.3 Experimental Procedure

3.3.1 Electrocatalytically Induced Liberation

The feed coal was first screened to the desired size fraction by mechanical screening, after which it was usually wet-screened to remove fine particulates of coal, dust and other extraneous matter. The coal was dried in an oven at 80°C for several hours, after which it was assayed for ash and sulfur content. The feed coal was now mixed with the acid electrolyte and brought to the desired reaction temperature in the reactor. Details

of the acid concentration, temperature etc. are described with the results in section 4.2. The coal-acid mixture was gently stirred for 15-18 hours. This was done to ensure complete wetting of the coal particles by the acid and to allow pyrite and other iron-bearing minerals to dissolve so that Fe^{3+} ions are available. After the conditioning period, a constant positive potential was applied to the electrodes. The current and the cumulative charge passed through the circuit was recorded at different time intervals for the duration of the experiments.

Most of the experiments were carried out at 60 to 80°C, with reaction times ranging from 3 to 30 hours. At the end of a reaction, the coal was placed on a screen and sprayed with tap water (pH $\simeq$5.5) until all of the liberated mineral matter passed through the screen. When the particle size of the feed coal was below 325 mesh, the liberated mineral matter was removed using a coarse filter paper (20-25μ pore size) or by a suitable flotation technique. The coal residue was heated at 80°C to dryness and analyzed for ash and sulfur content. In some cases, the liberated mineral matter that passed through the screen was collected along with the wash water. This solution was allowed to settle, decanted and filtered/centrifuged after which the residue was weighed and analyzed for ash content. This procedure was adopted whenever mass balance calculations were carried out.

3.3.2 Collection of Low Temperature Ash

The low temperature ashings of the various coals were accomplished by placing about 1.5 to 2.0 grams of the desired samples in Pyrex boats which could be inserted inside the chambers of the low temperature asher described earlier. The coal was spread thinly over the bottom of the boat and ridges were made in the sample surface to

increase the surface area for better efficiency. Oxidation of the sample occurred to depths of about 1 mm in a fresh sample, which was usually one-third to one-half the total depth. The process was interrupted at convenient intervals (usually 8-10 hours) to weigh and stir the sample. The coal samples were ashed until the color of the burning plasma in the oven changed from blue to the violet color of an oxygen discharge, showing that the oxidation of the coal samples had ended. Ashing was considered complete when three successive weighings (at intervals of at least a few hours) showed differences of 7 mg. or less. An additional criterion was that no unashed coal was evident upon visual inspection after stirring; some samples (particularly those of the -200 mesh particle size) failed to meet the latter criterion although they did meet the former one. The low temperature ashing procedure produced a powder of white or yellowish mineral matter which was analysed by X-Ray Diffraction.

3.3.3 Scanning Electron Micrographs

A monosize fraction of coal (usually below 200 mesh) was prepared by dry-screening. A separate sample was taken from this monosize sample by repeated riffling to ensure that a representative sample from the bulk was taken for the SEM analysis. Any substance to be analysed in an SEM must have a surface that is electrically and thermally conductive. Since coal samples do not meet this criteria, a layer of gold was sputter-coated over the mounted coal particles. In this technique, the mounted samples were placed in a chamber which was then evacuated to about 50 millitorr. Argon gas was passed through and the flow rate was adjusted to maintain a current of about 40 mA. Under these conditions, gold from a ring-shaped target was deposited on the sample. Following this treatment, the samples were placed inside the

SEM and photographs representing the lot were taken after examining several coal particles from various angles.

4.0 RESULTS AND DISCUSSION

4.1 Voltammetry and Coulommetry

4.1.1 Introduction

The results are divided into several sections. The first deals with the general electrochemistry of the EIL process since the process follows a chemical/electrochemical pathway; the chemical path being the reaction of ferric ions with coal while the electrochemical path is the oxidation of the ferrous ions at the platinum electrode. Hence electrochemical kinetics and mass transfer rates would have a significant impact on the overall kinetics of the EIL process. These may be studied by certain experimental techniques such as voltammetry and coulommetry carried out on the coal slurries. A short background note concerning these techniques is given below.

Cyclic voltammetry is a controlled potential technique in which the applied potential is varied linearly with time from an initial value, E_i, to some other value E_f.

At E_f, the direction is reversed and the potential sweep is repeated back and forth between the limits E_i and E_f . Cyclic voltammetry is a special case of Linear Sweep voltammetry where the starting potential, E_i, and the lower potential limit are the same. The waveform generator inside the potentiostat controls the starting potential, initial scan direction and rate, upper and lower potential limits etc. Consider the case of a platinum electrode immersed in a solution with bulk concentration C_b of species A. A sweep begins in the anodic direction from the initial potential that is below the reversible potential, E_r , for the anodic reaction

$$A \rightarrow B + e^- \qquad [4.1]$$

where species A,B represent the reduced and oxidized species, respectively. When the potential is above E_r, the anodic reaction can begin and an anodic current will flow. As the potential continues to rise, the rate of the reaction increases and hence the anodic current. If the supply of species A to the electrode surface cannot keep pace with the rate at which it is consumed, then the surface concentration at the electrode will diminish until it falls to near zero. Mass transport of species A to the electrode surface now controls the rate of reaction and the diffusion layer depletes as species A is consumed. If the concentration gradient of species A begins to decrease by the reaction, the current will decrease as well causing a peak in the voltammogram. If there is a continuous supply of species A to the electrode surface fast enough to support the electrode reaction, the current will contiually rise as the potential is raised and no peak will appear.

When the scan is reversed at the upper limit E_f, the anodic current will still flow as the potential is still above E_r . However, as the diffusion layer is further depleted the anodic current will continue to decrease. Eventually the potential will decrease below the reversible potential for reaction [4.1] and the reduction of B back to species A will occur causing a cathodic current to flow. The shape of the remaining portion of the

voltammogram is similar to that of the anodic scan for essentially the same reasons. The voltammetric technique is therefore useful for systems in which a succession of anodic and/or cathodic reactions occur since peaks corresponding to each one will appear. Furthermore, it is sensitive to reactions which proceed only to a small extent and to the electrosorption of species in monolayer amounts.

4.1.2 Voltammetry

Cyclic voltammetry was carried out to identify the electrochemical reactions taking place on the electrode. Although mass transfer processes occurring in a slurry matrix need not be the same for all coals, many of the coals examined under voltammetry exhibited similar current-potential behavior. Electrochemical activity generally arose at an applied potential of near 0.5V SCE and increased markedly above $\simeq$1.5V SCE due to oxygen production at the anode.

Figure 3 represents a typical voltammogram of the acid electrolyte during the EIL treatment of a Glamorgan seam coal. The coal was made into a slurry with 3.6M sulfuric acid without the addition of any ferric ions. The wide-scan started at 0.0V SCE in the anodic direction at a scan rate of 200mv/sec. and was reversed at 1.6V SCE. The presence of the anodic and cathodic peaks at $\simeq$0.5V SCE and $\simeq$0.3V SCE confirm the presence of a redox species in solution. These peaks were absent when coal was not present in the acid electrolyte indicating that coal played a part in the overall anodic reaction. To confirm this, ferric sulfate monohydrate (1.0mM) was added to the pure electrolyte. A 1.0V SCE potential was applied for several hours to ensure no oxidative species remained in solution. A sample of Glamorgan coal which had been previously washed in acid for several hours to remove all acid-soluble iron-bearing minerals was

then added to the solution. After a few minutes, the current began to increase, indicating that ferrous ions were being produced by some chemical reaction, possibly a combination of reactions [1.1] and [1.2]. A voltammogram of this system showed the presence of the Fe^{3+}/Fe^{2+} peaks. From electrochemistry, the first anodic and cathodic peaks correspond to the oxidation and reduction of the Fe^{3+}/Fe^{2+} redox couple, the reversible potential being located at approximately 0.44V SCE. The second anodic and cathodic peaks are associated with the electrolysis of water while the electrochemical activity near 1.5V SCE is caused by electrochemical oxidation of organic material leached from the coal (Taylor et al., 1985). Thus, currents below 1.0V SCE may be attributed to the oxidation of inorganic ions, particularly ferrous, while currents in 1.4 to 1.6V SCE region originate from the oxidation of organic material leached from the coals. Hence, as far as the EIL process is concerned, operating at potentials > 1.0V SCE wastes energy by dissociating water molecules and in oxidizing the coal itself.

4.1.3 Current versus Time Behavior

Figure 4 shows some typical examples of the current-time behavior of acidified coal slurries at potentials below 1.2V SCE. The current almost always dropped rapidly from its initial value and approached a steady-state value. These experimental observations along with the coal oxidation reactions [1.1], [1.2] and [1.3] suggest that coal is oxidized through an *ec'* type catalytic mechanism (Bard and Faulkner, 1980). At a potential of 1.0V SCE, the major electrochemical reaction occurring is that of ferrous oxidation and hence, the reaction current is a measure of the rate of oxidation of ferrous to ferric. The decrease in the reaction rates as shown by the curves is therefore primarily related to the amount of ferrous ions present in the system. The amount of ferrous ions is in

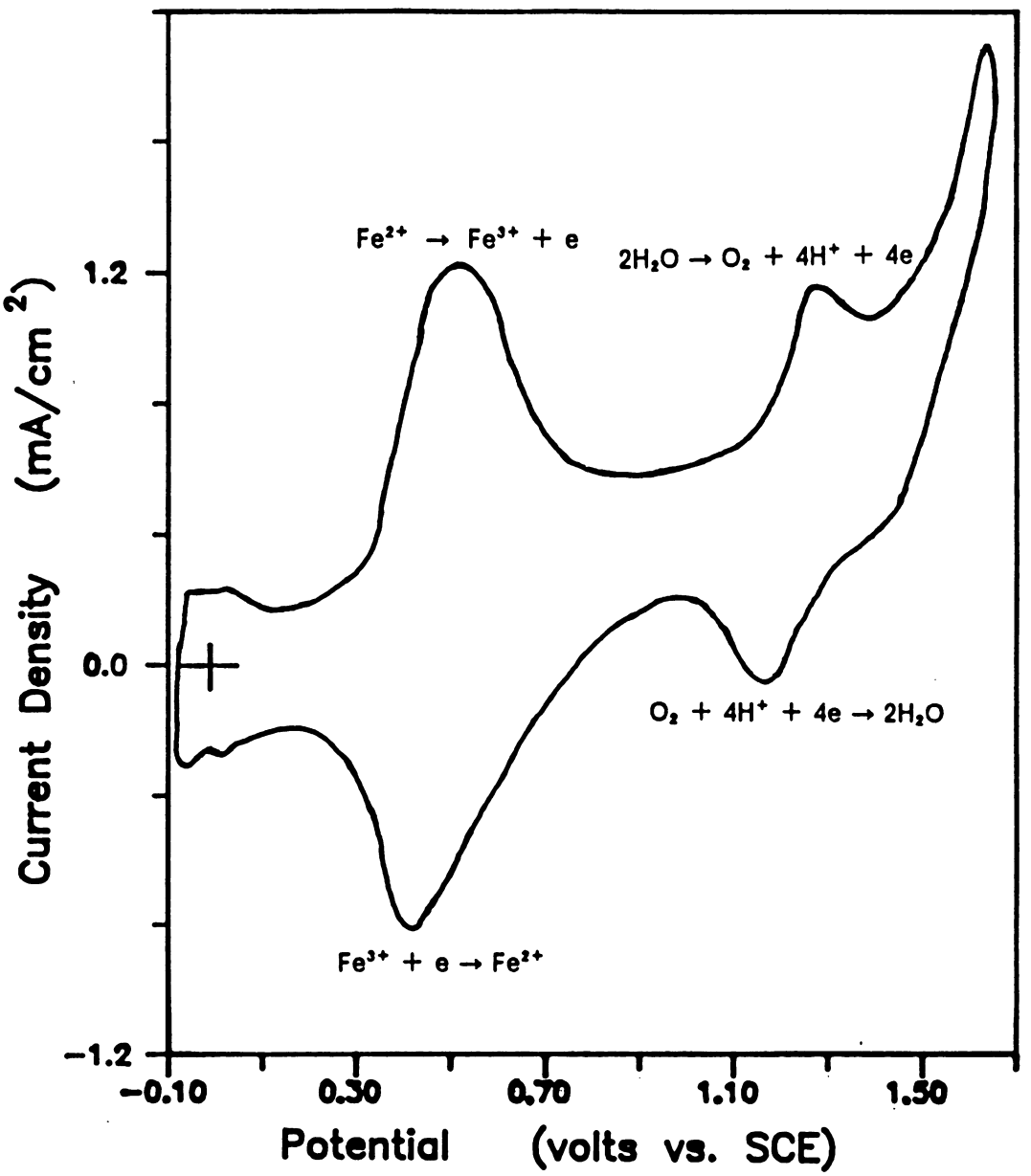

Figure 3. Typical Voltammogram of the Coal-Slurry During the EIL Process: Glamorgan coal in 3.63M sulfuric acid at 65°C after conditioning for 10 hrs. Scan rate = 200mV/sec.

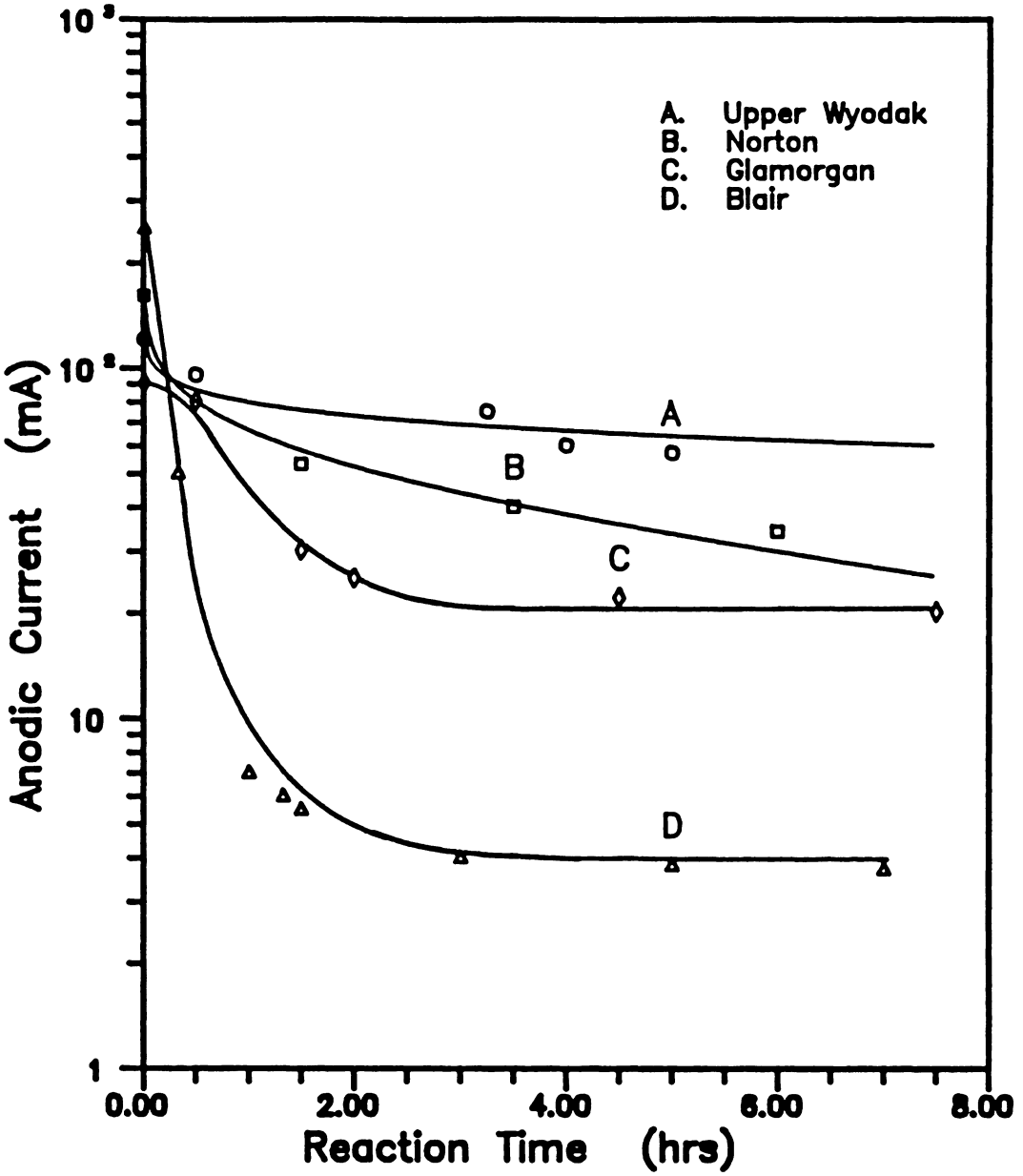

Figure 4. Typical Current-Time Behavior of Coal During the EIL Process: All coals were processed under similar conditions following a 12 hour conditioning period.

turn related to the reaction of ferric ions with coal which produces ferrous ions according to reactions [1.1] and [1.2]. The reaction of ferric ions with coal, as discussed in the literature, is limited to a few reactive carbon sites, probably associated with peripheral hetero-atoms or unsaturated carbon bonds in the coal structure. The decrease in the reaction rate could thus be linked to the disappearance of these sites during reaction, *i.e.*, by the transformation of one type of carbon bond to another. However, if the reaction of coal with ferric ion was straightforward, then the production of ferrous ion should cease after all these bonds were destroyed by the reaction. Since the limiting current remains at non-zero values, it is possible that new reactive sites are formed by the reaction. This provides a means for reactions [1.1] and [1.2]/[1.3] to continue indefinitely. The limiting current would thus correspond to the rate at which the rates of reactions [1.1] and [1.2]/[1.3] become equal.

Secondly, the gradual decrease in the reaction rate as represented by the current may be due to the formation of certain oxides containing hydroxyl, carbonyl or carboxyl groups that form on the coal surface. These oxides form whenever pure carbons are electrolysed in acid media (Panzer and Elving, 1975). Although coal is not a pure carbon, it is not unreasonable to expect certain portions of the macromolecule to behave as such.

The initial values of the currents depended primarily on the type of coal used and the time of contact between the coal and the acid prior to the application of a potential. The steady-state values that the current approached with time depended mainly on the type of coal used, although other factors such as acid concentration, reaction temperature, coal slurry concentration etc., were found to increase the steady-state value of the current for a given electrode geometry. The rate of fall in current to its steady-state value was different for each of the coals examined. Since the cell current is dependent on the amount of ferrous ions available for anodic oxidation, and the ferrous

ions are in turn generated by the reaction of the coal surface with ferric ions, the current-time curves indicate the relative reactivity of each coal to electrocatalytic oxidation by ferric ions.

It was found that freshly-prepared coal slurries invariably yielded smaller currents than identical ones that had been allowed to stand over a period of time prior to the application of a potential across the electrodes. Figure 5 shows current verses time behavior of Widow Kennedy coal under different conditions of the EIL process. 40 gms. of a -20+70 mesh sample of this coal assaying 26.3% ash was made into a slurry with 400.0ml. of a 1.0M sulfuric acid solution containing 10^{-3}M ferric sulfate monohydrate. Curve A shows the current-time response of this slurry after the coal had been allowed to soak in the acid for 24 hours before a potential of 1.0V SCE was applied to the electrodes. Curve B shows the current-time response of the slurry when the potential was applied immediately after the coal was mixed with the acid.

The high initial current observed in curve A indicates the oxidation of a large number of ferrous ions to the ferric state. These ferrous ions could only have been produced from the reaction of ferric ions with the coal as discussed earlier. The ferrous ions were then oxidized to ferric when the potential was applied and the current reaches a limiting value where the kinetics of ferrous oxidation by the electrode are balanced by the kinetics of ferric reduction at the reactive sites on the coal surface. When the potential was applied immediately following the addition of the coal to the acid, the observed initial current was much lower (curve B), but gradually approached the steady-state value of the current in curve A. This indicates that a smaller number of ferrous ions were available for oxidation at the beginning of the reaction, but as the reaction proceeded, the production of ferrous ions increased as shown by the increasing current. Since ferric ions can react with coal according to equations [1.2] and [1.3], it is theoretically possible to prolong this reaction indefinitely by constantly regenerating the

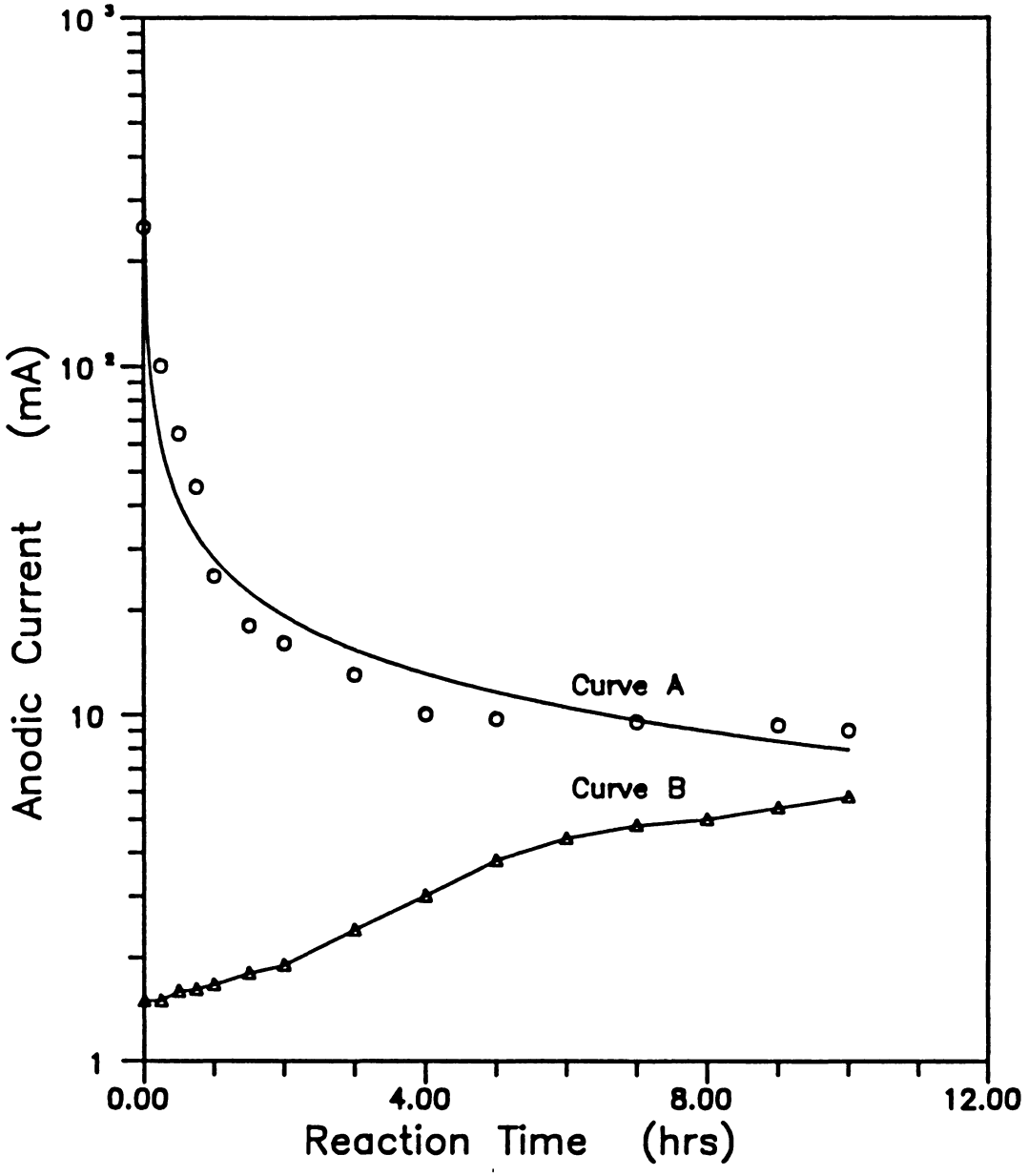

Figure 5. Current-Time Behavior of Widow Kennedy Seam Coal During EIL Treatment: Curve A = i-t behavior following acid soak for 24 hours. Curve B = i-t behavior without acid soak.

spent ions. Coughlin and Farooque (1979a) and Dhooge et al. (1982) were able to run coal-electrolysis experiments for over 100 hours with the current remaining at steady, non-zero values. After 10-25 hours of electrolysis, up to 90% of the current may be contributed by non-carbon dioxide forming organic reactions from dissolved coal products. The remaining 10% is caused by the direct oxidation of coal in contact with acid (Okada et al., 1981).

4.2 General Response of Different Coals to the EIL Process

4.2.1 Introduction

This section presents the results obtained by subjecting several different coal samples with the EIL process. Sulfuric and/or hydrochloric acids were used as electrolytes with or without the external addition of ferric ions. An electrochemical method was used to regenerate the spent electrocatalyst, which in this case was the Fe^{3+}/Fe^{2+} redox couple. Relatively coarse coals were used in these experiments, so that the processed coals could be washed on a screen to remove the liberated mineral matter.

The objective of this section is to discuss the potential application of the EIL process for a variety of coals. The experimental conditions necessary to produce the maximum removal of mineral matter from each of the coals tested varied from coal to coal. Several tests were conducted under different conditions to obtain the best ash removal results from each coal and only the results obtained under these conditions are reported. Unless otherwise noted, the experiments were not performed several times in order to provide an error analysis of the data, since the duration of each experiment was 2-3 days. Test results reported under other conditions are for the purpose of discussing trends in the cleanability of coals by the EIL process.

4.2.2 Glamorgan Seam Coal

A coal sample from the Glamorgan seam, assaying 1.65% ash and 0.6% sulfur, was tested in the stirred-tank reaction vessel (Figure 1). The experiments were carried out using a 3.6mol./ℓ sulfuric acid solution at 65°C. The coal was dry-screened into various size fractions and was pre-soaked for 12 hours prior to the treatment. A potential of 1.0V SCE was applied between the platinum working electrode and the SCE to regenerate the ferric ions. The results, shown in Figure 6, show that the percentage ash removal improved with decreasing particle size. A product coal assaying less than 0.8% ash could be obtained from a relatively coarse coal. Further tests were conducted by increasing the reaction time to 13 hours using a coarse (-16+20 mesh) and a fine (-100+140 mesh) fraction. As shown in Figure 7, the ash removal improved with increasing reaction time. The ash removal curve for the coarse coal flattened out after approximately 7 hours, while that for the fine coal continued to improve after 12 hours of treatment. However, the improvement became marginal after about 9 hrs.

Table 1 shows the results obtained with the finer size fractions of the Glamorgan coals using a 3.6mol./ℓ sulfuric acid solution and a potential of 1.0V SCE at 65°C. The -140+270 mesh coal had its ash content reduced from 1.25% to 0.4% after 4 hours of treatment. The -270+325 mesh coal had its ash content reduced from 1.23% to 0.32% after 10.5 hours of treatment. Coal recoveries (*i.e.*, recoveries of combustible material) are very high in both instances. The very modest power consumptions also shown in Table 1 are calculated for the electrochemical oxidation of ferrous ions to ferric.

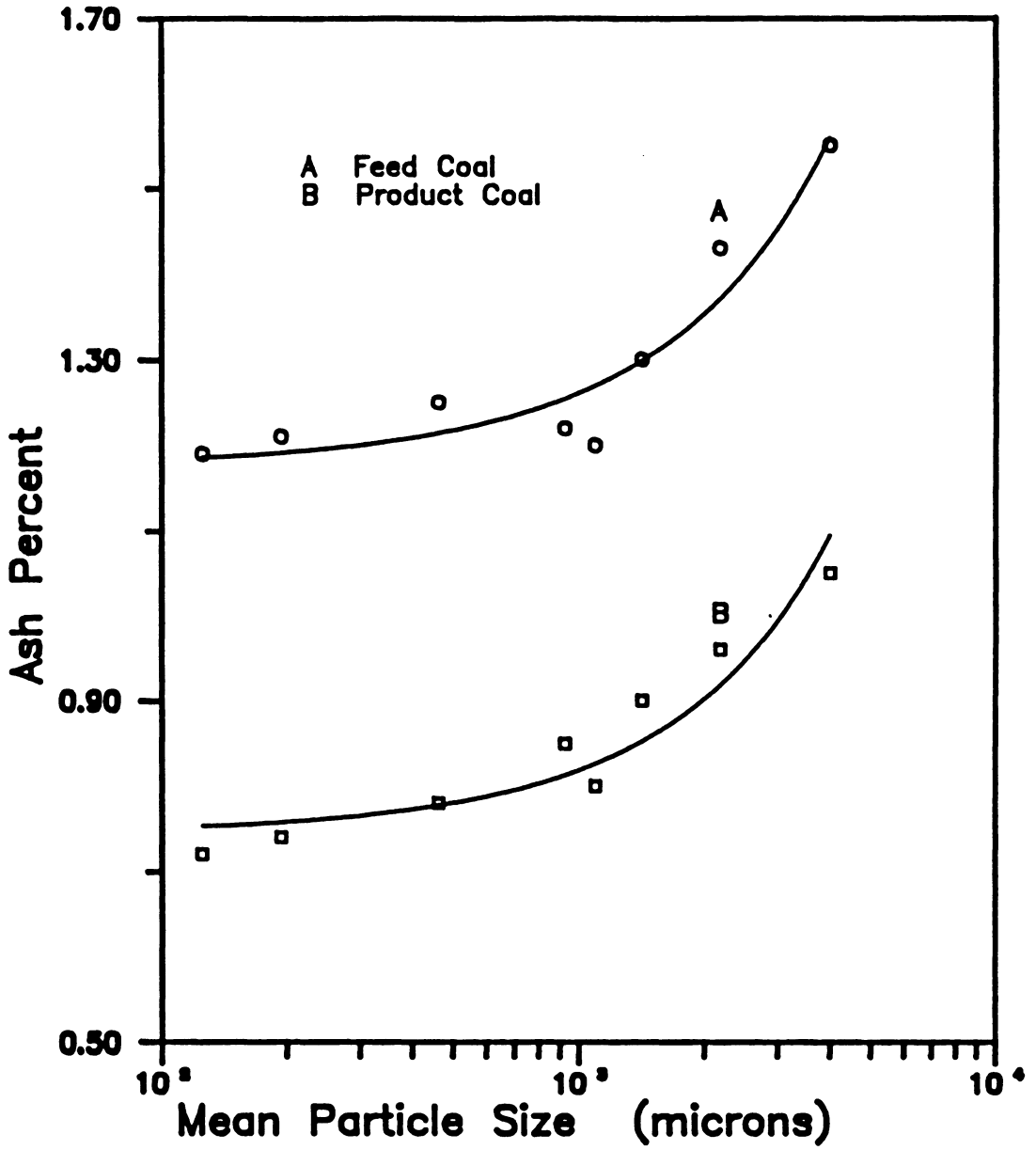

Figure 6. Effect of Particle Size on the Removal of Mineral Matter from Glamorgan Coal by the EIL Process: Electrolyte = 3.6M sulfuric, temperature = 65°C, treatment time = 4 hours, potential applied = 1.0V SCE

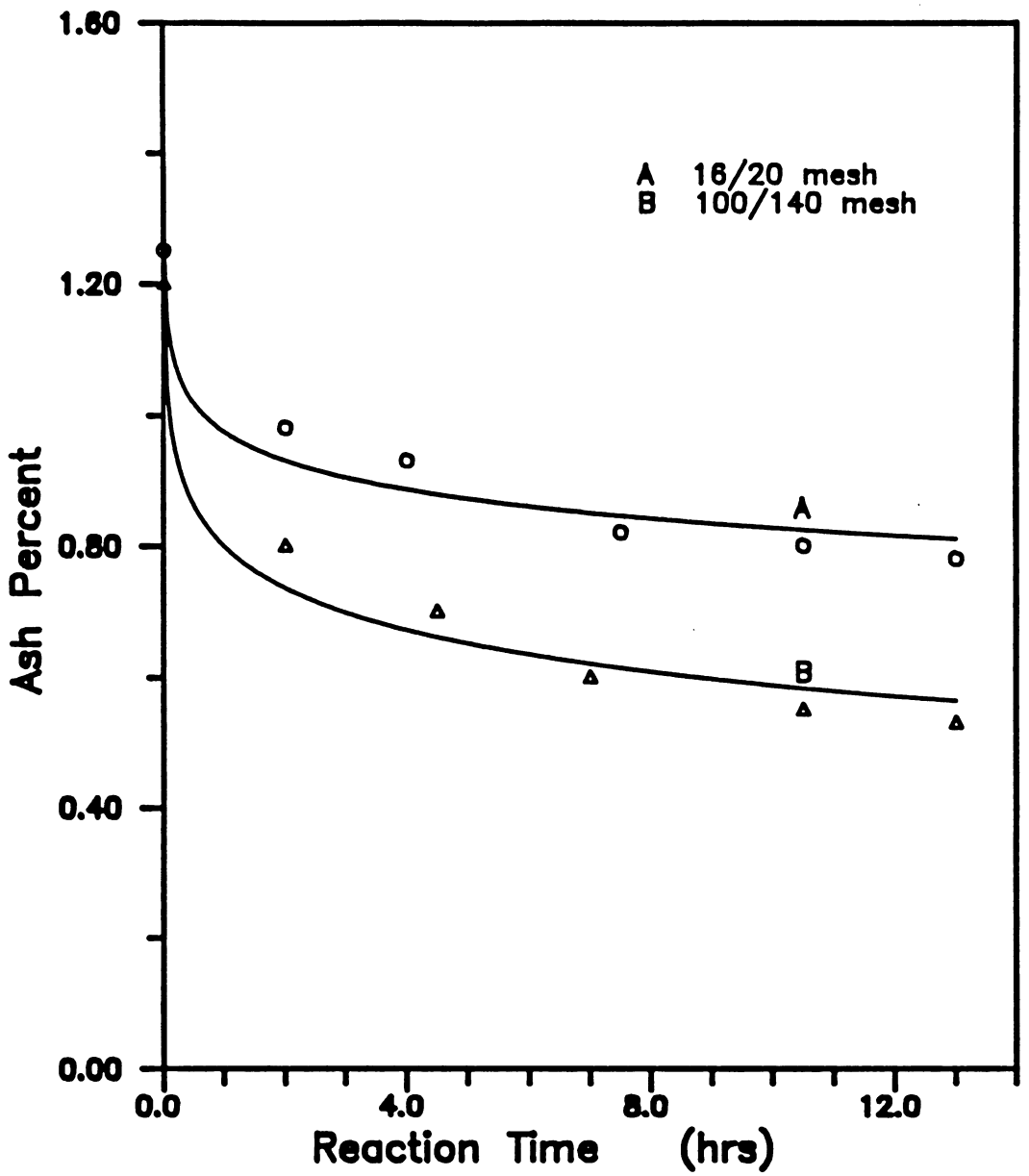

Figure 7. Effect of Reaction Time on the Removal of Mineral Matter from Glamorgan Coal by the EIL Process: Electrolyte = 3.6M sulfuric, temperature = 65°C, potential applied = 1.0V SCE

Table 1. Results of the EIL Treatment on Fine Sizes of Glamorgan Coal

Coal Size *(mesh)*	Reaction Time *(hours)*	Power Consumption *(Kwh/ton)*	Ash Content Feed *(% wt)*	Ash Content Product *(% wt)*	Coal Recovery *(% wt.)*
-140+270	4.0	1.81	1.25	0.40	98.26
-270+325	10.5	3.83	1.23	0.32	97.49

The effect of various acid electrolytes and electrolyte combinations on the removal of mineral matter was studied on relatively coarse sizes of Glamorgan coal. Starting with 3.6M sulfuric acid, the coal was cleaned down to 1.06% ash from 1.45%. An electrolyte containing 1.5M/ℓ sulfuric acid and 0.5M/ℓ hydrochloric acid reduced the ash content of the coal to 0.96%. The ash removal improved further when a solution of 3.4M/ℓ sulfuric and 1.1M/ℓ of hydrofluoric acid was used as an electrolyte. The addition of 10^{-3}M/ℓ of ferric sulfate monohydrate to this electrolyte reduced the ash content of the treated coal further down to 0.57%. When the temperature was increased to 80°C from 60°C, the product coal assayed 0.51%. The reaction time employed for all of these tests was 4 hours and the results represent the mean of two to three repetitions of each test. The mixture of sulfuric and hydrofluoric acid proved to be the best electrolyte for this coal. Further, the addition of ferric ions improved the removal of the mineral matter from the feed coal.

Table 2. Effect of Various Electrolyte Combinations on the EIL Treatment of Glamorgan Coal

Coal Size *(mesh)*	Electrolyte Used	Reaction Temperature *(°C)*	Ash Content Feed *(% wt)*	Ash Content Products *(% wt)*	Coal Recovery *(% wt)*
-07+12	H_2SO_4 (3.6M)	60	1.45	1.06	98.6
-20+60	1.5M H_2SO_4 + 0.5M HCl	60	1.28	0.96	96.5
-20+60	3.4M H_2SO_4 + 1.1M HF	60	1.28	0.73	96.0
-20+60	3.4M H_2SO_4 + 1.1M HF + 10^{-3}M $Fe_2(SO_4)_3$	60	1.28	0.57	96.8
-20+60	3.4M H_2SO_4 + 1.1M HF + 10^{-3}M $Fe_2(SO_4)_3$	80	1.28	0.51	96.2

Tests similar to those described above were conducted with coarse sizes of Glamorgan coal with the flow-through reactor and dilute sulfuric acid as electrolyte (pH 3.0). Platinum electrodes were used and a 1.0V SCE potential was applied for a 7 hour reaction period. Table 3 shows the results of these tests. The ash content of the feed coal was reduced from 1.65% to 0.89% with 7 hours of treatment at 65°C. The BTU content of the coal was unchanged by the treatment and the sulfur content decreased slightly. Table 3 also shows that the sulfur content of the coal was reduced by 3.33%. However, in coal analysis, sulfur is usually associated with the coal and hence, the removal of mineral matter from coal always results in an apparent *increase* in the sulfur content of the treated coal. In view of this, the small decrease in the sulfur content of the treated Glamorgan coal indicates that the actual amount of sulfur removed may be significant.

Table 3. EIL Treatment of Glamorgan Coal with the Flow-Through Cell

Coal Size *(mesh)*	Reaction Temperature *(°C)*	Ash Content Feed *(% wt)*	Ash Content Product *(% wt)*	Sulfur Content Feed *(% wt)*	Sulfur Content Product *(% wt)*	Coal Recovery *(% wt)*
-7+10	25	1.65	1.02	0.60	0.58	95.3
-7+10	65	1.65	0.89	0.60	0.59	93.7

To summarize, the EIL process reduced the ash content of Glamorgan coal from 1.2% to almost 0.3% with a coal recovery of over 95%. The removal of mineral matter improved with decreasing particle size, provided suitable separation methods were employed to separate the liberated mineral matter from the coal. The most suitable electrolyte for this coal was a mixture of sulfuric acid (3.4M) and hydrofluoric acid (1.1M) with 10^{-3}M of ferric sulfate. An extended reaction time provided better ash liberation although the bulk of the mineral matter was removed during the first six hours of treatment.

4.2.3 Widow Kennedy Seam Coal

The coal sample from the Widow Kennedy seam was first crushed and wet-screened to different size fractions. The -20+40 mesh fraction of the coal, assaying 23.4% ash, was treated by the EIL process using 3.6 mol./ℓ sulfuric acid solution in the stirred-tank reaction vessel at 65°C. The working electrode used in these experiments was a graphite rod held at 1.0V SCE. Table 4 shows the results of two sets of experiments. In one, the coal was treated continuously for 15 hours. In the other, the feed coal was treated in three consecutive stages of 5, 6 and 4 hours each, for a total of 15 hours. After each

stage of treatment, the coal was placed on a 40 mesh screen and sprayed with water to remove the liberated mineral matter.

Table 4. Effect of Multi-stage EIL Treatment on Widow Kennedy Coal

No of Stages	Reaction Time *(hours)*	Ash Content Feed *(% wt)*	Ash Content Product *(% wt)*	Coal Recovery *(% wt)*
1	15	23.4	8.5	95.5
3	5,6,4	23.4	3.5	94.6

The results show that the single-stage treatment reduced the ash content from 23.4% to 8.5% while the multi-stage treatment reduced it to 3.5% although both employed a 15 hr. reaction time span. During the multi-stage operation, the water-washing step between each reaction stage probably flushed away some or all of the reaction inhibitors discussed in section 4.1.3. More importantly, each water-washing step replaced the bulk acid surrounding the coals with fresh water, increasing the aqueous activity outside the coal particles. The difference in concentration between the solution outside a coal crevice and inside would now be larger than when the coal remained in the acid solution. This in turn would increase the osmotic pressures inside the coal crevices and enhance the removal of mineral matter. During the multi-stage operation described, this phenomenon would occur three times instead of just once, as in the single-stage operation, accounting for the improved mineral liberation from a multi-stage operation. The EIL process may therefore be applied in several stages for improved mineral liberation from this particular seam of coal.

In another set of experiments, the -3+7 mesh fraction of the Widow Kennedy coal was cleaned of its mineral matter in a laboratory scale dense medium bath to obtain a

float product coal assaying 5.3% ash. This cleaned coal was treated by the EIL process using the flow-through reactor (Figure 2 on page 45). The test was carried out using 2.4M and 3.6M sulfuric acid solutions at ambient temperature. The reaction time was 7 hours and a potential of 1.0V SCE was applied to a platinum electrode to regenerate the ferric ions. The results, given in Table 5 show that the EIL process also works on relatively coarse coal producing a low ash coal.

Table 5. Results of the EIL Treatment on a Coarse (-3+7 mesh) Widow Kennedy Coal Using the Flow-through Reactor.

Sulfuric Acid Concentration *(mol/ℓ)*	Ash Content *(% wt)*		Coal Recovery *(% wt)*
	Feed	Product	
2.4	5.3	1.01	98.2
3.6	5.3	0.99	98.1

More importantly, these experiments demonstrate that it is not necessary for coal particles to contact the electrodes for the EIL process to work. The most important part of the process is to continuously provide ferric ions to the coal surface. Regenerating the spent ions in the absence of the coal may be more efficient than doing it in the presence of coal because it can avoid the oxidation of the coal during the oxidation of the ferrous ions.

Table 6. Effect of Potential on the EIL Treatment of a -20 + 40 mesh Widow Kennedy Coal

Applied Potential *(V SCE)*	Charge Passed *(coulombs)*	Ash Content Feed *(% wt)*	Ash Content Product *(% wt)*
0.5	102.1	23.4	21.6
1.0	525.2	23.4	15.9
1.3	6125.7	23.4	14.7

Tests were conducted to determine the effect of the applied potential on the liberation of mineral matter from this coal. Platinum mesh electrodes were used and the tests were conducted using -20+40 mesh coal particles in an electrolyte containing 0.5M/ℓ hydrochloric and 1.5M/ℓ sulfuric acid at a temperature of 60°C. The tests were run at three different potentials, *i.e.*, 0.5, 1.0 and 1.3 volts SCE, and a 5-hour reaction time was employed in each of the experiments. The results show that the tests run at 0.5V SCE produced markedly inferior results that those run at higher potentials. Since the reversible potential of the Fe^{3+}/Fe^{2+} couple is around 0.77V SCE, the poor results obtained below this potential can be attributed to the lack of Fe^{3+} in solution. Increasing the potential beyond 1.2V SCE did not improve the mineral liberation significantly, as shown in Table 6. It is likely that at this potential, the coal itself was being directly oxidized during collisions with the electrode as shown by the over ten-fold increase in the amount of charge passed. This was also observed in the literature (Taylor et al., 1985). The competitive oxidation of the coal with the ferric ions may reduce the rate of regeneration of the spent ions which indirectly affects the mineral matter removal by the EIL process.

4.2.4 Powell Mountain Coal

A sample of Powell Mountain coal, assaying 2.6% sulfur and 9% ash, was treated with the EIL process as before, but without the addition of any acid. The test was conducted in distilled water at 65°C. A graphite electrode at 1.0 V SCE was used to regenerate the ferric ions. With this coal containing a large amount of sulfur, sufficient sulfuric acid and ferric ions would be generated from the electrochemical dissolution of the coal pyrite, as evidenced by the corresponding decrease in the solution pH. The EIL test was carried out in three successive stages with reaction times of 3, 5 and 8 hours each. The slurry was filtered after each stage and the filtrate was saved while the coal was wet-screened to remove the liberated mineral matter. The saved filtrate from each of the previous stages was used in the subsequent stages. The currents were very low in the first stage, indicating slow reaction rates. After each stage, the currents increased as the amount of ferric ions accumulated in solution, possibly through the oxidation of pyrite in the anodic environment of the EIL process via an autocatalytic pathway (Lalvani and Shami, 1986). The results, given in Table 7, show that the ash content of the coal was reduced from 8.2% to 5.3%.

Table 7. Removal of Ash & Sulfur from Powell Mountain Coal Without Using Acids

Particle Size *(mesh)*	Ash Content Feed *(% wt)*	Ash Content Product *(% wt)*	Sulfur Content Feed *(% wt)*	Sulfur Content Product *(% wt)*	Heating Value (MAF) Feed *(BTU/lb)*	Heating Value (MAF) Product *(BTU/lb)*
-60+100	8.4	5.7	2.7	2.0	14,832	14,854
-100+140	8.0	5.3	2.5	1.9	14,737	14,828

Although the ash removal was not as significant as when using acids, it is clear that the ash rejection was possible without using acids. It is likely that the pyrite contained in the coal sample undergoes anodic oxidation to yield a sufficient amount of ferric ions according to the reaction shown below.

$$FeS_2 + 8H_2O \rightarrow Fe^{3+} + 2SO_4^{2-} + 16H^+ + 15e^-$$

The ferric ions produced as such further oxidize the pyrite according to the reaction given below;

$$2Fe^{3+} + FeS_2 + 2SO_4^{2-} \rightarrow 3Fe^{2+} + 3SO_4^{2-} + 2S$$

These reactions have been well documented in the literature (see sec.2.2.2). The comparatively poor results may be due to the lack of counter-ions in the aqueous environment needed for the formation of an ionic double layer inside the pores and crevices of the coal. Further, chemical dissolution, if any, would be insignificant at the low acid strength.

4.2.5 Wyodak Seam Coal

The next coal tested was from the Middle Wyodak seam, assaying 4.7% ash and 0.44% sulfur. In one experiment, a -20+40 mesh coal sample was treated at 66°C for 5 hours using 3.6mol/ℓ of sulfuric acid and a potential of 1.0V SCE with platinum electrodes. The results are shown in Table 8. An excellent ash-rejection was obtained as the product coal assayed only 1.48% ash. In the next test, a fresh coal sample was treated using the filtrate obtained from the first test. After 5 hours of reaction time, the ash was reduced from 4.72% to 1.43%. These results indicate that in continuous operation, the reagent consumption can be minimized by recirculating the spent electrolyte.

Table 8. Removal of Ash & Sulfur from a -20+40 mesh Middle Wyodak Coal

Electrolyte Used	Ash Content (% wt)		Sulfur Content (% wt)		Heating Value (BTU/lb)	
	Feed	Product	Feed	Product	Feed	Product
3.6M H_2SO_4	4.72	1.48	0.44	0.63	10,413	10,947
Filtrate from above test	4.72	1.43	0.44	0.62	12,006	12,180

A coal sample (-60+150 mesh) from the Upper Wyodak seam, assaying 8.61% ash and having a calorific value of 9,189 Btu/lb, was tested with the EIL process for removal of mineral matter. The sample was treated first in a solution containing 0.5M/ℓ hydrochloric and 1.5M/ℓ sulfuric acid solution at 65°C using a platinum electrode at 1.0V SCE. After 7.5 hours of treatment, the coal was placed on a 150 mesh screen and washed of its liberated mineral matter. The washed coal, containing 5.2% ash was treated again with fresh electrolyte for another 7.5 hours under identical conditions. Table 9 lists the results of this test.

Table 9. Results of Repeated Processing on Upper Wyodak Coal

Test Stage	Reaction Time (hours)	Ash Content (% wt)		Sulfur Content (% wt)	
		Feed	Product	Feed	Product
1st.	7.5	8.61	5.19	1.5	1.5
2nd	7.5	5.19	2.26	1.5	0.5

The results show the second stage of treatment further reduced the ash from 5.19% to 2.3%. This is another example where a multi-stage treatment proved beneficial in obtaining a lower ash coal. It is likely that the EIL process removed the bulk of the non-sulfur bearing mineral matter in the first stage while the second stage removed sulfur-bearing mineral matter. This is shown by the decrease in ***both*** the ash and sulfur contents of the product coal in the second stage. Since the removal of the sulfur is dependent on the rate of pyrite leaching by the acid, it occurs at a slower rate as compared with the removal of ash, which occurs through the formation of ionic double layers and the development of an osmotic pressure. Further, the ash removal is too large to have been caused solely by the removal of pyritic sulfur.

4.2.6 Splashdam Seam Coal

A Splashdam seam coal (-20+40 mesh), assaying 8.8% ash, was treated by the EIL process at 68°C with 1.5 mol/ℓ sulfuric acid solution as electrolyte. A second test was conducted under identical conditions except that the electrolyte used in this test was a 3.6mol/ℓ solution of sulfuric acid. A third test was carried out under similar conditions by using a solution containing 0.5M/ℓ hydrochloric and 1.5M/ℓ sulfuric acid as electrolyte. The reaction time was 6 hours and a platinum electrode was used at a potential of 1.0V SCE. The results are given in Table 10.

Table 10. Effect of Electrolyte Concentration on the EIL Treatment of Splashdam seam Coal

Electrolyte Concentration *(mol/ℓ)*	Ash Content Feed *(% wt)*	Ash Content Product *(% wt)*	Coal Recovery *(% wt)*
H_2SO_4 (1.5M/ℓ)	8.8	2.5	96.2
H_2SO_4 (3.6M/ℓ)	8.8	1.5	95.7
HCl (0.5M/ℓ)	8.8	1.8	95.7
H_2SO_4 (1.5M/ℓ) + HCl (0.5M/ℓ)	8.8	0.9	93.6

The results show that the ash removal was improved at a higher sulfuric acid concentration for this particular seam. Of interest is the synergistic effect shown by the acid combinations of 0.5M hydrochloric and 1.5M sulfuric acid. When only 1.5M sulfuric acid was used in the EIL process, the product coal assayed 2.5% ash from a feed coal that assayed 8.8% ash. With 0.5M hydrochloric acid, the ash content of the product coals was reduced to 1.8%. However, the combination of the two acids at the same concentration in the EIL process reduced the ash content of the coal from 8.8% to 0.9%. Since this phenomenon was noticed with several other coals, this mixture of acids was used very frequently in the EIL process to obtain the optimum conditions for operating the EIL process.

4.2.7 Graphitic Anthracite

A graphitic anthracite sample, imported from Korea, containing 15% ash and 0.46% sulfur, was subjected to the EIL process. A particle size of -60+100 mesh was chosen for the tests with the stirred-tank cell (Figure 1 on page 44). The coal was

treated at 65°C in a mixture containing 0.5M/ℓ hydrochloric and 1.5M/ℓ sulfuric acid. A potential of 1V SCE was applied to a platinum mesh electrode to regenerate the ferric ions. After 3 hours of initial treatment, the coal was cleaned to 11.6% ash and 0.08% sulfur, as shown in Table 11. The cleaned coal was treated for a further 9 hours to obtain a coal containing 7.6% ash and 0.02% sulfur.

Table 11. Effect of Multi-stage EIL Treatment on a Graphitic Anthracite

Stage Number	Reaction Time *(hours)*	Ash Content *(% wt.)*		Sulfur Content *(% wt.)*		Coal Recovery *(% wt.)*
		Feed	Product	Feed	Product	
1	3	15.0	11.6	0.46	0.08	96.2
2	9	11.6	7.6	0.08	0.02	90.7

The results obtained with the EIL treatment of both the graphitic anthracite and the Elkhorn seam coal show that around 50% of the ash present in the feed coals was removed by the process along with coal recoveries of over 90%. Typical flotation results on -65+100 mesh coal rarely removes such a high degree of ash, mainly because flotation can remove only free mineral matter or coal-mineral composites, which would affect the coal recovery. Hence it is clear that some type of liberation of the mineral matter from the coal must take place in order to obtain the levels of ash rejection

4.2.8 Filter Cake Refuse

So far the EIL process was tested only with coals particles that fell into a selected size class. This was done to facilitate the separation of the coal from the liberated

mineral matter after the EIL treatment. The series of tests performed with a filter cake refuse was for the purpose of investigating the possibility of using the EIL process to recover a saleable product from plant refuse that is usually discarded. The refuse filter cake used in the following tests was obtained from the bulk flotation of Norton seam coal and assayed 44% ash. The coal sample contained a large amount of coal and mineral fines, from a visual observation. The electrolyte used was a solution containing 0.5M/ℓ hydrochloric acid and 1.5M/ℓ sulfuric acid. A potential of 1.0 V SCE was applied to a platinum electrode in the stirred-tank reactor. After 4 hours of treatment at 65°C., the coal was washed, dried and assayed for ash content. The results are shown in Table 12.

Table 12. Effect of EIL Treatment on Coal Plant Refuse

Sample Size *(mesh)*	Ash Content *(% wt)*		Coal Recovery *(% wt)*
	Feed	Product	
-400+0	44.0	9.32	52.0

The ash content of the refuse was reduced from 44.0% to 9.32% while the coal recovery was only 52%. Although 9.3% ash coal is not a superclean coal, the fact that 52% of the coal can be recovered from an extremely fine refuse is significant. The low recovery was due to the fact that the processed coal was cleaned of its liberated mineral matter by washing it on No.54 Whatman filter paper with an average pore size of 20-25μ. When the feed slurry was filtered through a similar filter paper without any EIL treatment, the product coal assayed 16.36% ash. Thus the EIL process must have caused some degree of liberation to occur, where the fines produced were small enough to pass through the filter paper. Furthermore, the mean particle size of the low

temperature ash obtained from Norton seam coal was less than 10μ. Thus it is possible that the EIL process caused the liberation of these microscopic mineral particles from the fine coal particles present in the filter cake refuse. Although some coal may have been lost by the post EIL wet-screening operation, it appears both by visual observation and analysis that the bulk of the material removed by the wet-screening stage contained most of the ash-forming minerals. A higher recovery would have been obtained if the processed coal had been cleaned of its liberated mineral matter using a process such as froth flotation or oil agglomeration before and after the EIL process. This is investigated with an Upper Freeport coal in section 4.3.

4.2.9 Kemmerer Seam Coal

A series of EIL tests were conducted on an Adaville No.1 sub-bituminous coal from the Kemmerer mine, Wyoming. A -20+60 mesh sample and a -200+325 mesh sample were treated using the acid mixture containing 5M/ℓ hydrochloric and 1.5M/ℓ sulfuric acid and a potential of 1V SCE. The treatment time was 12 hours at 65°C. Further tests were carried out by doping the electrolyte with ferric ions (from ferric sulfate monohydrate) to study the effect of ferric ion concentration on the removal of ash from the -200+325 mesh samples of this coal. The results are shown in Table 13.

Table 13. Results of the EIL tests conducted on Kemmerer Seam Coal

Coal Size *(mesh)*	Electrolyte Used	Ash Content Feed *(% wt)*	Ash Content Product *(% wt)*	Sulfur Content Feed *(% wt)*	Sulfur Content Product *(% wt)*	Coal Recovery *(%)*
-20+60	0.5M HCl+1.5M H_2SO_4	5.7	2.3	0.34	0.40	93.6
-200+325	0.5M HCl+1.5M H_2SO_4	3.6	1.5	0.33	0.38	95.9
-200+325	0.5M HCl+1.5M H_2SO_4 + 10^{-4}M Fe^{3+}	3.6	1.4	0.33	0.34	93.8
-200+325	0.5M HCl+1.5M H_2SO_4 + 10^{-2}M Fe^{3+}	3.6	1.5	0.33	0.39	95.1

The ash content of the -20+60 mesh coal was reduced from 5.7% to 2.3% while the sulfur content increased slightly. With the -200+325 mesh coal, the product coal assayed 1.5% ash with a coal recovery of 95.9%. When the tests were repeated under identical conditions, but with 10^{-4}M ferric ions added to the electrolyte, the product coal still assayed around 1.5% ash. Even when the ferric ion concentration was increased to 10^{-2}M, the product coal did not show any improvement in its ash rejection. These results indicate that the addition of the ferric ion electrocatalyst did not appear to have much effect on the removal of ash from the Kemmerer seam coal. However, since the results are comparable with the test results obtained from other coals, it is possible that with this coal, the presence of the acid was sufficient to cause the surface oxidation and the ensuing formation of the double layers inside the pores and cavities of the coal.

4.2.10 Upper Freeport Seam Coal

An Upper Freeport coal (-28 mesh x 0), assaying 24.5% ash and 1.68% sulfur, was treated with the EIL process using 2 mol/ℓ hydrochloric acid solution for 5 hours. The ferric ions were regenerated on a platinum electrode at 1.0 V SCE. After the initial 5-hour treatment, the processed coal was washed of its liberated mineral matter on a 400 mesh screen which unfortunately allowed most of the fine coal to pass through as well.

Table 14. Results of the EIL tests conducted on Upper Freeport Coal

Stage Number	Reaction Time *(hours)*	Ash Content *(% wt)*		Sulfur Content *(% wt)*		Coal Recovery *(%)*
		Feed	Product	Feed	Product	
1	5	24.5	7.7	1.71	0.64	65
2	5	07.7	3.7	0.64	0.63	86

The product coal obtained by the EIL treatment assayed 7.7% ash and 0.64% sulfur, as shown in Table 14. The recovery was relatively low (65%) because a significant amount of the fine coal particles passed through the 400 mesh screen along with the liberated mineral matter. The coal was treated in the second stage in the same manner; the ash content was further reduced to 3.7%, but the sulfur content remained about the same. The coal recovery was higher (86%) because most of the fines had already been removed in the first stage.

4.2.11 Elkhorn Seam Coal

A relatively high-ash coal from the Elkhorn seam assaying 13.87% ash was obtained from the United Coal Co., VA, along with a lower ash coal from the Elkhorn #3 seam from the Consol Coal Co., PA. To avoid confusion, the latter will be referred to as Consol Coal, while the former as Elkhorn seam coal.

The Elkhorn seam coal was treated with the EIL process at 65°C. using 3.6mol/ℓ sulfuric acid at a potential of 1.0V SCE. Two different size fractions of this coal were tested by the EIL process.

Table 15. Results of the EIL Treatment of Elkhorn Seam Coal

Particle Size *(mesh)*	Ash Content Feed *(% wt)*	Ash Content Product *(% wt)*	Coal Recovery *(% wt)*
-20+60	13.87	8.01	92.7
-60+100	12.01	7.74	91.3

The results shown in Table 15 indicate that a product coal containing 7.74% ash may be obtained from this feed coal with high coal recoveries. The ash removal improved with decreasing particle size as expected.

The sample of coal obtained from the Consol Coal Co., assayed 7.92% ash at a particle size of -12+16 mesh. This was subjected to the EIL process at 55°C. The electrolyte contained 0.5M/ℓ hydrochloric and 1.5M/ℓ sulfuric acid. The ash content of the feed coal was reduced from 7.92% to 1.25% in 5.5 hours. This is shown on Figure 8. The removal of ash becomes marginal after about 5 hours.

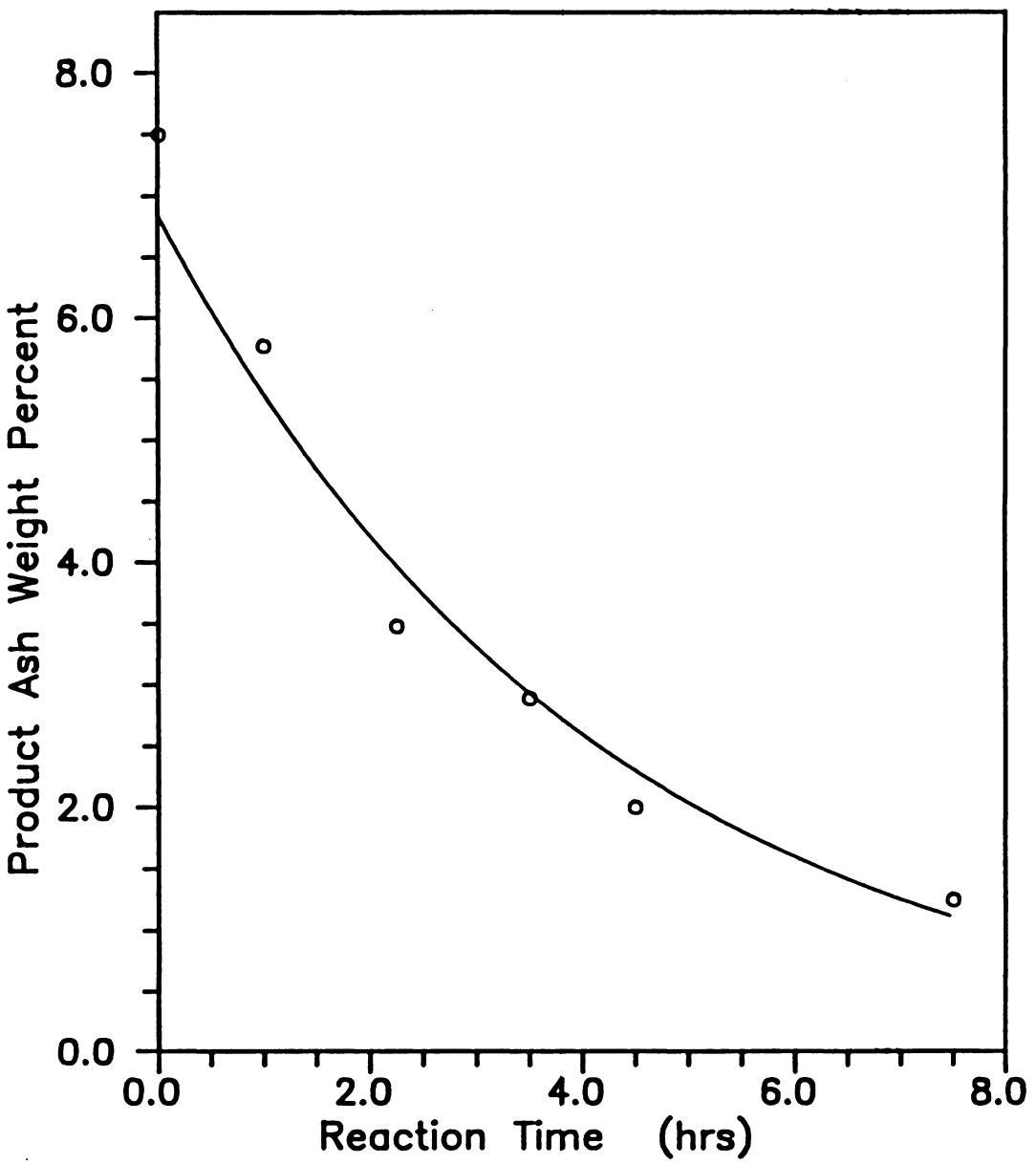

Figure 8. Effect of Reaction Time on the Removal of Mineral Matter from Consol Coal

4.2.12 General Discussion

Since coal is highly heterogeneous and its properties may vary even within a given seam, the results are specific for the coals studied and will not necessarily be representative of other coals. However, the results from the range of coals studied do permit some cautious generalizations.

The best coal-cleaning results obtainable with the EIL process are summarized in Table 16. The type and rank of the feed coal (if known) is given alongside, while further information on the coal is available in the Appendices.

Table 16. Summary of Coal Cleaning Results from the EIL Process

Coal Seam	Rank	Ash Content (wt %) Feed	Product	Percent Removal	Percent Recovery
Glamorgan	bituminous	1.2	0.3	74.2	97.5
Widow Kennedy	bituminous	23.4	3.5	85.1	90.3
Powell Mtn.	bituminous	8.0	5.3	33.7	91.2
Middle Wyodak	subbituminous	4.7	1.4	69.7	89.9
Upper Wyodak	subbituminous	8.6	2.3	73.7	92.3
Splashdem	bituminous	8.8	0.9	89.8	93.6
Graphitic Anthracite	Anthracite	15.0	7.6	49.3	87.2
Kemmerer	subbituminous	3.6	1.4	61.1	93.8
Upper Freeport		24.5	3.7	84.9	56.0
Elkhorn	bituminous	13.8	7.7	44.2	84.6

Most of the coals responded favourably to the EIL treatment, although some did better than others. Optimum conditions for the treatment varied from coal to coal, but all coals showed an improvement in the ash liberation with decreasing particle size and reaction temperature.

The results, in general, show that the recoveries of combustible materials are exceptionally high in nearly all of the cases. During multi-stage processing of coals that were difficult to clean, a trade-off occurs between improved ash removal and decreased recovery. The high recoveries of combustibles suggests that the liberation of minerals from coal by the EIL process should proceed via a highly efficient process. With conventional liberation processes, which rely on size reduction, the mineral liberation may be due to random fracture, resulting in the production of a large amount of composite particles (or middlings). Since the EIL process produces only a minimum of fines (as evidenced by high coal recoveries and the visible absence of fine coal during processing), it is likely that the process induces fracture primarily along grain boundaries, which helps minimize the production of composite particles to improve coal recovery.

From the data available on the feed coals tested, there appears to be no correlation between the type of coal and its response to the EIL treatment. In general, most of the low-rank coals responded readily to the EIL treatment to produce clean product coals. A possible reason may be the higher moisture contained in the pores and crevices of these coals that permits the rapid migration of ions during the initial stages of the EIL process to form ionic double layers. However, good coal cleaning results were also obtained with the graphitic anthracite, whose moisture content was lower than that of the low rank coals. The reasons for the different responses of coals to the EIL treatment may therefore be more complex and dependent on a several other variables, requiring further investigation.

The results presented are only those of coals that responded favourably to the EIL process. However, out of the several coals tested, some did not show any reduction in ash and sulfur content when treated by the EIL process. The response of these coals were only marginally improved even when the conditions of the EIL treatment were

made severe by using higher acid concentrations (up to 5.0 M/ℓ), higher temperatures (up to 80°C) etc. Table 17 shows some of the typical coal cleaning results obtainable from the coals that did not respond well to the EIL process. In some cases, the addition of ferric ions did not improve the ash rejection of the coal tested.

Table 17. Coals with Limited Response to the EIL Process

Coal Seam	EIL Process Conditions			Ash Content		Percent Removal
	Temperature	Electrolyte	Added Fe^{3+}	Feed	Product	
Sahara	80°C	5M H_2SO_4	none	6.59	6.32	4.1
Sahara	80°C	1M H_2SO_4	4mM/ℓ	6.59	5.24	20.5
Norton	75°C	5M H_2SO_4	none	4.63	4.02	13.2
Blair	80°C	1M H_2SO_4	4mM/ℓ	6.59	5.24	20.5
Splashdem	31°C	1M H_2SO_4	none	44.24	28.87	34.74
Splashdem	31°C	1M H_2SO_4	1mM/ℓ	44.24	27.92	36.88

The ash removal results shown in Table 17 indicate that the EIL process was not very effective in removing much of the mineral matter from these coals. The Sahara seam coal, which originated from the Illinois #6 seam, showed hardly any cleanability with the EIL process within the range of testing. Valid reasons for this behavior are not known as this point.

With the run-of-mine, high-ash Splashdem seam coal (which was unlike that tested in section 4.2.6), the addition of ferric ions barely improved the removal of mineral matter as compared with the removals obtained without the addition of ferric ions. Furthermore, these coals did not show any significant difference when they were treated solely with acid (*i.e.*, no potential was applied to regenerate the spent ferric ions). Several reasons may account for this unexpected behavior. Firstly, the feed coals

assayed 44.24% ash and it is possible that the bulk of the ash removal from 44.24% down to 28.87% may ***not*** have been caused by the EIL mechanism as most of the mineral matter was in the free state. The decrease in ash content may have been caused by the dissolution of acid-soluble minerals present in the free state. Secondly, the feed coal was run-of-mine and the test sizes were obtained by dry screening and thus the feed coal would have contained fine particles of dust and mineral matter as adherents on the coal surface. These adherents are seldom removed by dry screening, but would have been removed by the wet-screening stage following the EIL treatment. Thirdly, the EIL process is most efficiently used when it is used to clean coals that have been pre-cleaned to remove all liberated mineral matter and it is with such coals that its effects are clearly seen. While it is suspect that the acids present in the system may be responsible for the removal of ash by dissolution, it is again unlikely since the majority of the mineral matter present in coal is not soluble in acid under the conditions of the EIL process (Fan et al., 1984b). Furthermore, the theory of fluid flow through a porous, anisotrophic material such as coal indicates that purely diffusion controlled migration of a fluid into the porous medium will ***not*** take place without an external driving mechanism (Marcus, 1962). Further work discussed in section 4.8 addresses the issue of acid dissolution of the mineral matter.

4.3 The EIL Process Combined with Microbubble Flotation

4.3.1 Introduction

Although the EIL process can remove mineral matter from coal, the extent of the removal was limited by the simple wet-screening separation technique employed. The screens could only separate liberated particles that were smaller than the screen aperture and hence, any liberated mineral matter that was coarser than the screen aperture could not be separated by the wet-screening process. In such a situation, the EIL process followed by a wet-screening step would not show the full extent of liberation occuring during the process. It was, therefore, necessary to test the EIL process in conjunction with another separation technique such as microbubble flotation that can remove both coarse and fine liberated mineral matter.

4.3.2 Upper Freeport Coal

A sample of Upper Freeport coal assaying 24.5% ash and 1.68% sulfur was processed in combination with froth flotation and the microbubble flotation process. The -28×0 mesh coal was initially subjected to froth flotation using a Denver laboratory flotation machine. After two stages of flotation, consuming 1.0lb/ton of kerosene and 0.2lb/ton Dowfroth M-150, a clean coal product assaying 4.8% ash with 82.8% recovery was obtained. The clean coal product was pulverized for 15 minutes in an attrition mill to

liberate the finely disseminated mineral matter. The mill product was subjected to four stages of batch microbubble flotation tests, consuming a total of 1.0lb/ton of kerosene and 4.0lb/ton of Dowfroth M-150. The ash content of the coal was reduced to 1.8% with 73.2% recovery.

The cleaned coal product from the microbubble flotation test was then subjected to the EIL process. It was treated in 2.0 mol/ℓ hydrochloric acid solution for 4 hours in the stirred-tank reactor. After the treatment, the coal slurry was subjected to single-stage microbubble flotation using 1.0lb/ton of kerosene and 0.6lb/ton of Dowfroth M-150. The cleaned coal product obtained as such assayed 1.16% ash, and the coal recovery was 82% for the microbubble flotation step as shown in Table 18.

Table 18. EIL Treatment on Upper Freeport Coal with Microbubble Flotation

Stage Number	Process	Ash Content Feed	Ash Content Product	Recovery per Stage
1	2 Stage Froth Flotation	24.50	4.80	82.8
2	Attrition Grinding and 4-Stage Microbubble flotation	4.80	1.80	73.2
3	EIL treatment and single stage microbubble flotation	1.80	1.16	82.0

These results indicate that when processing a feed coal containing a large amount fines, it is imperative that no size-based separation technique such as wet-screening be used during the post EIL stage. Failure to do this resulted in low recoveries, as shown in Sections 4.2.8 and 4.2.10. Improved results may have been obtained if a flotation technique had been used in all of the cases. Furthermore, the results confirm that the

EIL process essentially liberates mineral matter from coal, since the feed coal to the EIL process is free of all liberated mineral matter. This is an excellent example where the EIL process can be used efficiently to extend the range of coal cleaning. With several stages of combined EIL treatment and microbubble flotation, it will be possible to produce superclean or even ultraclean coals with high coal recoveries.

4.4 *EIL Treatment without Regeneration of Ferric Ions*

In the examples presented earlier, the ferric ions were regenerated by oxidizing the ferrous ions on the surface of a graphite or platinum electrode held at a potential of 1.0V SCE. However, it was considered that by providing a sufficiently large amount of ferric ions in the system, the EIL process could be as effective without the use of an electrode and an applied potential. To demonstrate this effect, a set of simple ferric-ion leaching experiments was carried out using relatively concentrated solutions of ferric sulfate on three different coal samples. The typical amounts of Fe^{3+} added during the EIL process were in the order of $10^{-3}M/\ell$, with electrolytic regeneration. Since no regeneration was to be employed in this set of tests, the amounts of Fe^{3+} added was increased by 3 orders of magnitude to provide a sufficient number of ferric ions to react with the coal.

Three samples of coal from the Norton, Splashdam and Blair seams were used in these tests. In each test, a 20-gram sample was mixed with 100 ml of 1.0M ferric sulfate solution and left in a water bath at 65°C. To prevent the breakage of the coal particles, no mechanical stirring was used, except for occasional agitation by hand. After 12 hours of treatment, the coal samples were wet-screened by hand using plenty of water to wash off any ferric sulfate crystals adhering to the coal. The liberated ash particles passed through the screen while the coal particles were retained on the screen; the Norton seam coal was washed using a 230 mesh screen, while the Splashdam and Blair seam coals were washed using a 200 mesh screen. The products remaining on the screen were then subjected to simple skin flotation in which the coal particles floating on the surface of the water were carefully skimmed off and analyzed. The cumulative ash contents and recoveries of the coals are given in Table 19.

Table 19. Results of the EIL Treatment without Ferric Ion Regeneration.

Product	Norton Seam (-100+230 mesh)		Splashdem (-80+200 mesh)		Blair (-140+200)	
	Ash%	*Recovery*	*Ash%*	*Recovery*	*Ash%*	*Recovery*
Float	3.3	14.7	1.8	34.3	1.2	50.7
Screen	12.7	71.4	2.5	92.5	1.7	99.3
Feed	16.9	100.0	3.6	100.0	2.0	100.0

Although the extent of ash removal was not as good as those obtained under applied potential conditions as in the EIL process, the results nevertheless demonstrate that ferric ions are mainly responsible for the liberation in these series of tests, particularly since no acids were used in the tests. The concentrated ferric solution provided a large number of ferric ions to react with the sessile bonds in the coal, but these ions, once reacted, remained as ferrous ions in solution since no regeneration techniques were used. The ferrous concentration will affect the ferric reduction by causing reaction [1.1] to reverse. More importantly, the ferric/ferrous ion ratio will decreased and this is known to affect the kinetics of any ferric-ion leaching operation (Dutrizac and MacDonald, 1974). This situation may be contrasted with the case where these ions are oxidized back to ferric *in-situ* by, for example, an electrode as in the EIL process. The ferric/ferrous ratio will now be maintained at an optimum value. Further, the regeneration step prevents the accumulation of ferrous ions that could interfere with the free migration of ferric ions to the reaction sites on the coal surface.

Secondly, the presence of a large amount of ferric or ferrous ions results in a form of chemisorption of these compounds on the coal surface. When the samples were washed with tap water during the wet-screening stage, the high pH ($\simeq$ 5-6) of tap water may cause the ferric or ferrous to precipitate as $Fe(OH)_3$ or $Fe(OH)_2$ on the coal

surface, which would report as ash when the product coal was assayed. These adherents may be removed only by a laborious procedure involving several stages of soaking and washing with water or strong acid treatment. The use of a dilute solution of ferric ions coupled with continuous regeneration of the spent ions (as in the EIL process) provides the same effect while eliminating the difficult step of removing the chemisorbed iron compounds from the surface of the coal.

4.5 Comparison of the EIL Treament with Ferric Leaching

4.5.1 Introduction

The previous section discussed the possibility of operating the EIL process without the application of an oxidizing potential to regenerate the spent ferric ions. This was achieved by utilizing concentrated solutions of ferric ions in the process. Qualitatively, it was possible to remove a portion of the ash present in the coal by this method. This section presents the results of a few tests that compare the efficiency of ash removal by this method with the usual EIL process (*i.e.*, when the ferric ions are regenerated using a potential).

4.5.2 Taggart Seam Coal

A coal sample from the Taggart seam assaying 1.66% ash and 0.6% sulfur was treated with an acidified solution of 1.0mol/ℓ ferric sulfate solution and the solution was acidified with 1.0mol/ℓ sulfuric acid solution. The particle size of the coal used for these tests was -140+200 mesh and the coal was mixed with the acidified ferric sulfate solution to make up a slurry containing 10% solids. The reaction was carried out at 65°C in the stirred tank reaction vessel. No attempt was made to regenerate any of the spent ferric ions. Samples of the treated coal were withdrawn at various time intervals ranging from 3 to 7 days. The treated coal samples were wet-screened several times with excess water

to remove liberated mineral matter as well as any ferric sulfate adhering to the coal particles. The samples were analyzed for ash and sulfur after being dried completely in an oven.

A sample from the same feed coal was treated with the EIL process under identical conditions as before, except that no ferric solutions were used. The treatment was carried out for 18 hours with 1.0mol/ℓ at a potential of 1.0V SCE after which the treated coal was wet-screened, dried and analyzed for ash content. Figure 9shows the percent ash removal of the product coal with time of treatment for the ferric sulfate leach and the EIL process. At the end of 7 days, 26.5% of the ash had been removed by leaching with ferric sulfate. In contrast, the EIL process removed 35.5% of the ash in 18 hours.

Similar tests were conducted with a pre-cleaned Norton Seam Coal assaying 8.0% ash and 1.47% sulfur. The feed coal had to be treated for several days in a solution containing 1.0M/ℓ sulfuric acid and 1.0M/ℓ ferric sulfate solution to effect a significant reduction in its ash content. As Figure 10 shows, the ash and sulfur content of the product coal at the end of 35 days was 5.5% and 1.19% respectively. The identical coal, when treated with the EIL process for 16 hours at 1.0V SCE with an electrolyte consisting of only of 1.0M/ℓ sulfuric acid resulted in a product coal assaying 4.04% ash and 1.31% sulfur. The only difference between these two processes was the application of a potential for the regeneration of ferric ions. More importantly, the regeneration of the ferric ions maintains the Fe^{3+}/Fe^{2+} ratio as high as possible. During the simple ferric leaching process, the ferric ions react with the *free* pyrite in the coal. In addition, the ferric ions may diffuse through the coal matrix and react with the pyrite entrapped between coal macerals. The diffusion of both reactants and products through the pore structure of coal in a ferric sulfate leaching operation is known to be rate limiting (Shimada et al., 1984). As such, the authors found that the reaction times typical for 30-50% removal of mineral matter was $\simeq$96 hours. This may be contrasted with the EIL

process where the removal is effected by the osmotic pressure inside the coal matrix and thus, the reaction times are decreased by over 50%.

From these two examples it can be seen that mineral removal by the EIL process is not solely due to ferric or acid leaching, although a certain portion of the minerals removed from the coal may be attributed to this.

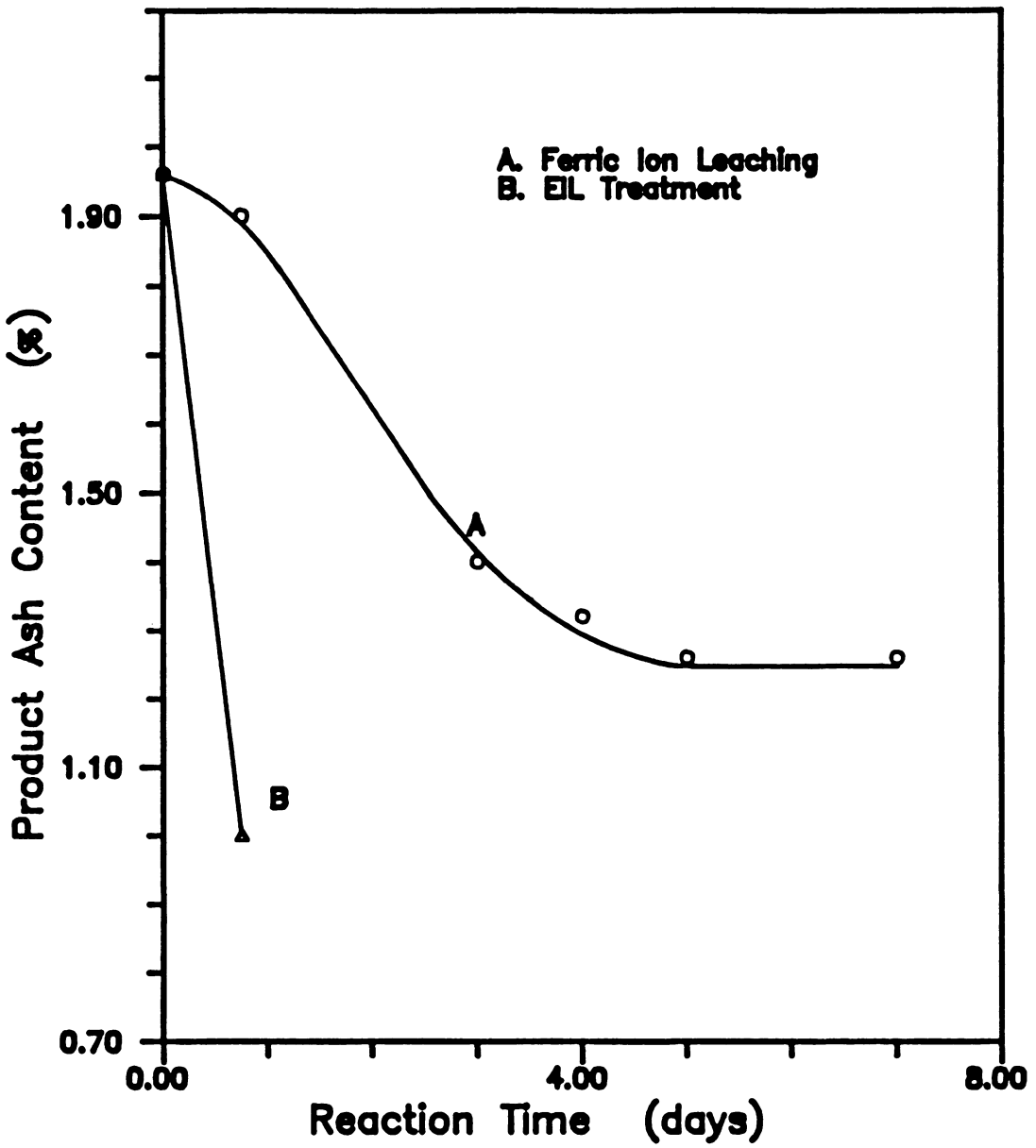

Figure 9. Comparative Ash Removal Rates of Ferric-Ion Leaching and EIL Treatment-Taggart Seam Coal: Taggart seam coal treated with 0.05M ferric ions at 65°C. Particle size = -140 + 200. EIL treatment conducted at 65°C in 1.0M sulfuric acid with similar coal and no added ferric ions.

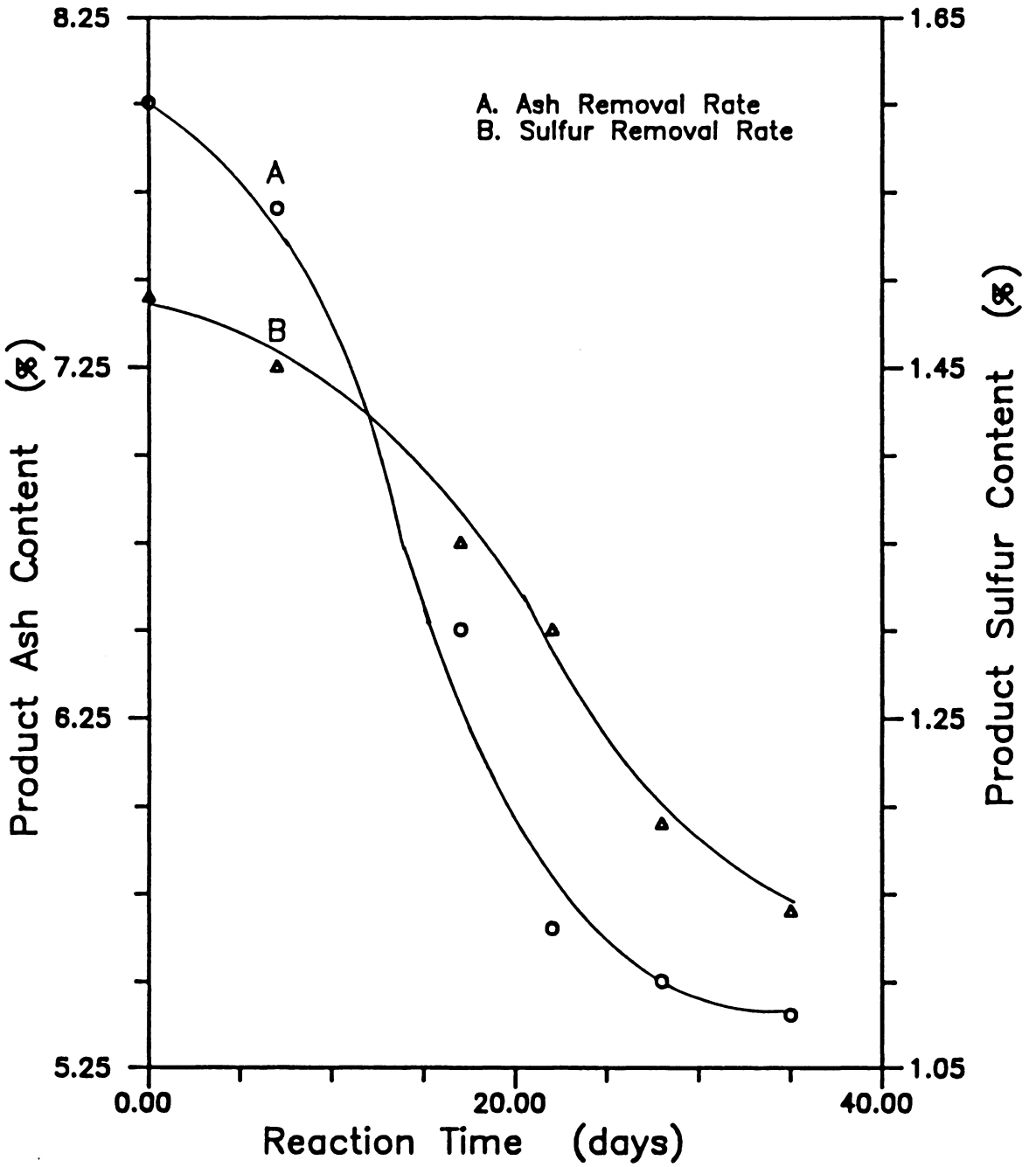

Figure 10. Demineralization Rates of Norton Coal with Ferric-Ion Leaching: -100 + 230 mesh Norton seam coal in 1M ferric-ion solution at 65°C.

4.6 EIL Treatment with Alternate Methods of Ferric Regeneration

4.6.1 Regeneration of the Electrocatalyst with Oxygen

The results shown in Tables 1 to 17 have been obtained by regenerating the ferric ion electrocatalyst with an electrochemical method. Since the application of a potential to the solution oxidizes the ferrous ion to the ferric state, it should be possible to replace the electrochemical method with a kinetically slower, but more economical method of regeneration. Tests were conducted by operating the EIL process while continually saturating the electrolyte with oxygen to regenerate the spent ferric ions by a simple aeration technique.

A Wyodak coal sample of size -100+200 mesh was contacted with a mixture containing 5% hydrochloric acid and 15% sulfuric acid by weight. No ferric ions were added to the mixture. No mechanical stirring was employed to prevent the particles from breaking by agitation. A gentle stream of oxygen was blown into the supernatant solution for 5 days before taking the sample out and screening it at 200 and 325 mesh. The -325 mesh fraction was discarded and the -100+200 and -200+325 mesh fractions were analyzed for ash content. The results are given in Table 20.

Table 20. Results of the EIL Treatment with Wyodak Coal Using Oxygen

Products	Size *(mesh)*	Weight *(%)*	Ash *(%)*	Cumulative Ash *(%)*	Cumulative Recovery *(%)*
Feed Coal	-100+200	100.00	6.29	--	---
Clean Coal	-100+200	35.05	2.37	2.37	36.52
Clean Coal	-200+325	47.02	3.20	2.85	88.44
Refuse	-325+0	17.91	22.03	6.29	100.00

The results show that this simple technique can remove ash from the coal, producing a 2.85% ash coal from a 6.29% ash feed coal with 88.44% recovery. Note that there was a significant size reduction of the feed coal as a results of the process, which was unlike the test results obtained with the EIL technique. The loss of 0.02% is attributed to losses incurred during the collection of material after the EIL treatment.

A comparative treatment of the same Wyodak coal was carried out under similar conditions but instead of the oxygen, a potential of 1.0V SCE was used to regenerate the spent ferric ions. The reaction was carried out at an ambient temperature as before and the reaction time was increased to 12 hours to somewhat compensate for the slower kinetics at the lower temperature. A potential of 1.0V SCE was applied to regenerate the spent ferric ions. From the results summarized in Table 21, the application of the 1.0V SCE oxidation potential to regenerate the ferric ions resulted in a considerable reduction in the reaction time and a decrease in the ash content of the product coal as well.

Table 21. Results of the EIL Treatment with Wyodak Coal for Two Methods of Ferric Ion Regeneration

Method of Regeneration of Spent Ferric Ions	Reaction Time *(days)*	Ash Content Feed *(% wt)*	Ash Content Product *(% wt)*	Coal Recovery *(% wt)*
Bubbling Oxygen	5	6.29	2.85	88.4
Oxidizing Potential	0.5	6.29	1.95	89.3

A similar set of tests were conducted with a -100+140 mesh Pittsburgh #8 seam coal. The feed coal assayed 7.46% ash and 1.99% sulfur. In this set of experiments, the coal was slurried with a solution of 1.0M sulfuric acid containing 0.1M ferric ions. The temperature of the reaction was maintained at 54°C. A stream of oxygen was bubbled through the solution using a coarse glass frit for 2.5 days after which the sample was wet-screened, dried and assayed. The product coal contained 5.16% ash and 1.36% sulfur. The test was repeated under identical conditions, but instead of the oxygen, a 1.0V SCE potential was applied to the slurry via platinum electrodes. The reaction was carried out for 6 hours at 54°C after which the coal was wet-screened and assayed as before. Table 22 summarises the results of these tests.

Table 22. Results of the EIL Treatment with Pittsburgh #8 Coal for Two Methods of Ferric Ion Regeneration

Method of Regeneration of Spent Ferric Ions	Reaction Time *(days)*	Ash Content Feed *(% wt)*	Ash Content Product *(% wt)*	Sulfur Content Feed *(% wt)*	Sulfur Content Product *(% wt)*
Bubbling Oxygen	5.0	7.46	5.16	1.99	1.36
Oxidizing Potential	0.25	7.46	4.37	1.99	1.51

The results show that the oxidation of the spent ferric ions by electrolysis is a superior method of regeneration under similar experimental conditions. Although it may be possible to improve the rate of ferrous oxidation by oxygen by altering other process variables, the results obtained in the present work indicate the superiority of the electrochemical oxidation in the EIL process. However, it is not certain whether the application of the potential improved the overall kinetics of the process by improving the kinetics of the ferric ion regeneration. The liberation of mineral matter by the EIL process involves the series of steps listed in section 5.2. It is possible that the application of a potential may improve the kinetics of some or all of these steps to yield an overall improvement in the liberation of mineral matter. The application of the potential may increase the rate of reaction of the ferric ions with the coal surface by oxidizing parts of the coal surface to simpler organic compounds that could react more readily with the ferric ions. Furthermore, the relatively rapid kinetics of electrochemical oxidation maintains the ferric/ferrous ratio as high as possible. This is a thermodynamically desirable condition for the dissolution of the pyrite by ferric ions as the rate depends on the ferric ion concentration and the ferric/ferrous ratio.

4.7 Mass Balance Studies

4.7.1 Introduction

The foregoing sections presented the theoretical basis of the EIL process and the experimental results obtained so far. Although the process is essentially a method of removing ash from coal, it is possible that certain components of the mineral matter may be removed by chemical dissolution because the process uses up to 3.6 mol/ℓ of acid. Therefore it is necessary to establish mass balance diagrams for the process. These studies were undertaken to investigate the percentage of mineral matter dissolved by the acid and the percentage actually liberated by the EIL process.

Two coal samples were selected for these tests; a high-ash coal from the Widow Kennedy seam assaying 27.5% ash and a low-ash sample from the Middle Wyodak seam assaying 2.83% ash. Each feed sample was thoroughly washed and wet-screened to remove dust and other fine particulates that might be adhering to coarse particles prior to any analysis. The sample was subjected to the EIL treatment using the stirred tank reaction vessel with an acid electrolyte. The treatment was carried out for 6 hours after the coal had been conditioned in the same electrolyte for 10 hours. A potential of 1V SCE was applied to a platinum electrode to regenerate the spent ferric ions in solution.

Following the EIL treatment, the electrolyte was separated from the treated coal by filtration. The residue remaining on the filter paper and the treated coal were wet-screened, and the underflow containing the liberated mineral matter and fine particulates of coal was collected along with the wash water. The underflow was

allowed to settle over a period of time after which the water was decanted away and the balance centrifuged. The solid residue from the underflow together with the feed and product coals were all analysed for their ash content. The mass of ash present in the feed, product and underflow were determined from the ash assays.

4.7.2 Widow Kennedy Coal

Figure 11 shows a mass balance diagram of the EIL process with the Widow Kennedy seam coal. For the sake of simplicity, all combustibles are denoted by *C* and all non-combustibles by *NC*. 50.00 gms. of the -20+70 mesh feed coal was treated with 756.0 gms. of 1.0M HCL as electrolyte. The reaction temperature was 70°C. The mass of the ash in coal was obtained from the masses of the coal and its respective ash percentages in the different stages of the process. The Parr formula was used to correct ash weights to mineral weights. The diagram shows the mass balance of a feed coal containing 13.76 gm. ash subjected to the EIL process. The resulting product coal contained 3.55 gm. ash and the tailings contained 7.55 gm. of ash. Thus the total ash removed from the feed coal was 13.76-3.55 = 10.21 gm. Since 7.55 gm. of this was present in the underflow, the balance 2.66 gm. of ash was removed with the acid electrolyte when it was filtered off from the coal. Hence 2.55 gm. of the total 10.21 gm. of ash removed from this coal was due to dissolution in the acid. Thus 78.20% of the ash in the coal may be removed by the EIL process of which 18.53% was removed by dissolution and 54.8% was removed by liberation.

To complete the mass balance however, it is necessary to determine the dissolved mineral content of the filtrate. At the time these experiments were conducted, it was not possible to conduct analyses on the filtrate due to a breakdown in the Atomic

Absorption apparatus. However, this was done at a later stage and is discussed in section 4.8.

4.7.3 Middle Wyodak Coal

The other sample of coal selected for this series of tests was processed in a similar manner except that the electrolyte used contained 0.5M/ℓ hydrochloric and 1.5M/ℓ sulfuric acid in solution. A low-ash coal from the Middle Wyodak seam assaying 6.29% ash was used fro the tests. Figure 12 shows the amount of ash in the coal before and after the coal was treated by the EIL process. The 2.83 gm. of ash in the feed coal was distributed as 0.76 gm. in the product coal, 1.12 gm. in the underflow and the remaining 0.95 gm. as dissolved matter in the electrolyte. Thus, 73.14% of the ash was removed from the feed coal with 39.57% removed by liberation and 33.56% removed by dissolution. The results obtained from the preceding tests are summarized in Table 23.

The methods described above are not completely error-free. The amount of mineral matter attributed to dissolution by the acid was obtained by difference and not actual measurement. Thus experimental losses will be included with the proportion of mineral matter supposedly dissolved by the acid.

Secondly, the pore size of the filter paper used was around 20 to 25μ, and the mean particle size of the low-temperature ash of most of the coals tested was around 10μ Thus, a large portion of the liberated mineral matter would have passed through the filter paper and would be reported as ***dissolved*** mineral matter. Furthermore, when the low temperature ash of the Widow Kennedy and Middle Wyodak coals were isolated and treated with the identical acid as used in the EIL tests for the mass balance studies, the

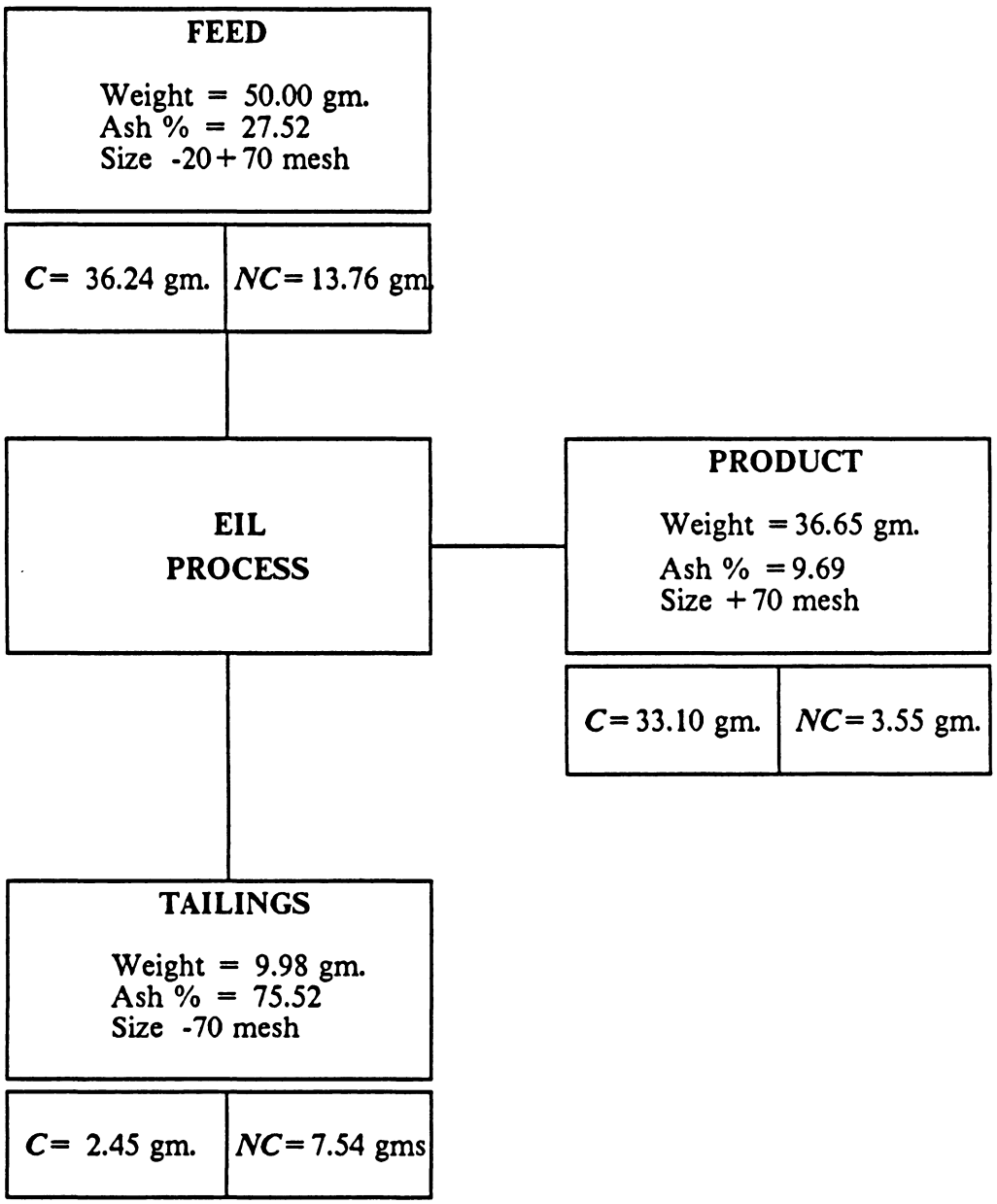

Figure 11. Mass Balance of Widow Kennedy Seam Coal: *C* = Combustible Material, *NC* = Non-combustible Material.

percent ash dissolved was much lower than that shown in Table 23 Finally, errors in weighing would be reflected in the mass-flow calculations.

Table 23. Ash Removal by Dissolution and by Liberation

Coal Seam	Percent Ash Removed		
	Dissolution	*Liberation*	*Total*
Widow Kennedy	18.53	54.8	78.20
Middle Wyodak	33.56	39.57	73.14

Out of the many oxides present in coal, only those of Fe, Ca, Mg, Na and K are basic and can lend themselves to dissolution by the acid electrolyte. A study on the behaviour of mineral matter during the alkaline leaching of coal (Fan et al., 1984b) indicated that the minerals predominant in coal, namely quartz, kaolin and pyrite were almost always insoluble in concentrated or dilute sulfuric or hydrochloric acid, whether hot or cold. Acid-soluble products were only obtained if these minerals were reacted first with an alkali in an autoclave at temperatures around 250°C to form sodium hydroaluminosilicates. Thus the relatively large proportion of ash removed by the EIL process cannot be wholly due to acid dissolution. Although it may be possible that certain acid-soluble minerals may be holding acid-insoluble minerals in position in the coal matrix, it is highly unlikely that this may be the case in all of the particles of the various coals tested by the EIL process. Furthermore, it is unlikely that a polar substance such as an acid can penetrate inside the pores of a non-polar substance such as coal without an external driving mechanism (Marcus, 1962). It is proposed that it is the osmotic pressure that provides the driving force for the acid to penetrate the coal matrix. Initially, the osmotic pressure build-up forces water into the crevice to cause

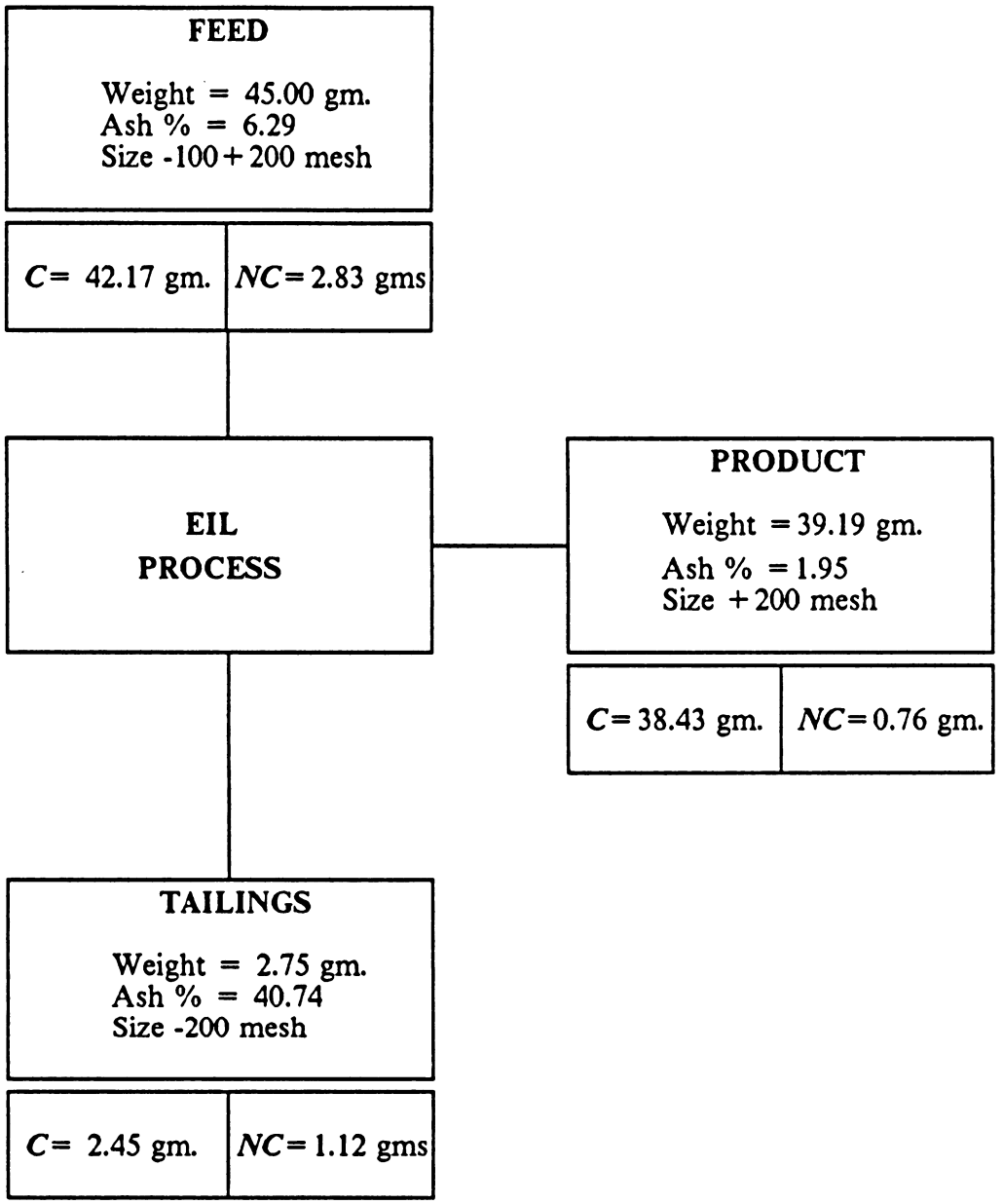

Figure 12. Mass Balance of Middle Wyodak Coal: *C*= Combustible Material, *NC*= Non-combustible Material.

partial fracture. The bulk solution now flows into the increased volume inside the pore caused by the fracture. A double layer now forms deeper inside the crevice by (a) the exposure of a fresh coal surface to the bulk solution and (b) the oxidation of the coal by ferric ions. An osmotic pressure develops in this region caused by the interaction of the double layers and water flows deeper into the crevice to cause further cracking of the crevice. The bulk solution (acid) flows into the increased volume caused by the cracking and the process is repeated until sufficient acid has penetrated the pore structure of coal to cause the dissolution, if any, of acid-soluble minerals. More commonly however, the flow of the water into the coal crevice under the osmotic pressure causes the fracture of the crevice and the loosening of the mineral matter entrapped inside it.

4.8 Analysis of the Mineral Matter Present in Coal

4.8.1 Particle Size Analysis

The primary objective of this exercise was to determine the type, size and distribution of the mineral matter in a given sample of coal. This was particularly important for conducting accurate mass balance studies. However, a true representation of particle size is often difficult to realize due to irregularities in the shape of the particles comprising the mineral matter. For this reason, equivalent diameters are frequently used to report the size of irregularly shaped particles, where the equivalent diameter refers to the diameter of a sphere which behaves similarly to an irregularly shaped particle under a given influence.

Numerous techniques are available for determining the particle size distribution of a powder and their range usually depends on the physical parameter used to measure the particle size. An electrical sensing technique based on the *Coulter Principle* was used in this work due to its low detection limit ($\simeq 0.3\mu$) and good reproducibility. However, any size analysis technique has the inherent problem of missing particles finer than some finite lower limit. This may be indirectly obtained from a mass balance which blends the size analysis data from several ranges to get a complete distribution. These inherent problems were accounted for by an automated technique (Mankosa, 1986), which provided a complete, mass balanced size distribution from the Elzone 80XY particle size analyzer described in section 3.

The low temperature ash (LTA) obtained from several feed coals was analyzed by the Elzone particle size analyzer. The mean particle size of the ash in all of the coals

examined varied from 5-10μm, making it ideally suited for x-ray diffraction analysis. Figure 13 and Figure 14 show the particle size distribution of the low temperature ash from the Widow Kennedy seam and the Middle Wyodak seam. The mean particle size of the low temperature ash from these coals lies between 12-14μ. Thus it is possible that during the mass balance studies discussed in the previous section, any ash ***liberated*** by the EIL process would be lost by passage through the filter paper and would be accounted as dissolved material. Further, the collection of any liberated ash presents considerable difficulty in that it has to be isolated from an acid solution. Even with repeated washings of the liberated ash, there is always some acid that remains with the ash. When the ash is dried prior to weighing, the acid solution becomes concentrated and behaves as concentrated sulfuric acid. Added to this is the difficulty of washing a fine powder such as the liberated ash without any loss of material. To overcome this, the spent electrolyte was analyzed for anions and cations from which the weight of ash dissolved was back-calculated using several assumptions. As a first step, the nature of the minerals present in the Middle Wyodak seam needed to be determined by X-Ray Diffraction.

4.8.2 X-Ray Diffraction Analysis

The x-ray analysis of the LTA is described in section 3.2.8. A primary objective was to determine the type of minerals present in the feed coals and to study trends, if any, between the response of a given coal to the EIL process and its mineral constituents. A number of considerations were made in analyzing the XRD patterns obtained, given that a complex mixture of minerals would undoubtedly be involved. Phases were identified by considering the d-spacings calculated for the 2θ values. Peak

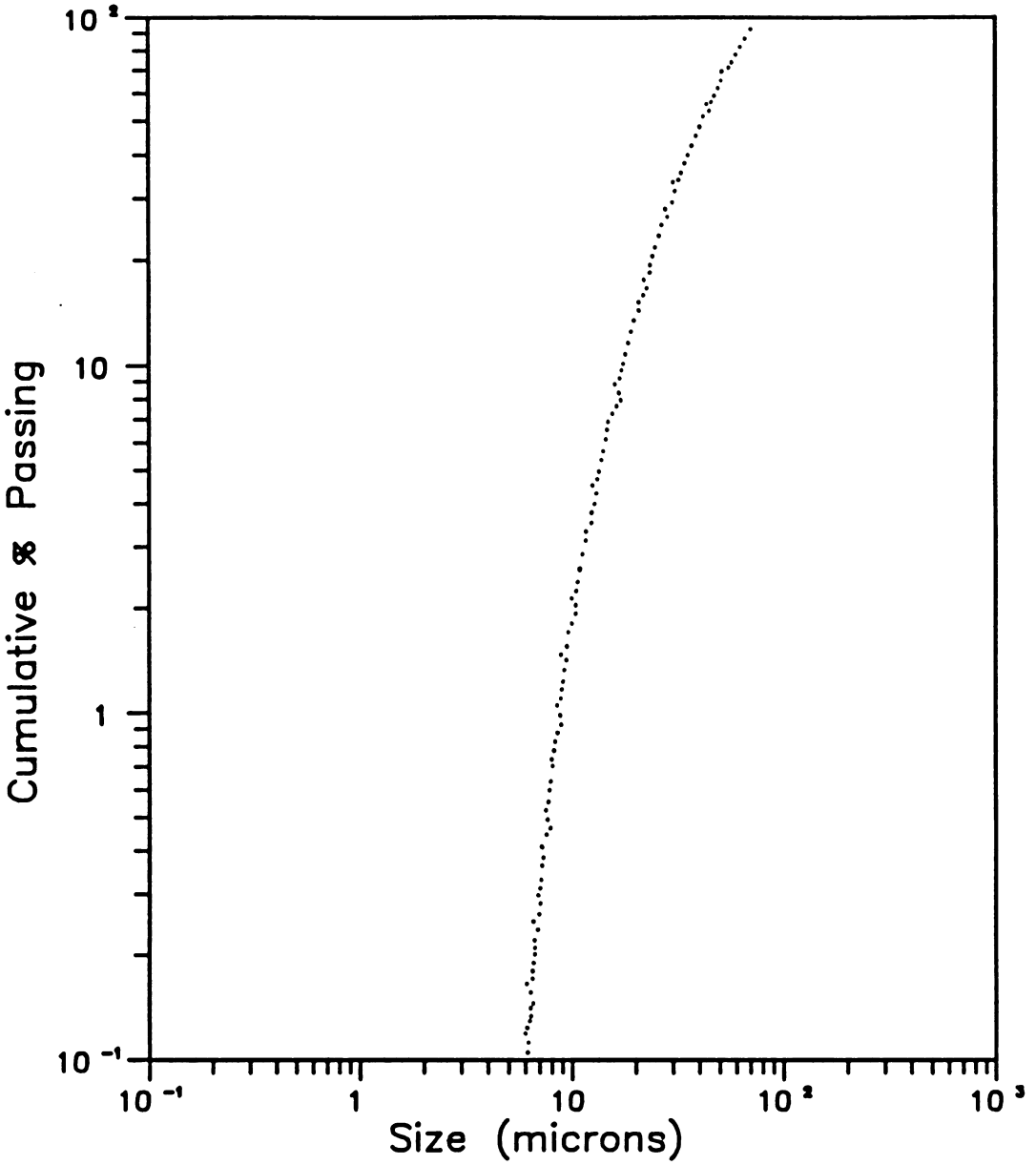

Figure 13. Particle Size Distribution of the Low Temperature Ash from Widow Kennedy Seam Coal: Distribution plotted as a function the cumulative percent passing through a given size

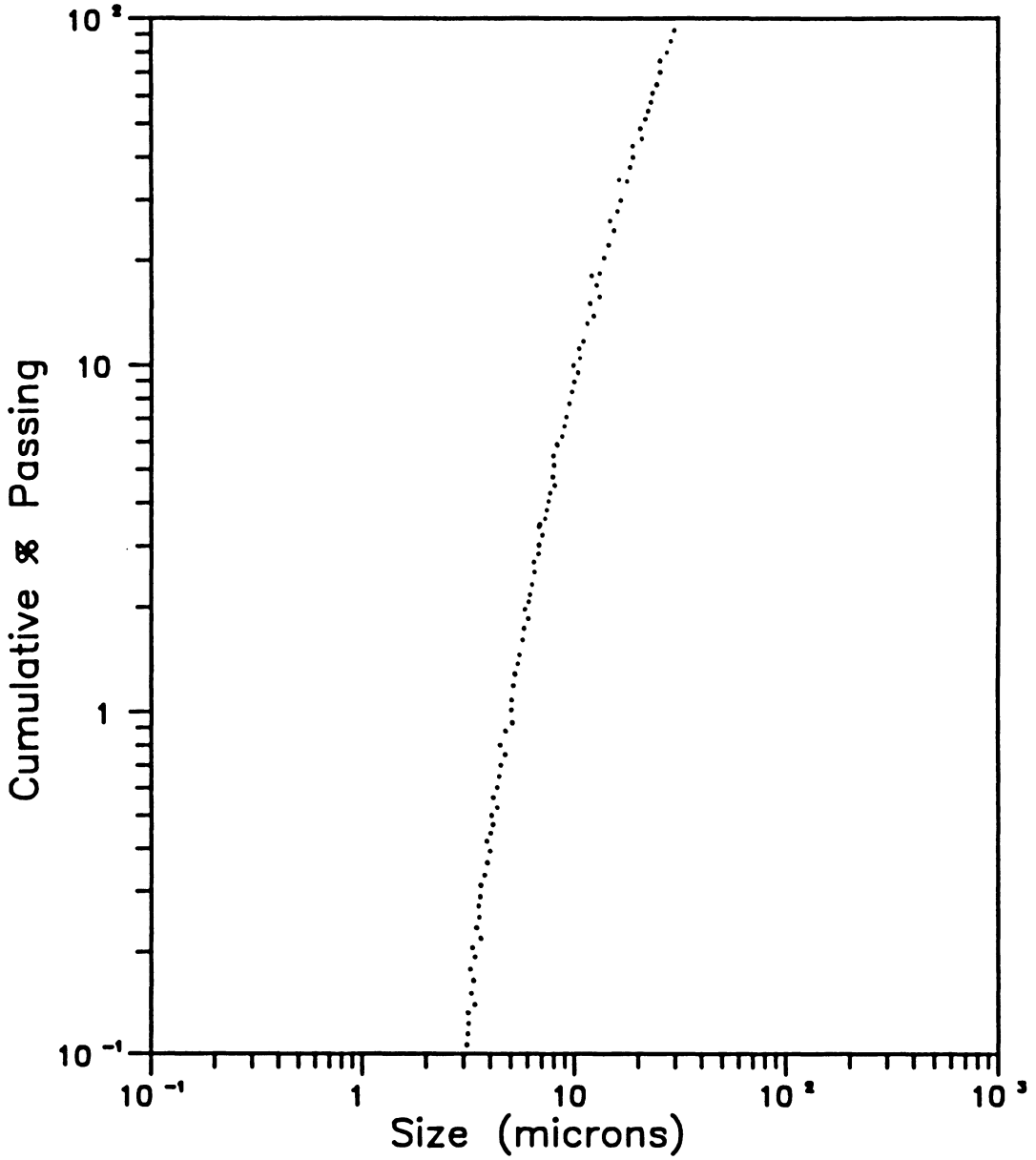

Figure 14. Particle Size Distribution of the Low Temperature Ash from Middle Wyodak Seam Coal: Distribution plotted as a function the cumulative percent passing through a given size

interference, which occurs whenever several species have similar interplaner spacings, creates some difficulty when resolving certain peaks in the XRD pattern. Furthermore, preferred orientations of clay minerals and their degree of crystallinity can greatly affect and alter the intensity distributions and XRD maxima, particularly in the case of kaolinites. Because of these influences, no quantitative conclusions were drawn from the peak intensity data. XRD results from the LTA of several feed and product coals are discussed below.

4.8.2.1 Middle Wyodak Coal

The LTA of this feed coal showed the presence of quartz, kaolinite, calcite and siderite. Peaks corresponding to pyrite were extremely weak or absent altogether in the XRD pattern. The product coal showed a similar pattern corresponding to the same minerology.

Table 24 lists the analysis of the spent acid after the EIL treatment of Middle Wyodak coal. The following assumptions were made in order to back-calculate the actual amounts of mineral matter dissolved by the acid.

1. The X-Ray analysis was 100% correct in identifying quartz, kaolinite calcite and siderite as the ***only*** mineral species present in Middle Wyodak coal.

2. All iron present in solution was obtained ***only*** from the whole or partial dissolution of siderite

3. All calcium present in solution was obtained ***only*** from the whole or partial dissolution of calcite

4. All aluminum present in solution was obtained ***only*** from the whole or partial dissolution of kaolinite

5. The silica present in solution was from the partial dissolution of both quartz and kaolinite.

Table 24. Analysis of the Spent Acid after the EIL Treatment of Middle Wyodak Coal

Element *(Total)*	Quantity Present *(mg/l)*
Iron	48.6
Calcium	41.2
Magnesium	248
Silica (SiO_2)	7.1
Aluminum	16.4
Carbonate	<1.0
Nitrate	<0.01
Sulfate	134,000

On the basis of these assumptions, the amounts of quartz, kaolinite, calcite and siderite removed by dissolution amount to a total of 202.81 mg. Referring back to Figure 12, 0.95 gms. of mineral matter was attributed to dissolution in acid. According to the above calculations, only 0.20 gms. was dissolved in acid. Accordingly, 0.75 gms. of mineral matter was ***liberated*** and not dissolved. This material would have passed through the filter paper as its size consist may have been below the D-50 mean size as shown in Figure 14 on page 115. On the basis of these calculations, the proportion of mineral matter ***dissolved*** by the acid is 7.06% while the proportion of mineral matter ***liberated*** by the EIL process is 66.08% making a total removal of 73.14%. However, due to the several assumptions made, the conclusions are questionable.

The remaining part of this section discusses the X-Ray Diffraction analyses conducted on several coals as regards their mineral consituents.

4.8.2.2 Pittsburgh #8 Feed Coal

The major minerals present were kaolinite and illite. Calcite peaks were correspondingly weak and shifted, indicating the presence of iron or magnesium substitutes in its crystal structure. This coal responded well to the EIL process although the major minerals present in the feed coal were acid-insoluble silicates.

4.8.2.3 Blair Seam Feed Coal

The XRD pattern showed the presence of quartz, kaolinite and illite. In addition, fairly prominent peaks for siderite were present. Very little pyrite was detected. During the EIL treatment of this coal, it is probable that the majority of the ferric ion catalysts were derived from siderite.

4.8.2.4 Splashdam Seam Feed Coal

Strong peaks for illite and quartz were present along with weaker peaks for kaolinite and mixed forms of calcite. Small peaks for anhydrite were detected as well.

4.8.2.5 Powell Mountain Feed Coal

The presence of pyrite and kaolinite were shown by prominent peaks. The quartz peaks were relatively smaller as well as those corresponding to carbonate-type minerals. As it was possible to clean this coal using ***water*** as an electrolyte with the EIL process, the demineralization of this coal cannot be attributed to mere dissolution of the mineral matter.

4.8.2.6 Elkhorn #3 Feed and Product Coals

The dominant minerals detected were illite, quartz, kaolinite and pyrite. Small quantities of calcite, siderite or their combinations were detected as well. The product coal showed little or no illite as peaks corresponding to illite were not present. Part of the XRD of the feed coal LTA is shown in Figure 15, and that of the corresponding product coal is given in Figure 16. A comparison of the relative peak heights of quartz and kaolinite show that these heights are considerably reduced in the product coal. Qualitatively, this indicates the removal of quartz and kaolinite from the feed coal by the EIL process, both of which are insoluble in acid.

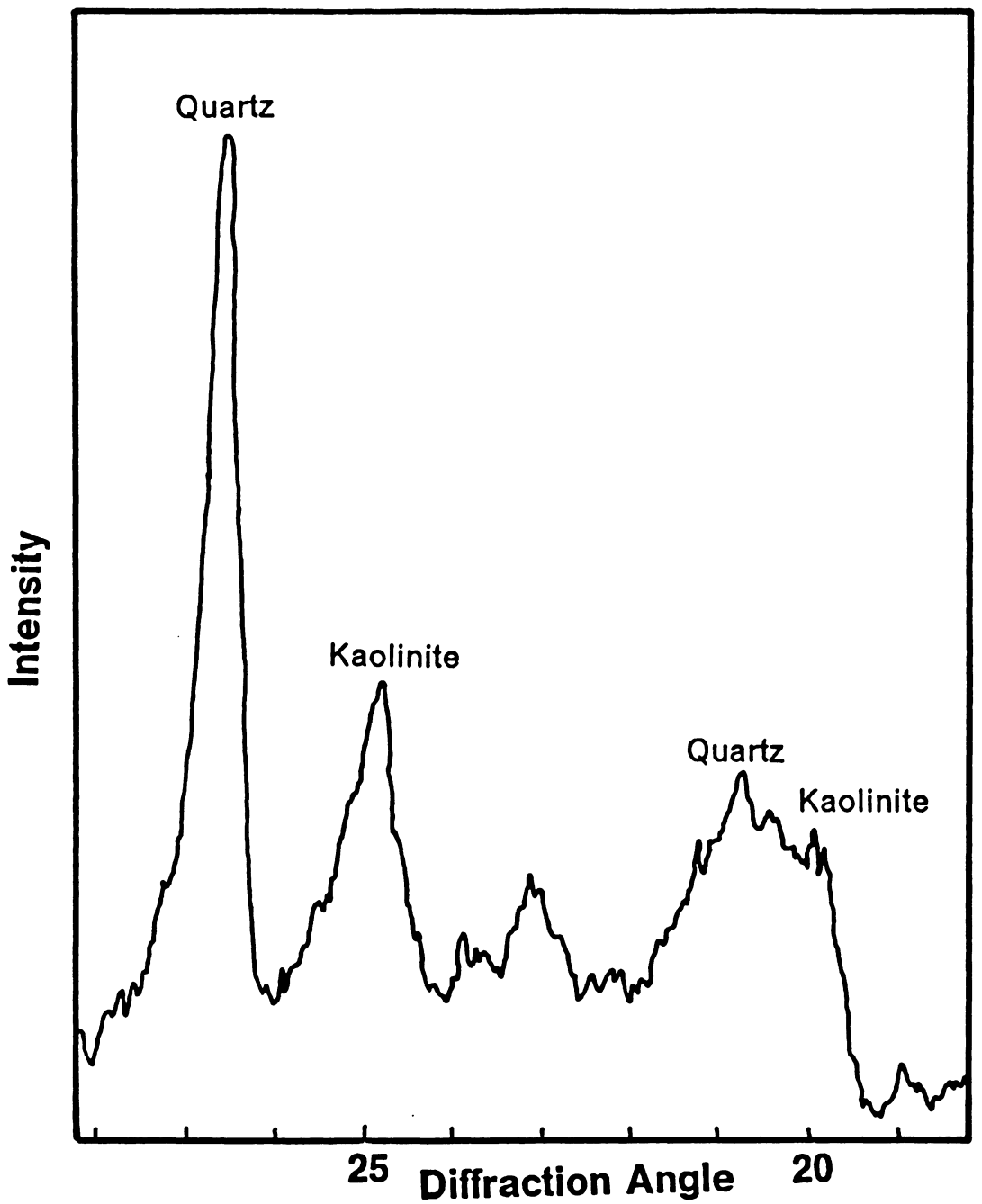

Figure 15. XRD patterns of Consol Coal LTA before EIL Treatment: LTA obtained from wet-screened Consol coal

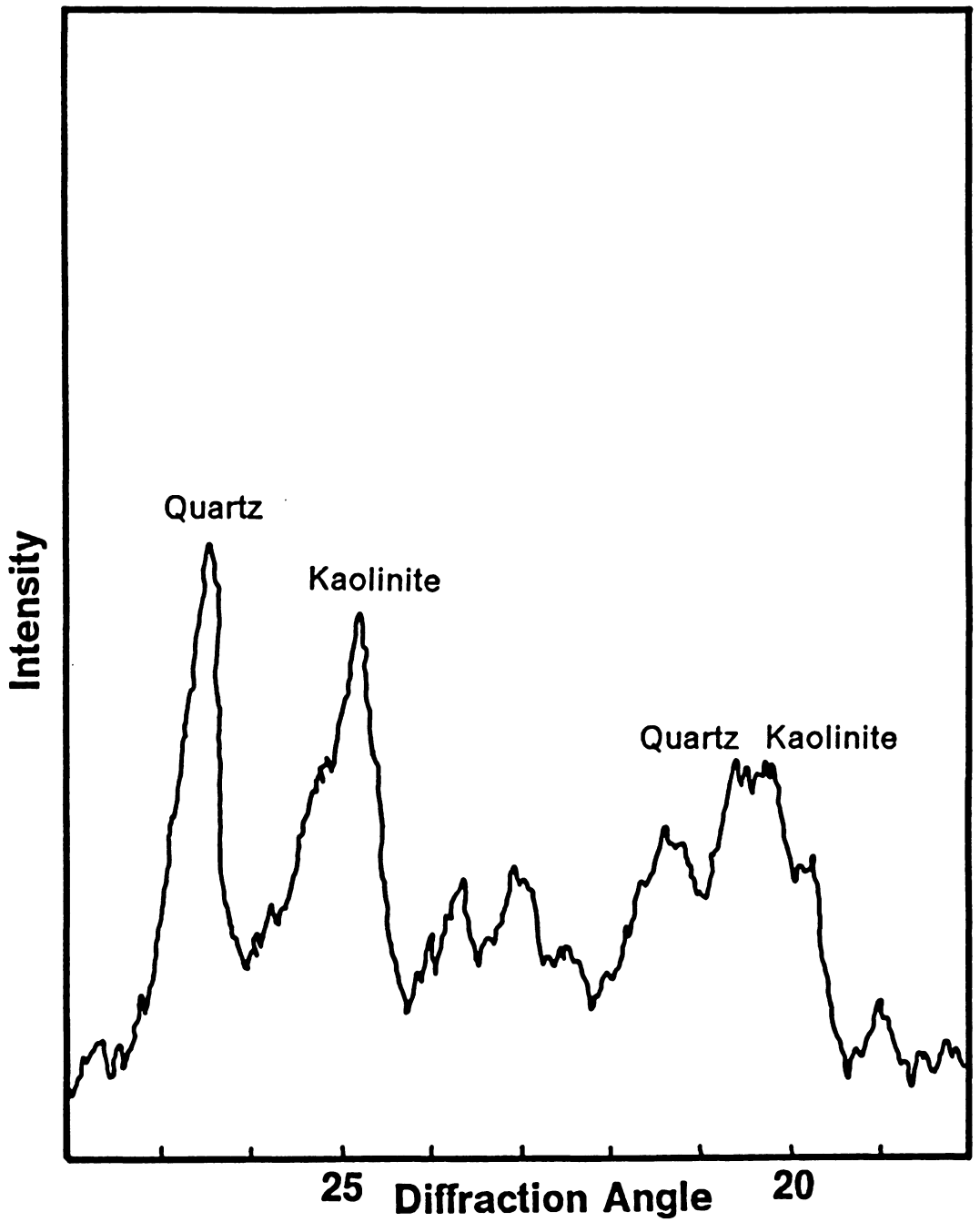

Figure 16. XRD patterns of Consol Coal LTA after EIL Treatment: LTA obtained from EIL-treated Consol coal. EIL treatment carried out with 1M sulfuric acid at 65°C for 5 hours.

4.9 Comparison of the EIL Treatment with Acid Leaching

4.9.1 Introduction

The EIL test results conducted on a variety of coals usually showed some degree of demineralization. While it is certainly plausible that minerals such as calcite and dolomite, if present in coal, may be dissolved by an acid, the percent ash removed from most coals during the EIL process could not be solely attributed to the dissolution alone as discussed in the previous sections. Some comparative tests were conducted with four different samples of coal to determine the extent of demineralization by the acid alone.

4.9.2 Wet-Screened Feed Coals

With each coal, two similar samples were prepared by repeated riffling and sampling. A 45 gm. sample was mixed with 750 ml. of 1.0mol/ℓ of sulfuric acid for 4 to 6 hrs. at 65°C. A potential of 1.0V SCE was applied to one of the mixtures via platinum electrodes as in the EIL process. The other sample had only the electrodes inserted into the mixture, but without any potential applied. This was done to ensure identical reactor geometry for both comparative tests. After the desired time of reaction, the coal samples were carefully screened, washed and dried under identical conditions, after which they were analysed for ash content. The results of each of these tests are given in Table 25.

Table 25. Comparative Coal Cleaning Results of Acid Treatment and the EIL Process

Sample Type	Feed Ash	Product Ash	
		Acid Treatment	EIL Process
Norton Seam	30.81%	20.67%	18.76%
Consol-Mathew	7.64%	6.02%	4.42%
Wyodak-Anderson	5.01%	2.98%	1.14%
Pittsburgh #8	10.83%	4.01%	3.11%

The results shown in the table indicate that the EIL process improved the removal of mineral matter from coal by a small, but consistent amount over the acid treatment. When the coal was treated with the acid, ferrous and/or ferric ions were initially released into solution by reaction of the acid with the *exposed* coal pyrite or other ferruginous minerals. The ferric ions react with the coal surface to oxidize it whilst increasing the positive charge on it by elecron abstraction from sessile bonds on the coal (Kreysa and Kochanek, 1985). The ferric ions are thus reduced to ferrous and remain in solution. However, the ferrous ions can undergo *slow* oxidation in the acidic environment. The open circuit potential of the system is over 0.56V SCE, which is high enough to oxidize ferrous to ferric. When a potential was applied to the system (as in the EIL process), the ferrous ions are rapidly regenerated, the rate of reaction being faster than that under open circuit conditions. This in turn increases the positive charge on the coal at a faster rate and hence the double layer interaction and eventually, the pressure inside the pore. The larger pore pressures developed on the average by the EIL process result in greater fractures and liberation of mineral matter over that obtained under open circuit conditions.

4.9.3 Dry-Screened Feed Coals

Most of the comparative tests between acid treatment and EIL process produced a small, but consistent improvement in the removal of ash. However, with a dry-screened coal sample the improvement was more substantial. Table 26 shows the results of comparative tests between acid treatment and the EIL process conducted in turn with a wet-screened and a dry-screened feed coal sample from the Widow Kennedy seam. The feed size of the coal used was -100+270 mesh and was treated in 1.0mol/ℓ sulfuric acid solution at 65°C for a period of 10 hours following a 12 hour conditioning period.

Table 26. Comparative Coal Cleaning Results of Acid Treatment and the EIL Process using Wet/Dry Screened Widow Kennedy Coals

Conditions	Feed Type	Ash Content		Percent Removal
		Feed	Product	
Acid Treatment	Dry-Screened	26.56	16.01	39.72
EIL Process	Dry-Screened	26.56	11.56	56.47
Acid Treatment	Wet-Screened	21.34	15.86	25.67
EIL Process	Wet-Screened	21.34	15.12	29.15

The percent ash removal with the dry-screened feed coal was 39.72% with acid treatment and 56.47% with the EIL process. The EIL process improved the removal of ash by 16.75%. When the same coal sample was wet-screened and fed to each of the processes in turn, the percent ash removal was 25.67% and 29.15%. In this case, the EIL process improved the ash rejection by only 3.48%. This might suggest that some active species, essential for the EIL process, was lost during the wet-screening step of the feed coal. The spent acid after treating the wet-screened coal by the EIL process

showed little or no discoloration whereas the spent acid from treating a dry-screened coal was straw-colored. This coloration was not due to suspended particulates in the solution and was not observed when either a dry-screened or a wet-screened coal was treated only with acid. It appears, therefore, that some unknown species may have an important electrocatalytic role during the EIL process.

Table 27 lists the analysis of the spent acid obtained after the EIL treatment of the dry-screened coal. The presence of iron confirms its role as an electrocatalyst for the EIL process. However, it is not clear at this stage whether the presence of the other elements play a role in activating the iron catalyst.

The pH of the acid solution during the EIL process was found to ***increase*** with reaction time when the potential was applied. Further, in some of the examples of coal-cleaning presented earlier, the acid was reused two to three times over and in some cases, several times over. The pH of the solution decreased after successive testing until it passed beyond the lower detection limit of the pH meter. Hence the sulfuric acid does not appear to be consumed by the EIL treatment and this was also observed by Farooque and Coughlin (1979c) during the electrolysis of coal in acidified slurries. If the ash removal phenomena of the EIL process was wholly due to acid dissolution of the mineral matter, the acid strength should decrease with time and usage. Thus, it cannot be conclusively stated that the ash removal from coal by the EIL treatment is entirely due to the dissolution of soluble species.

Table 27. Analysis of the Spent Acid after the EIL Treatment of Widow Kennedy Coal

Element *(Total)*	Quantity Present *(mg/l)*
Iron	353
Calcium	2.72
Magnesium	1.33
Silica (SiO_2)	94.6
Aluminum	158
Carbonate	<1.0
Nitrate	<0.01
Sulfate	120,000

4.10 Scanning Electron Microscopy

4.10.1 Introduction

Scanning electron photomicrographs of some of the coals studied were taken to observe changes in its surface morphology before and after processing. The feed coal was first split into two representative samples by repeated riffling. One sample was treated by the EIL process using a mixture containing 0.5M/ℓ hydrochloric and 1.5M/ℓ sulfuric acid at 65°C for 6 hours. The other sample was treated under identical conditions, but without the application of a potential as in the EIL process. After processing, the coals were wet-screened, dried and riffled to obtain representative samples for microscopic analysis. Photomicrographs were taken of the feed coal and the two product coals. The surfaces were further characterized using Energy Dispersive X-Ray analysis (EDX) to confirm the presence of mineral matter as it appeared on the photomicrographs of the coals.

4.10.2 Jacob Ranch Coal

Figure 17 (top) shows the typical surface morphology of a feed coal from the Jacob Ranch mine in the Middle Wyodak seam. The large gray inclusion near the center of the photomicrograph showed the presence of aluminum, silicon and calcium during EDX analysis. The mineral particle may be held in place by (a) acid-soluble minerals such as carbonates or (b) by compressive stresses between the walls of the coal pore and the mineral particle, created during the formation of the coal bed. Alternatively, a

combination of (a) and (b) may hold the particle in place inside the coal pore. The removal of such a mineral particle from the coal surface requires the penetration of the acid into the space between the clay particle and the coal to dissolve the mineral. This would also be affected by the diffusion of the dissolution products out of the space. The spacing between the coal and the mineral particle in a typical crack is in the order of 1.0-0.75μm, and may be even smaller beneath the surface of the coal. Thus, it is unlikely that this could take place within the reaction time span of the EIL process ($\simeq$4-6 hrs) without an external driving mechanism, such as an osmotic pressure. If the mineral were held together as in (b), an additional step would be required to break the compressive stress between the coal surface and the mineral. Hence the removal of such mineral matter from the coal surface may involve more than a simple acid dissolution mechanism.

Smaller mineral inclusions were seen scattered throughout the micrograph. These minerals appeared to be adhering to the coal surface, but were probably included inside tiny cracks on the coal surface and held in place by methods similar to those discussed above. The minerals may be only as large as they appeared on the micrograph or may extend deep into the pore with their remaining portions hidden beneath their visible sections.

Figure 17 (bottom) shows the surface of this coal when treated with hydrochloric acid. The fine particulates of mineral matter seen on the surface of the feed coal were not present, indicating that the acid treatment may have dissolved or liberated them out of the coal. However, large inclusions of mineral matter were still visible on the surface as shown by the arrows on the photomicrograph. The EDX spectra of these particles showed the presence of Al, Si and Ca, identifying them as mineral matter.

The two photomicrographs of Figure 18 show the surfaces of two different macerals of the Jacob Ranch coal after the EIL treatment. The EIL treatment for this

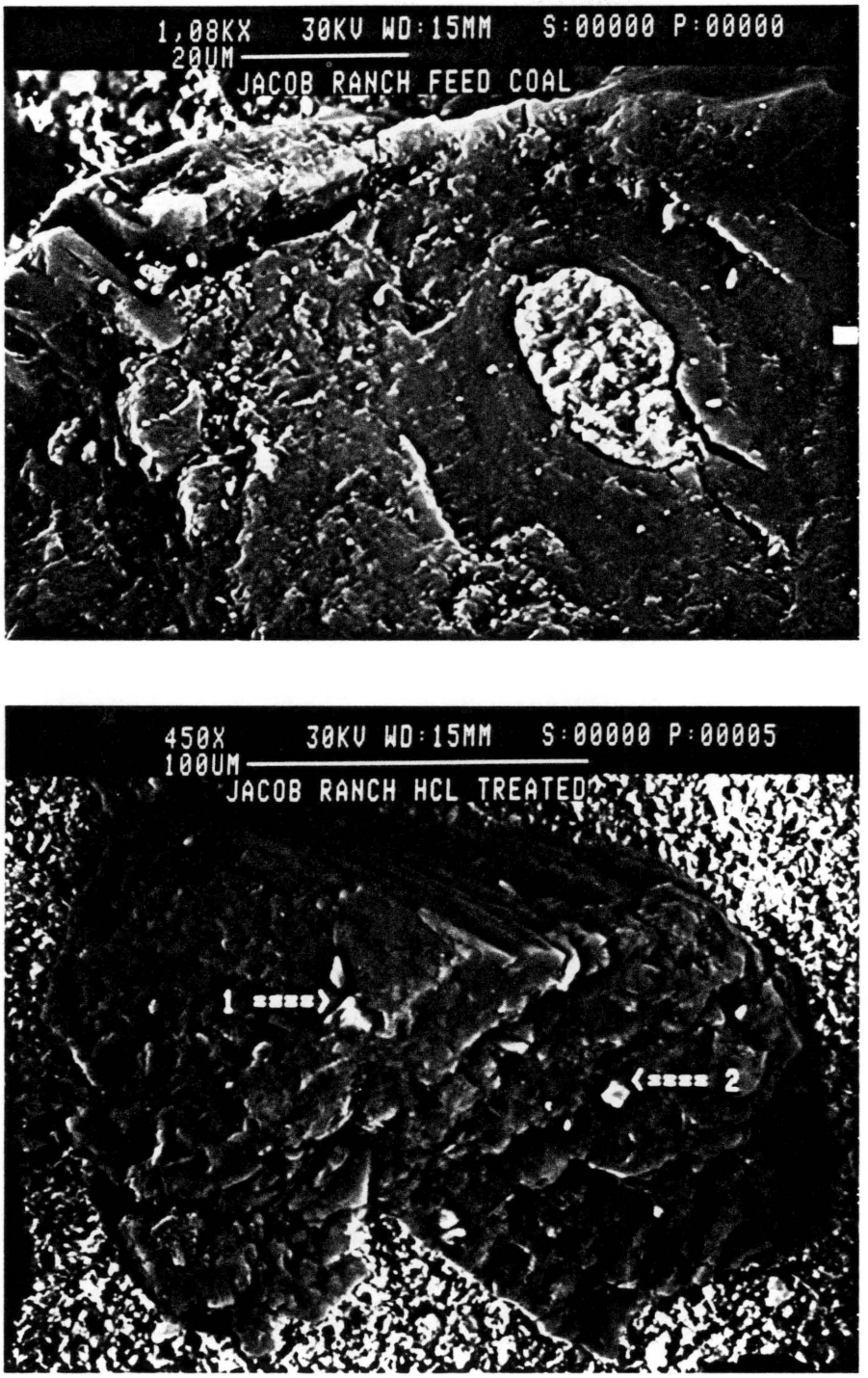

Figure 17. Photomicrographs of Jacob Ranch Coal: (Top) Feed coal surface, -150 + 230 mesh. (Bottom) Surface of acid treated coal.

coal was carried out with $10^{-3}M/\ell$ of Fe^{3+} added to the acid electrolyte. A characteristic surface of the coal showed that pits and cracks had formed on the coal surface after the EIL treatment. The pits may have been the locations where mineral matter once resided in the coal, in a manner not unlike that shown in the micrograph of the feed coal (Figure 17). It seems likely that these mineral particles were removed from the coal by the osmotic pressure mechanism discussed in Section 5. Although the surface of the EIL-treated coal was marked with large cracks, there was no significant size reduction of the coal by the EIL treatment. The cracks, therefore, did not penetrate deep enough to cause particle breakage, but were only sufficient to cause partial fracture of the coal along bedding planes. The areas pointed to by the arrows in the lower photomicrograph show the beginning stages of some smaller cracks on the surface of the coal. The fact that no significant size reduction was observed in the product coals seems to suggest that the cracking may not propagate across the entire particle.

4.10.3 Consol Coal

Figure 19 (top) shows the typical surface of a coal sample obtained from the Consol Coal Co., PA. This sample belonged to the Elkhorn #3 seam. The coal macerals encapsulated mineral matter between longitudinal crevices, shown by the arrows in the photomicrograph. Most of the mineral matter was extremely fine (below 0.5μm) in size, although a few relatively large mineral particles were observed as well. When the coal was acid treated (Figure 19, bottom), the large mineral particles appeared to have been removed by the acid treatment process, although most of the finer particles were still intact. Several particles of the product coal appeared as shown in Figure 20, (top), where vacant pits were clearly visible. The arrows in Figure 20 (top) point to some

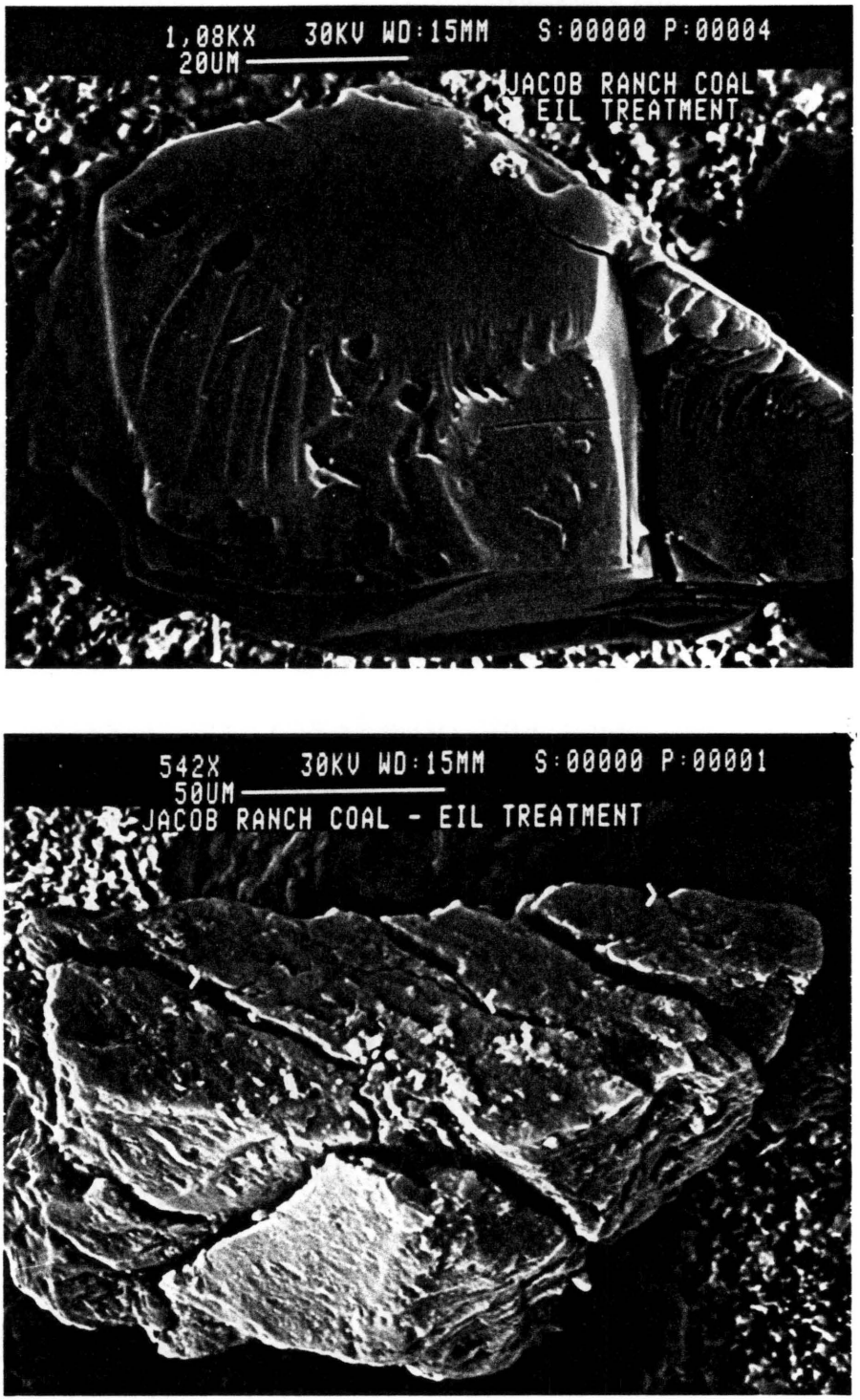

Figure 18. Typical Surfaces of EIL-Treated Jacob Ranch Coal: (Top) Empty pits where mineral matter previously resided. (Bottom) Appearance of cracks following EIL treatment.

empty spaces which may have been occupied by pyrite framboids similar to those surrounding the empty spaces. An enlargement of the area indicated by the arrow in the lower left hand corner is shown in the photomicrograph below it. In the lower right hand corner are empty spaces where pyrite framboids may have existed since the shapes of these empty spaces closely resemble those of the crystals particles beside them. Since pyrite is not very soluble in acid under the conditions of the EIL treatment (Biegler and Swift, 1979), the removal of these framboids from their individual crevices in the coal would require an external force such as an osmotic pressure.

4.10.4 Widow Kennedy Coal

The feed coal from the Widow Kennedy seam showed a large number of mineral particles on its surface (Figure 21, top). These particles may be held in place on the coal surface by the adhesion mechanisms or by the compressive forces. The acid-treated coal showed a similar morphology of such mineral particles remaining on the surface, although their frequency was reduced in the majority of the coal particles examined (Figure 21, bottom). The same feed coal treated by the EIL process showed a much cleaner surface as compared with the feed coal, even at a higher magnification (Figure 22, top).

The acid treatment had not removed much of the large clusters of pyrite present in the feed coal as shown on Figure 22, (bottom). This was not unexpected since pyrite is almost insoluble in acid under the present experimental conditions. The EIL treatment however, removed a significant portion of the pyrite framboids present in the feed coal. This was evidenced by the presence of pits and cracks on the surface of the coal (Figure 23, top). The cracks appeared to propagate to and from empty pyrite

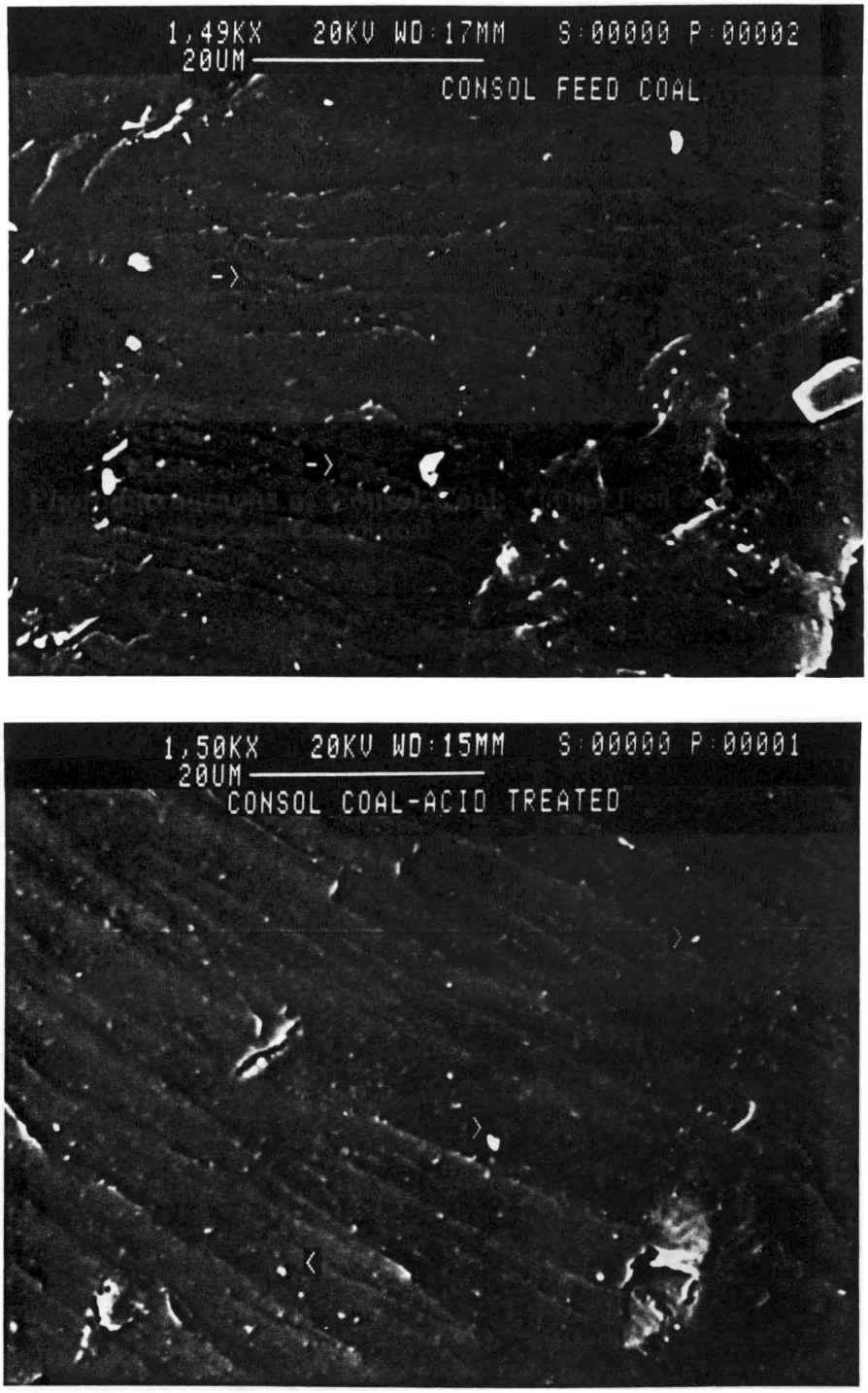

Figure 19. Photomicrographs of Consol Coal: (Top) Feed coal -140 + 270 mesh. (Bottom) Acid treated Consol coal

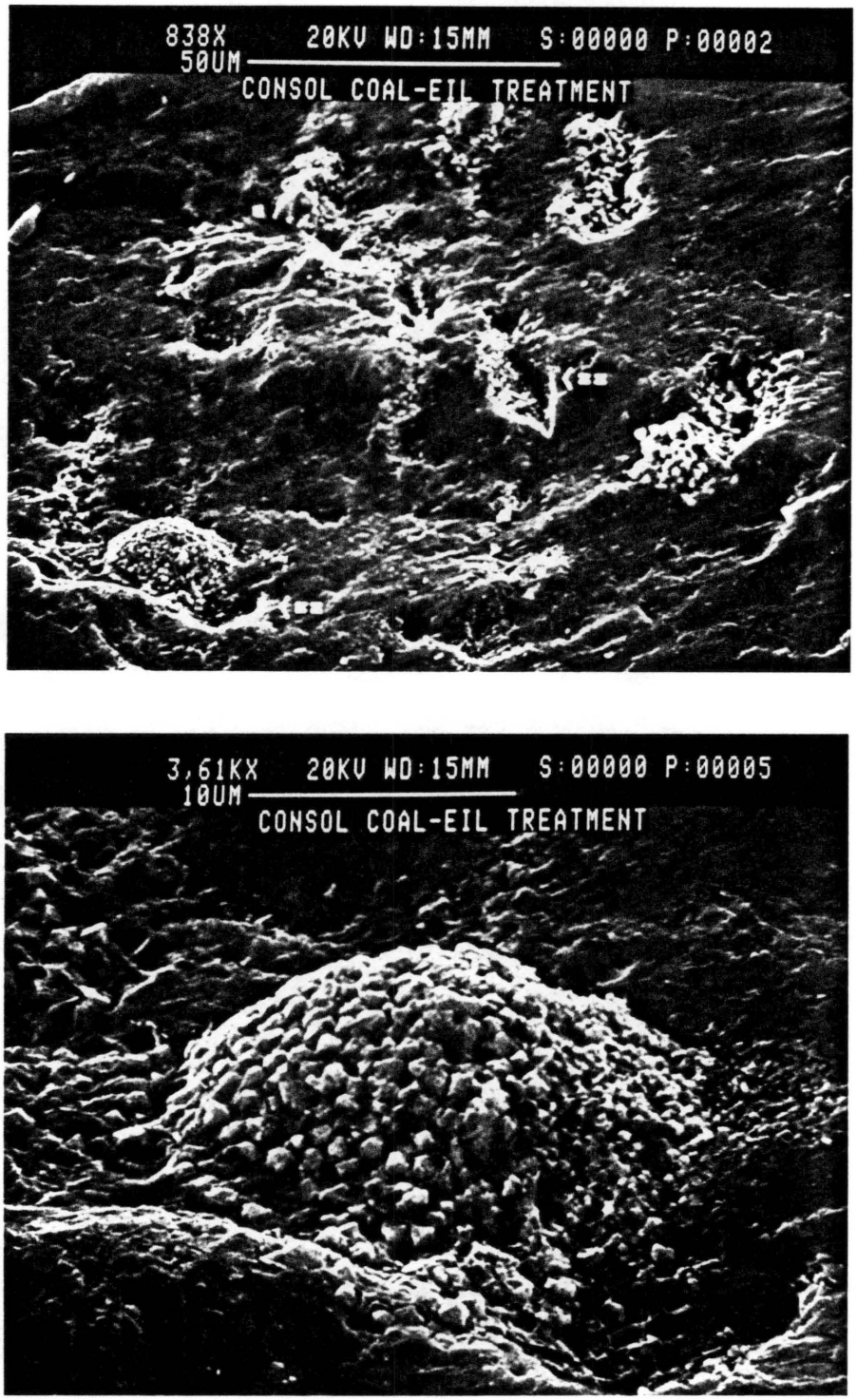

Figure 20. Typical Surfaces of EIL-Treated Consol Coal: (Top) Arrows indicate former pyrite inclusions. (Bottom) Enlargement shows details of former pyrite sites.

inclusions in most cases. Arrow A points to a pyrite framboid that was not removed by the EIL treatment. The compressive stresses holding it to the coal surface may have been larger than the osmotic pressure developed between it and the coal surface, thereby preventing its liberation. Arrow B points to three empty sites where pyrite inclusions had been located. This section is shown enlarged in the lower photomicrograph. If the removal of the pyrite from the coal was primarily due to ferric-ion leaching, which is basically a dissolution process, it is unlikely that an exposed pyrite inclusion (such as that shown by Arrow A), will remain intact after the treatment. Futhermore, all of the exposed pits are completely empty, as the EDAX analysis did not show the presence of any iron or other minerals inside the pits. Thus it is possible that the majority of the pyrite framboids were removed by a non-dissolution type liberation process, which caused a clean removal of the pyrite. These facts suggest that the bulk of the pyrite removal was caused by the osmotic pressure mechanism.

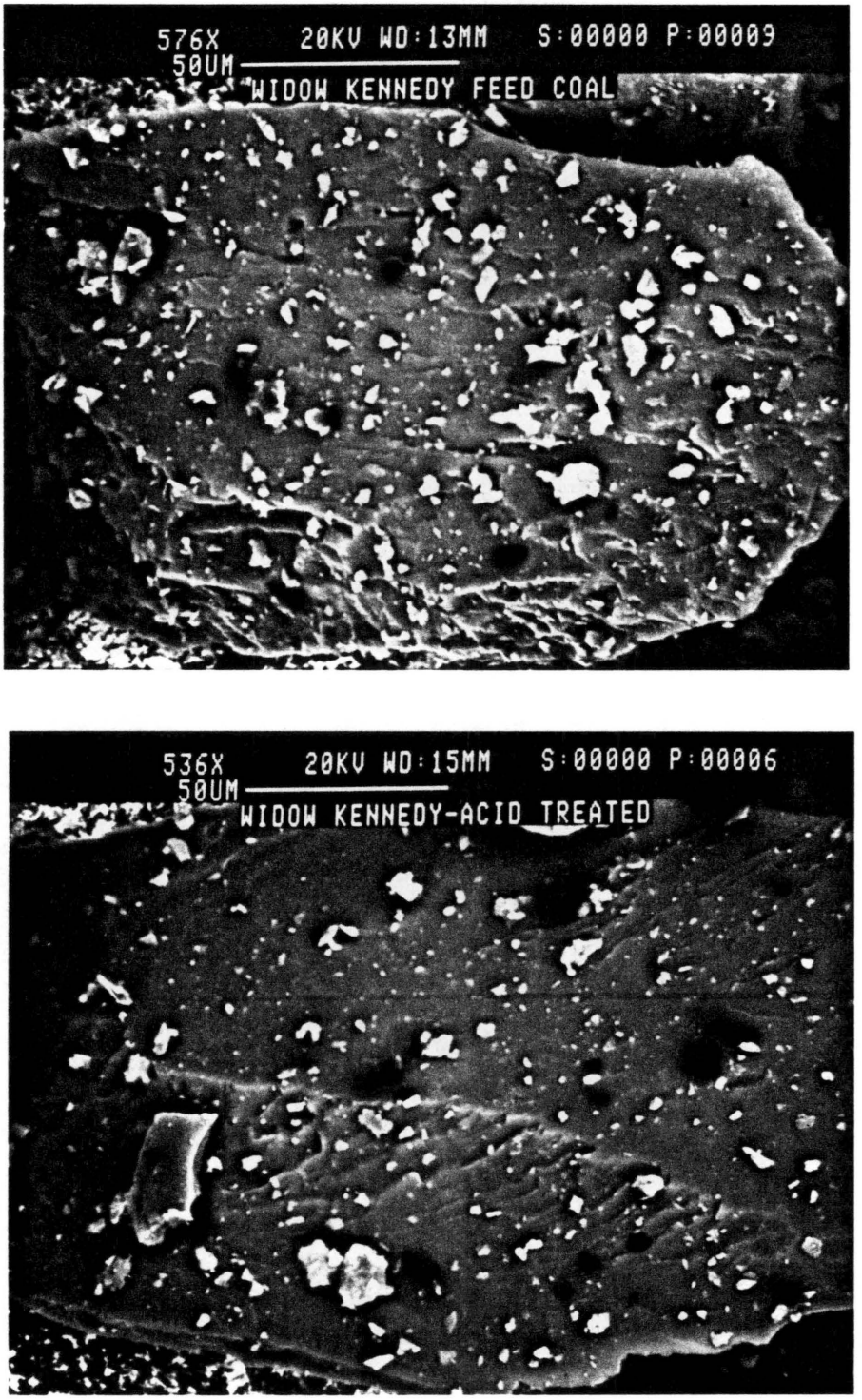

Figure 21. Photomicrographs of Widow Kennedy Coal: (Top) Feed coal -140 + 270 mesh. (Bottom) Acid treated Widow Kennedy coal.

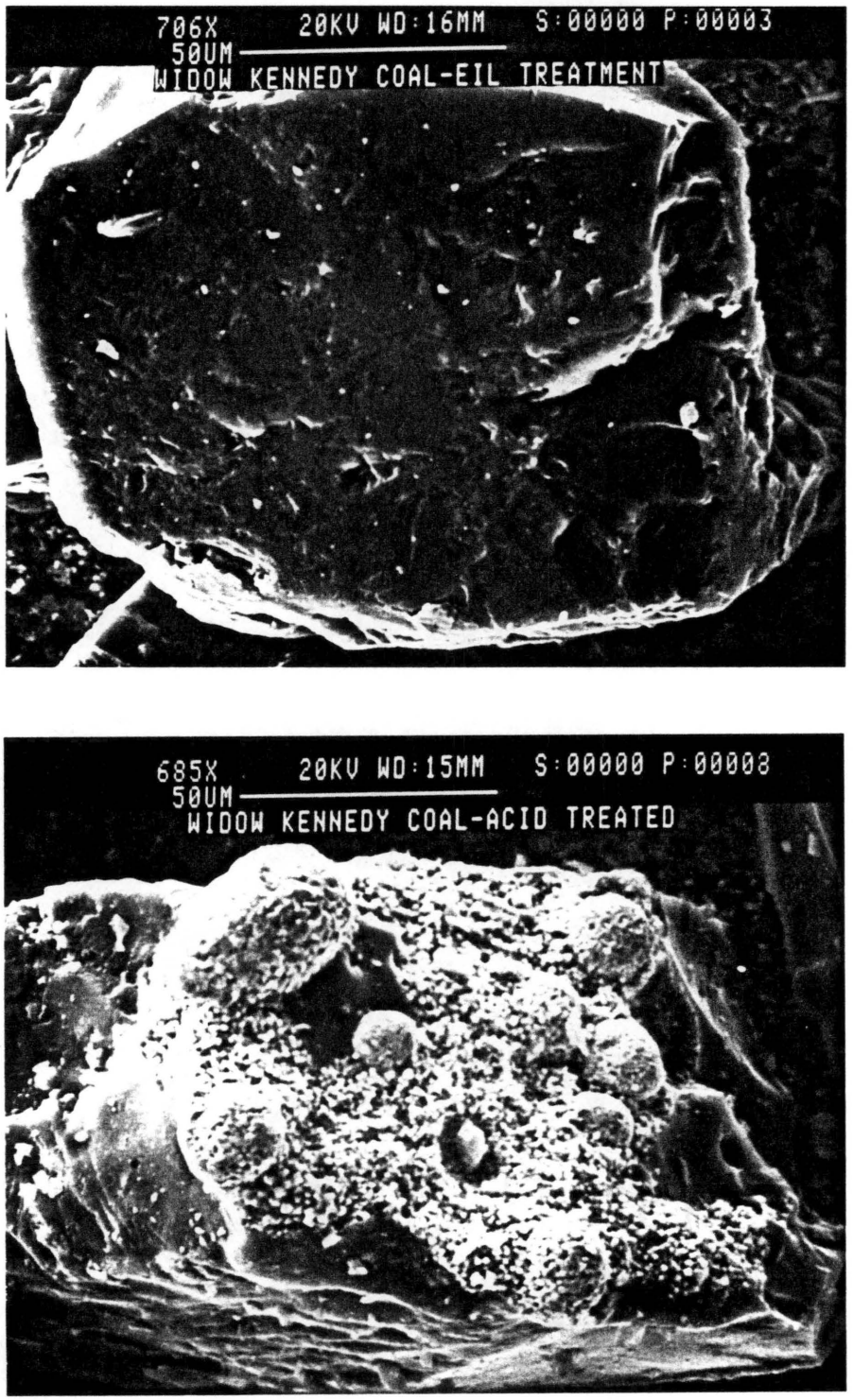

Figure 22. Typical Surfaces of Treated Widow Kennedy Coal: (Top) Surface of EIL treated coal. (Bottom) Pyrite clusters in acid treated Widow Kennedy coal.

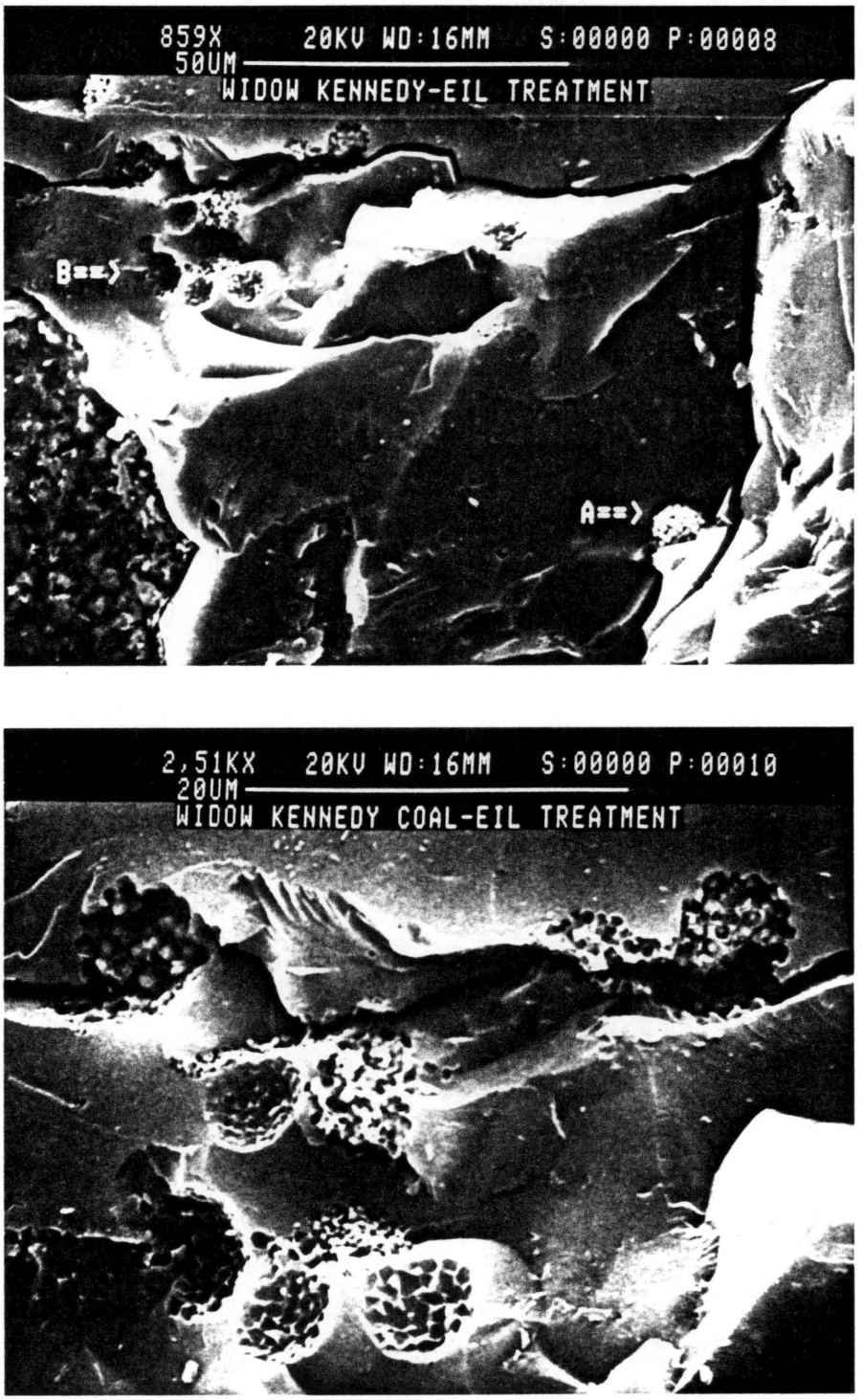

Figure 23. Typical Surfaces of EIL Treated Widow Kennedy Coal: (Top) Unremoved coal pyrite (A) and former pyrite sites (B). (Bottom) Enlargement of former pyrite sites.

5.0 THERMODYNAMIC MODELLING OF THE EIL PROCESS

5.1 Introduction

The preceding sections have illustrated the applicability of the EIL process towards coal cleaning. The EIL process involves a build-up of osmotic pressure inside the crevices and grain boundaries in the coal maceral. The development of the pressure is a result of several reaction stages, one of which may be rate controlling. A thermodynamic analysis may be used to calculate a numerical value for this pressure. If the analysis indicates that the pressure would be significantly large, then it is likely that this pressure fractures the coal to liberate the trapped mineral matter.

Although the concept of a repulsive force existing between charged double layers is well documented in the literature, it has not yet been applied to coal and to coal-cleaning. The primary task in applying an existing concept towards a new process is a systematic analysis of the process. Although thermodynamics, equilibrium or

non-equilibrium, can provide a conceptual frame work which facilitates the analysis of a process, a full understanding of the process requires a kinetic description. This would ideally be based on detailed models involving sub-processes, but the present level of understanding of the EIL process barely allows such detailed models to be developed. A singular objective of this analysis is, therefore, to determine the thermodynamic feasibility of the EIL process.

As time is not a factor in an equilibrium, equilibrium thermodynamics can only be used to predict certain transformations which would occur in a system under changing conditions. However, without the factor of time, the rates at which these transformations occur cannot be predicted. However, equilibrium thermodynamic considerations are not totally useless, even in situations where equilibrium is not maintained. Several thermodynamic functions, called "state functions" (examples include the internal energy, enthalpy, entropy and free energy of the system) can be assigned numerical values based solely on the state of the system prior to a process and the state of the system following the process. Of particular interest is the free energy which can be described as the Gibbs free energy or the Helmholtz free energy depending on the constraints within which the reactions take place. From the Gibbs free energy function, the values of an important thermodynamic variable, the chemical potential, may be calculated. The transfer through space of a component within a system (or across system boundaries) is dependent upon the gradient of the chemical potential of that component along the path of transfer. Equilibrium thermodynamic considerations thus indicate the end results of a process occurring within a system, although the exact details of the process itself may not be known.

5.2 *Analysis of the EIL Process*

A study of the EIL process requires two areas of investigation; (a) the thermodynamic feasibility of the process and (b) the kinetics of the said process. The first step, therefore, is to enumerate the various sub-processes involved in this process. It is assumed that ferric ions are already present in the system, either by external addition or by reaction of the acid with the iron-bearing minerals in coal.

5.2.1 Reaction Stages of the EIL Process

1. Diffusion of the ferric ion from the solution to the coal surface through the electrolyte.

2. Reaction of ferric ion with sessile bonds in the coal matrix. These bonds may involve oxidation of the hydroquinone/quinone or other groups present in coal to oxidize it via positively charged intermediates.

3. Movement of anions towards the positively-charged coal surface, setting up an ionic double layer. If these ions accumulate inside a pore or crevice on the coal surface, the chemical potential of water inside the pore or crevice will be decreased.

4. Flow of water into the pore due to the osmotic pressure caused by the difference in the chemical potential of water inside and outside the pore.

5. Increase of pressure inside the pore resulting in the ejection of mineral matter inside it. In the case of mineral matter that is held too tightly inside the pore, the pore fractures due to the increasing osmotic pressure and liberates the mineral matter entrapped inside it.

6. Regeneration of ferric ion from the spent ferrous ions at the electrode surface.

Steps 1-6 may now be repeated endlessly to force the electrolyte into the pore structure of the coal and to unlock the mineral matter entrapped deeper inside the pore. Since a certain portion of the mineral matter present in coal may be removed by dissolution, the following steps may occur simultaneously with those listed above.

7. Diffusion of the acid and ferric ions to the crevices in coal.

8. Reaction of ferric ions and/or sulfuric acid with the mineral matter entrapped inside the coal crevice.

9. Diffusion of dissolved mineral matter and ferrous ions out of the crevice filled with sulfuric acid and ferric sulfate solution. The ferrous ions result from the reaction of ferric ions with the mineral matter in coal.

Steps 7 to 9 constitute the basis of coal cleaning by ferric-ion leaching (Meyers, 1977; Dutrizac, 1974). However, in order to contact and dissolve mineral matter trapped inside a narrow pore on a coal particle, the acid or ferric solution must first flow into the pore. The characteristic pore radius of most coals ranges from 5 to 7 Å (Spitzer et al., 1977), although it may be larger with some coals. The theory of fluid flow through a

porous, anisotrophic material such as coal indicates that purely diffusion controlled migration without an external driving force cannot occur (Marcus, 1962). A simple application of Darcy's law for the flow of fluid through a porous medium such as coal indicates that the flow is proportional to the pressure gradient. Thus without an external driving force such as a pressure gradient, the acid will not flow into the pore structure of coal on its own accord. Even if highly reactive surface sites are present along the depth of the pore, the migration of ferric ions into the pore will be affected by the microscopic size of the pore. In addition, the presence of dissolution products remaining inside the pore will affect the diffusion of the reactant molecules into the pore (Shimada et al., 1984). The dissolution products inside small cavities are *not* easily removed and are dependent on the nature of the secondary fluid flow (*i.e.*, trapped eddies) inside the cavity (Alkire and Reiser, 1984). Unless secondary fluid motion inside the cavity is increased (for example, by an ingress of water from outside the cavity), the dissolution products tend to remain inside the cavity and adversely affect the kinetics of dissolution. Thus, the dissolution of mineral matter by acid or ferric ions inside the pores and crevices of coal, if any, will not occur without a driving force.

5.2.2 The EIL Mechanism

Mineral particles are usually associated with the coal in the form of inclusions in the coal matrix. If the mineral is acid-soluble and exposes a large surface area, it will dissolve in the acid, the kinetics following a mechanism similar to the Shrinking Core Model (Levenspiel, 1975). However, most mineral matter found in coal consists of clays and sulfides which are usually insoluble in acid under the experimental conditions of the EIL process. These minerals are usually present as inclusions in the pore stucture of

coal. During the EIL process, the rate of dissolution of an ***acid-soluble*** mineral trapped deep inside a narrow coal pore would depend on steps 7 to 9 listed earlier, which may be the rate determining step. Most mineral matter that is not in the free state is present in coal as shown schematically in Figure 24. One end of the pore or crevice in which the minerals are trapped is exposed to the surface of the coal particle and is in contact with the solution. The minerals are either too large to pass through the opening (Figure 24 (A)), or are compacted together so tightly that a physical force is required to push them out (Figure 24 (B)).

The ferric ions react primarily with the sessile bonds bonds of the coal matrix, but they may also react with stronger bonds after prolonged oxidation. Each ferric ion on reaction with the coal oxidizes the coal surface by removing an electron from it. The ferric ion is reduced to ferrous while the coal surface acquires a positive charge due to the loss of an electron from one of its sessile bonds. The ferrous ion is oxidized to ferric by the anode (or any other regenerative technique) and the process continues until there are no more sessile bonds left in the coal matrix for oxidation. However, as the coal surface becomes increasingly positive by oxidation, ferric ions will have an increasingly difficult time to gain access to the coal surface.

On a microscopic scale, the surface of coal is rarely smooth; it is marked with cracks, crevices and pores, many of which encapsulate mineral matter. Thus, a charged layer growing along two opposite walls of a crevice for example, will eventually overlap. At this stage, the positive and negative layers tend to inhibit the further passage of cations and anions into the pore. Anions attempting to migrate through such pores are repelled as well as cations because cations must remain with their anionic counterparts to retain the electrical neutrality of the bulk solution. The excess charged species inside the pore over that of the bulk reduces the chemical potential of water inside the pore. Driven by this difference, uncharged water molecules pass through the double layer,

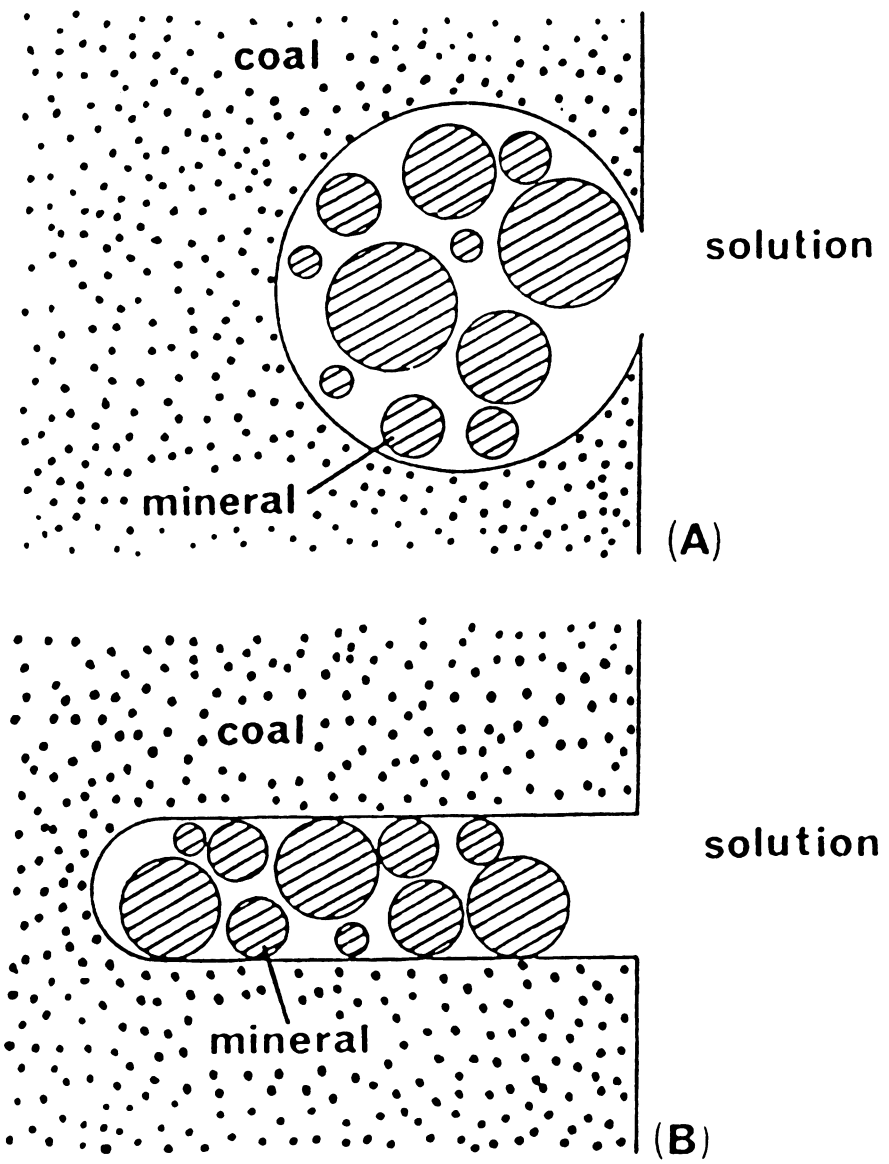

Figure 24. Schematic Representation of Mineral Matter Trapped Inside the Pores and Crevices of Coal.: Shaded areas represent mineral matter and dotted areas represent the coal matrix.

whereas the dissolved ions tend to be prevented from doing so by the charged bilayer. Osmosis results in a net passage of water from the bulk solution into the more concentrated solution inside the pore. If this solution is contained inside a rigid, confined pore space, the water flow will result in an increased hydrostatic pressure that will eventually raise the activity of water inside the pore. The osmotic flow will cease when the aqueous activities of the solutions inside and outside the pore are equal. If the confined pore space is unable to withstand the increased hydrostatic pressure, it will fracture, either partially or completely and cause (a) the solution to flow deeper into the pore and/or (b) the liberation of any entrapped mineral matter. Ferric ions may now react with sessile bonds further inside the pore and the above process repeats itself, forcing the bulk solution deeper into the pore and causing further liberation of the mineral matter. The movement of the anions towards the positive charges along the crack walls will partially account for crack propagation as each anion will carry its hydration layer along with it. The EIL mechanism for the removal of minerals or the penetration of the solvent into the pore structure of coal is summarized in Figure 25.

5.3 Estimation of the Osmotic Pressure Inside a Coal Pore

5.3.1 The Fundamental Osmotic Equation

The driving force for osmosis is the chemical potential difference of water on either side of the medium separating the two solutions. The medium may be a semi-permiable

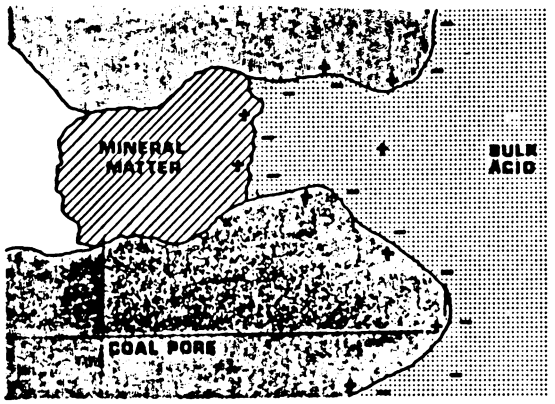

Step I: The coal surface aquires a positive surface charge in the the acidic medium (pH $\leq$1.0). A double layer of counter-ions forms along the coal surface.

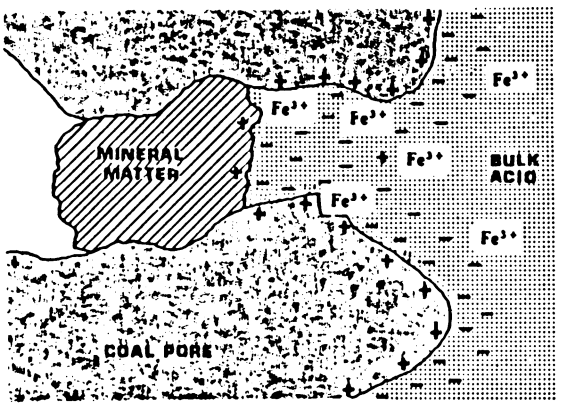

Step II: The reaction of ferric ions with the coal increases the charge on the coal and attracts more counter-ions to the vicinity of the coal surface.

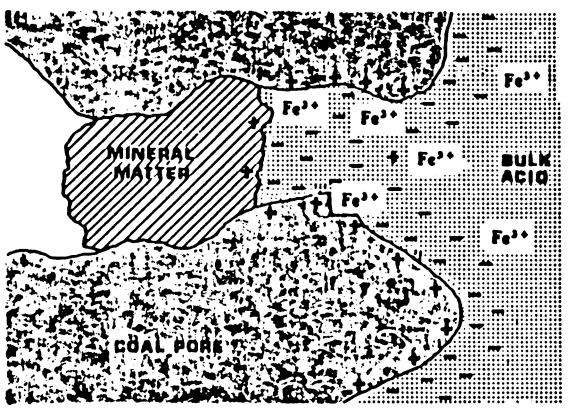

Step III. The increased ion concentration inside the pore reduces the aqueous chemical potential. The hydrostatic pressure inside the pore increases to equalize the aqueous chemical potentials inside and outside the pore.

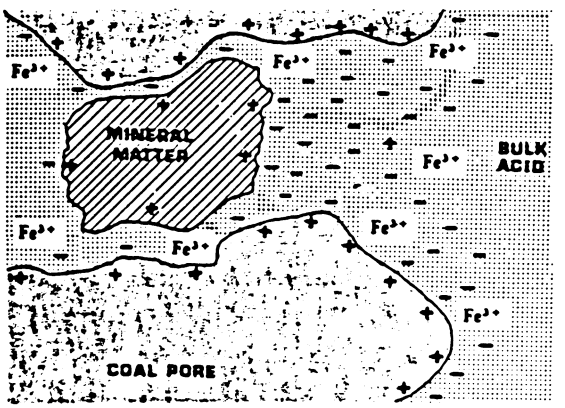

Step IV: The increased hydrostatic pressure fractures the pore and loosens the mineral particle. This in turn allows the electrolyte to penetrate further into the pore. Steps I-IV may be repeated to liberate other mineral particles embedded deep inside the pore.

Figure 25. Stages in the Liberation of a Mineral Particle Inside a Coal Pore during EIL Treatment.: Shaded areas = mineral matter, Dotted areas = acid solution, Dark areas = Coal matrix

membrane of animal (natural) or chemical (synthetic) origin or a charged bilayer of ions. Osmotic equilibrium is independent of how the membrane acts so long as it is permiable only to solvent (water) ions.

In the case of a coal pore, let the aqueous chemical potential inside and outside the pore be μ_I and μ_O respectively. P_I and P_O denote the pressures inside and outside the pore.

At equilibrium, the chemical potentials are the same; *i.e.*,

$$\mu_I(P_I) = \mu_O(P_O) \qquad [5.1]$$

Since the solution inside the pore is at a higher pressure than the solution outside, its aqueous chemical potential is increased by an amount given by

$$\int_{P_O}^{P_I} \frac{\partial \mu}{\partial P}\, dP$$

Thus equation [5.1] may be written as

$$\mu^{std} + RT \ln A_I + \int_{P_O}^{P_I} \frac{\partial \mu}{\partial P}\, dP = \mu^{std} + RT \ln A_O \qquad [5.2]$$

where A_I and A_O are the aqueous activities inside and outside the pore.

From thermodynamics, $\frac{\partial \mu}{\partial P}\, dP = \overline{V}$, where $\overline{V}$ is the partial molar volume of water. Equation [5.2] becomes

$$RT \ln A_I + \int_{P_O}^{P_I} \overline{V} dP = RT \ln A_O \qquad [5.3]$$

If the variation of the partial molar volume with pressure is assumed linear, the integral in equation [5.3] may be simplified to

$$RT \ln \frac{A_O}{A_I} = \overline{V}_m (P_I - P_O) \qquad [5.4]$$

where $\overline{V}_m$ is the mean partial molar volume of water inside and outside the pore. Since the osmotic pressure, $\Pi = P_I - P_O$

$$\boxed{\Pi = \frac{RT}{\overline{V}_m} \ln \frac{A_O}{A_I}} \qquad [5.5]$$

Hence the osmotic pressure inside the pore may be calculated if the mean partial molar volume and the activity of water inside and outside the pore are known. The ensuing sections discuss how these parameters may be calculated.

5.3.2 Activity of Water Outside the Pore

Methods of calculating the activity of water in electrolyte solutions were discussed in section 2.3.4. For this study, a statistical method was adopted. The osmotic coefficients of aqueous sulfuric acid solutions previously measured by several workers were represented by a semi-empirical equation (Rard et al., 1976). This equation is accurate to within ±0.5% in predicting the osmotic coefficient, Φ, for sulfuric acid

solutions at 25°C from concentrations ranging from 0.1-27.7 mol./kg.water. A minimum of seven polynomial coefficients were necessary to represent the experimental data in an equation of the form

$$\Phi = 1 - (\frac{A}{3}) m^{0.5} + \sum_{i=1}^{7} A_i m^{r_i} \qquad [5.6]$$

where A = 4.0743. The 7 coefficients A_i and powers, r_i which were determined by Rard et al. (1976) using a least-squares fit, are listed in Table 28. The errors in the A_i's increase as the powers increase, being 1.6-1.9% for the first five terms and 3.2-3.4% for the two highest powers.

Table 28. Empirical Parameters for the Osmotic Coefficient Equation

i	r_i	A_i
1	0.750	-5.545523727×10
2	0.875	2.087446992×10^2
3	1.000	-2.887967991×10^2
4	1.125	1.777105198×10^2
5	1.250	-4.112741365×10
6	3.125	$2.039232617 \times 10^{-3}$
7	3.375	$-6.467613632 \times 10^{-4}$

The activity of water may now be calculated from the following equation (Harned and Owen, 1958).

$$A_w = \exp - (\Phi \nu m M) \qquad [5.7]$$

where

A_w = Activity of water

v = Number of ions produced per molecule of dissolved solute

m = Molality of the solution in moles/Kg. water

M = Molecular weight of the solvent in Kg./mole

5.3.3 Activity of Water Inside the Pore

It is possible by thermodynamic means to determine the composition of ions that probably constitute the charge in an electrical double layer. Early studies on the adsorption of anions and cations on mercury led to methods of calculating Γ_+ and Γ_-, the excess of cations and anions in the double layer (Grahame and Soderberg, 1954). Ferric ions are not the only oxidants that render the coal surface positive. Coals oxidized without ferric ions may behave in the same way, except that in the presence of ferric ions, the oxidation may be intensified. If no specific adsorption occurs, the SO_4^{2-} counter-ions are adsorbed only by electrostatic attraction. Two opposing forces keep these counter-ions against the charged walls of the coal pore: the electrostatic attraction towards the charged surface and the Brownian diffusion flux away from the high concentration zone near the surface. When these opposing fluxes are just in balance, the system is in equilibrium and steady-state profiles of concentration and potential are established.

The net flux, N_i, of the negatively-charged counter-ions towards the charged coal surface may be obtained by applying the Nernst-Planck equation,

$$N_i = -D_i \frac{dC_i}{dx} + D_i \frac{C_i z_i F}{RT} \frac{d\psi}{dx} \qquad [5.8]$$

where z_i and C_i are the charge and concentration of the counter-ion. F is Faraday's constant and D_i is the ionic diffusivity.

At steady state, $N_i = 0$, so that

$$\frac{dC_i}{dx} = \frac{C_i z_i F}{D_i RT} \frac{d\psi}{dx} \qquad [5.9]$$

Equation [5.9] may be integrated to

$$C_i(x) = C_i^b \exp\left(-\frac{z_i F}{RT} \psi_{(x)}\right) \qquad [5.10]$$

where C_i^b is the concentration in the bulk of the solution and x is the distance measured normal to the charged pore wall. Equation [5.10] predicts the concentration of any adsorbed species, $C_i(x)$, if the potential at x and the bulk concentration are known. However, since potential is a variable and will change with distance x from the pore wall, it is necessary to derive an expression to relate the potential with distance in order to use equation [5.10].

Figure 26 depicts a typical coal pore during the EIL process. The charged surface and its anion dominated adsorption layer together define the Guoy double layer. If the pores are sufficiently large that the traversing ions are not influenced by the electrical field surrounding the pore walls, there will be no build-up of osmotic pressure as ions can flow freely in and out of the pore and equalize concentrations. Ferric ions will continue to react with the coal surface and increase its surface charge by electron abstraction until the ensuing double layers begin to effectively overlap. This restricts the further flow of charged ions and permits only the flow of uncharged water molecules in and out of the pore. When this stage is reached, the electrochemical potential gradient of the adsorbed ions is related to the potential gradient by the following equation;

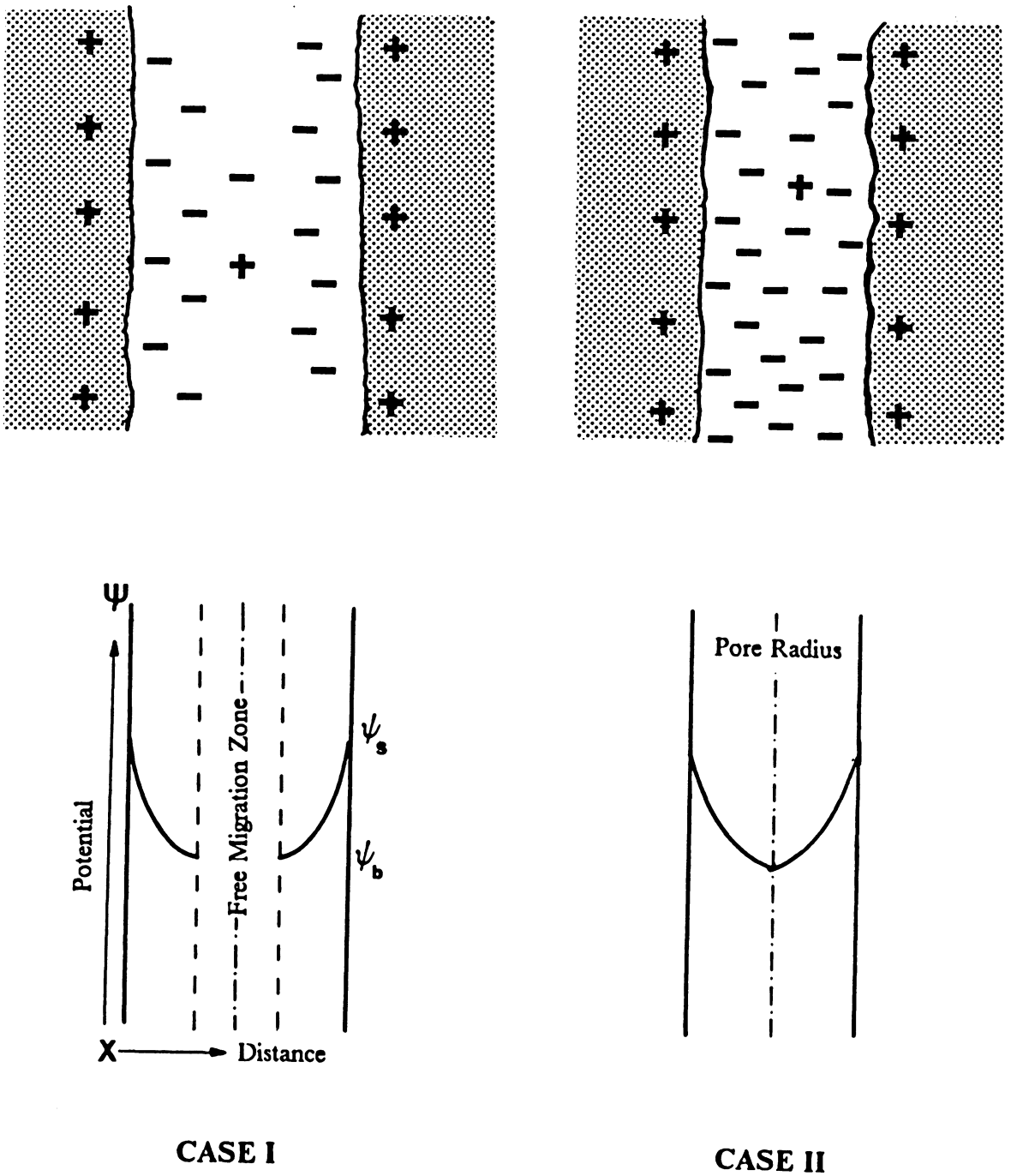

Figure 26. Double-Layer Conditions Inside a Coal Pore: Case I-No double layer overlap permits free flow of ions in and out of the pore. Case II-Double layer overlap prevents free flow of ions and creates an osmotic pressure inside the pore.

$$\frac{\partial \mu_i}{\partial x} = - z_i e \frac{\partial \psi_x}{\partial x} \qquad [5.11]$$

where μ_i is the electrochemical potential and z_i is the number of charges carried by the ith species inclusive of sign, e is the elemental charge of an electron and x is the distance measured outwards from the coal surface. ψ_x is the potential at x with respect to potential of the bulk solution, taken as zero.

If n_i represents the number of ions of type i per unit volume of solution and k, is the Boltzmann constant,

$$\mu_i = \mu_i^{std} + kT \ln n_i \qquad [5.12]$$

By differentiating equation [5.12] and substituting from equation [5.11]

$$\frac{d \ln n_i}{dx} = - \frac{z_i e}{kT} \frac{d\psi_x}{dx} \qquad [5.13]$$

Integrating and using the boundary condition $\psi = 0$ when $n_i = n_i^{bulk} = n_i^b$

$$n_i(x) = n_i^b \exp\left(- \frac{z_i e}{kT} \psi_x \right) \qquad [5.14]$$

where $n_i(x)$ represents the number of ions per unit volume at a distance x from the coal surface.

An expression for ψ_x may be obtained from the Poisson equation, written in one-dimension.

$$\frac{d^2 \psi_x}{dx^2} = - \frac{1}{\varepsilon \varepsilon_0} \rho_x \qquad [5.15]$$

where ρ_x is the space charge density given by;

$$\rho_x = \sum_{i=1}^{n} n_i e z_i = \sum_{i=1}^{n} n_i^b e z_i \exp\left(\frac{- z_i e \psi_x}{kT} \right) \qquad [5.16]$$

Combining eqns. [5.15] and [5.16] and dropping subscripts,

$$\frac{d^2\psi}{dx^2} = \frac{e}{\varepsilon\varepsilon_0} \sum_{i=1}^{n} n_i^b e z_i \exp\left(\frac{-z_i e \psi}{kT} \right) \qquad [5.17]$$

Integrating [5.17] and using the boundary condition that $\frac{d\psi}{dx} = 0$ at $\psi = 0$

$$\left(\frac{d\psi}{dx} \right)^2 = \frac{2kT}{\varepsilon\varepsilon_0} \sum_{i=1}^{n} n_i^b \left[\exp\left(\frac{-z_i e \psi}{kT} \right) - 1 \right] \qquad [5.18]$$

Since sulfuric acid is present primarily in the form H^+ and HSO_4^- at pH $\leq$ 2.0, it may be considered a symmetric electrolyte. Equation [5.18] will simplify to

$$\frac{d\psi}{dx} = -\left(\frac{8kTn^b}{\varepsilon\varepsilon_0} \right) \sinh\left(\frac{ze\psi}{2kT} \right) \qquad [5.19]$$

An expression for the variation in potential with distance from the wall of the cavity may be obtained by rearranging and integrating equation [5.19],

$$\int_{\psi_0}^{\psi} \frac{d\psi}{\sinh\left(\frac{ze\psi}{2kT}\right)} = -\left(\frac{8kTn^b}{\varepsilon\varepsilon_o}\right)\int_0^x dx \qquad [5.20]$$

where ψ_0 is the potential at $x=0$. Integrating equation [5.20]

$$\frac{2kT}{ze}\ \ln\left\{\frac{\tanh\left(\frac{ze\psi}{4kT}\right)}{\tanh\left(\frac{ze\psi_0}{4kT}\right)}\right\} = -\sqrt{\frac{8kTn^b}{\varepsilon\varepsilon_0}}\ x \qquad [5.21]$$

Let $\kappa = \sqrt{\frac{2n^b z^2 e^2}{\varepsilon\varepsilon_0 kT}} = \sqrt{\frac{2NC^b z^2 e^2}{\varepsilon\varepsilon_0 kT}}$ where N is the Avogadro number and C^b is the bulk molar acid concentration. Equation [5.21] thus becomes

$$\frac{\tanh\left(\frac{ze\psi}{4kT}\right)}{\tanh\left(\frac{ze\psi_0}{4kT}\right)} = e^{-\kappa x} \qquad [5.22]$$

Setting $e^{-\kappa x}\ \tanh\left(\frac{ze\psi_0}{4kT}\right) = \chi$, equation [5.22] can be written as,

$$\frac{ze\psi}{4kT} = \frac{1}{2}\ln\left(\frac{1+\chi}{1-\chi}\right)$$

or

$$\psi = \frac{2kT}{ze}\ln\left(\frac{1+\chi}{1-\chi}\right) \qquad [5.24]$$

Equation [5.24] relates the change in potential with distance in the double layer surrounding the charged coal surface. The expressions for χ and for κ have been defined earlier.

The values of χ for different values of x may now be substituted in equation [5.10] to obtain a relationship between the change in the counter-ion concentration with distance from the charged surface. However, equation [5.10] provides a value for the concentration inside the pore at only ***one point.*** and this cannot be taken as a representative ionic concentration of the solution inside the pore. An average concentration inside the pore may be obtained by calculating the first moment of the surface concentrations, $C_i(x)$, obtained from equation [5.10] for values of x measured from the pore wall throughout the thickness of the double layer, according to the equation given below.

$$\frac{\sum_{j=1}^{n} x_j C_i(x_j)}{\sum_{j=1}^{n} x_j} \qquad [5.25]$$

where $\sum_{j=1}^{n} x_j$ = an average pore radius or crevice width.

5.3.4 Partial Molar Volume of Water

The third unknown in the general equation for osmotic pressure is the mean partial molar volume of water in the sulfuric acid solution inside the pore and in the bulk. The partial molar volume of water *(PMVW)* is a function of the solution concentration. A

short note on partial molar volumes is given prior to discussing the method used to obtain an expression relating the *PMVW* to the acid concentration.

5.3.4.1 Ideal Solutions

A solution is considered ideal when the partial molar volume of a component in that solution is the same as the molar volume of that component in the pure state; *i.e.*, there is no volume change in the mixture when the components are mixed together. However, sulfuric acid solutions are not ideal except at very low concentrations.

5.3.4.2 Partial Molar Properties

If M represents any molar thermodynamic property (*i.e.*, volume, enthalpy, entropy, etc.,) of a solution in which i is any single component, the partial molar property of component i in that solution is given by

$$\hat{M}_i = \left[\frac{\partial(nM)}{\partial n_i} \right]_{T, P, n_j, n_k \ldots} \qquad [5.26]$$

where n_i, n_j, n_k ... are the number of moles of components i, j, k ... in solution.

The partial molar property of component i, designated by the symbol $\hat{M}_i$, reflects the contribution of component i to the total property of the solution. If the total property of interest is the volume of the solution made up of a moles of component A, b moles of component B etc., the total volume of the mixture is given by

$$V_{net} = \sum a\hat{V}_A + b\hat{V}_B + c\hat{V}_C \ \ldots \qquad [5.27]$$

or, in general,

$$V_{net} = \sum_{i=a}^{n} n_i \hat{V}_i \qquad [5.28]$$

5.3.4.3 Partial Molar Properties of Water in Sulfuric Solutions

If equation [5.28] is applied to a binary system consisting of sulfuric acid and water,

$$V_{net} = n_w \hat{V}_w + n_a \hat{V}_a \qquad [5.29]$$

where

n_a = number of moles of sulfuric acid in solution,

$\hat{V}_a$ = partial molar volume of sulfuric acid,

n_w = number of moles of water in acid solution,

$\hat{V}_w$ = partial molar volume of water in acid solution.

However, this expression is not in a convenient form to obtain partial molar volumes from experimental data and is usually transformed to the form shown in equation [5.30]. This somewhat tedious derivation is found in Smith and Van Ness (1987).

$$\hat{V}_w = V_{avg} - X_a \frac{dV_{avg}}{dX_a} \qquad [5.30]$$

where V_{avg}, the average molar volume of the solution, is given by

$$V_{avg} = \frac{V_{net}}{n_a + n_w} \qquad [5.31]$$

and X_w, the mole fraction of sulfuric acid in solution is given by

$$X_a = \frac{n_a}{n_a + n_w} \qquad [5.32]$$

Values for V_{avg} are calculated by carefully adding known volumes of concentrated sulfuric acid to water and measuring the final volume of the solution, after equilibration. From the number of moles of water and acid added together, values for V_{avg} are calculated using equation [5.31].

Figure 27 shows the change in V_{avg} with X_a for the binary sulfuric acid-water system. Values of the derivative $\frac{dV_{avg}}{dX_a}$ are obtained by the slopes of the lines drawn tangent to the curve at several points. The tangent intercepts on the vertical axis yield the partial molar volumes of water as X_a, the acid mole fraction varies from 0 (pure water) to 1 (pure acid), (Smith and Van Ness (1987).

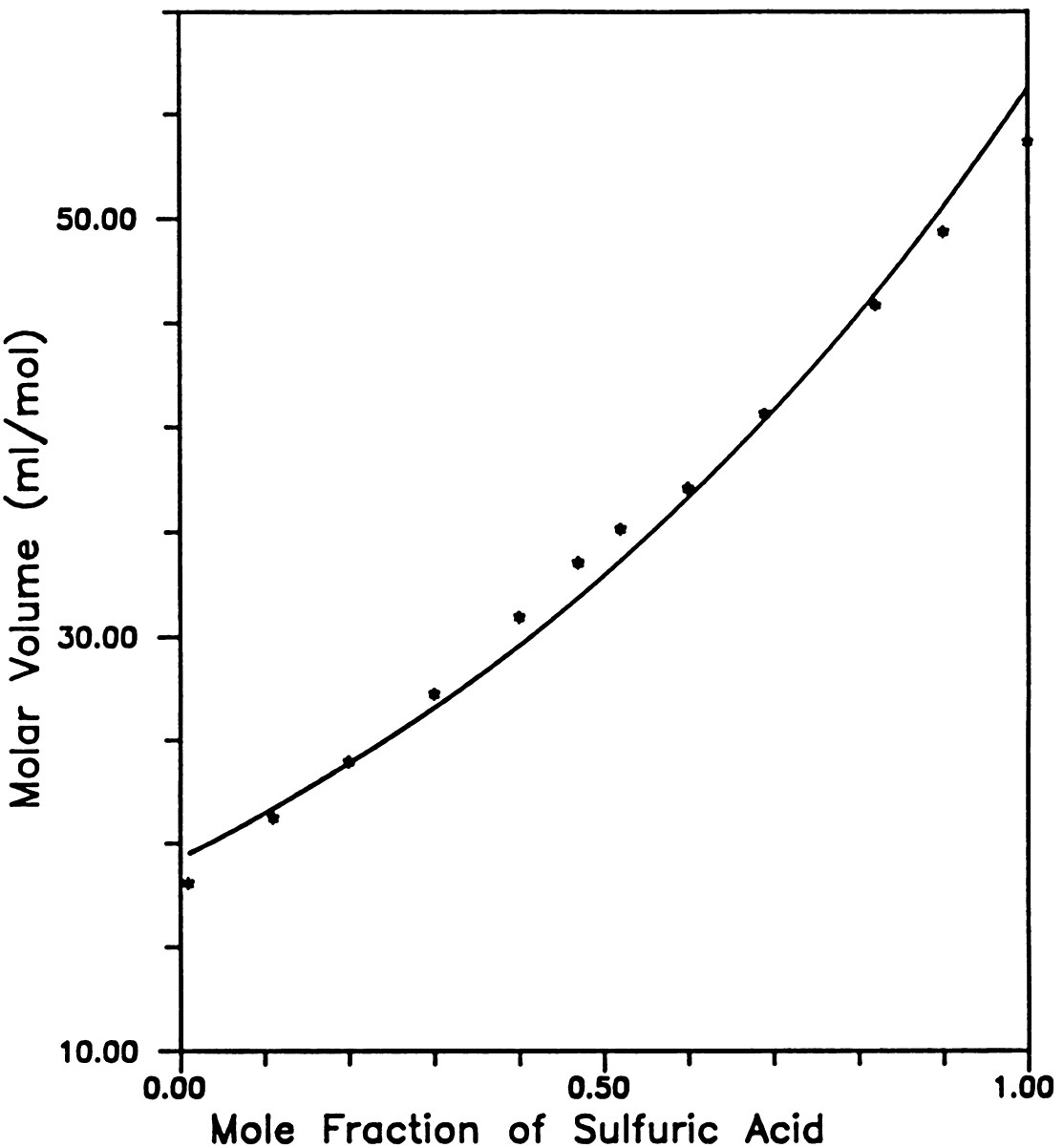

Figure 27. Molar Volumes for the Sulfuric Acid-Water System

Table 29. Partial Molar Volumes of Water in Sulfuric-Acid Solutions

Mole Fraction	Molar Concentration *moles/ℓ*	Partial Molar Volume *(ml).*
0.0	0.00	18.0
0.1	4.60	17.9
0.2	7.86	17.5
0.3	10.29	17.0
0.4	12.17	16.5
0.5	13.67	16.0
0.6	14.89	15.5
0.7	15.90	14.0
0.8	16.76	13.5
0.9	17.50	11.0

Table 29 lists the partial molar volumes of water in sulfuric acid solutions obtained by this procedure. The acid concentrations are given in mole fractions and molar units. Nevertheless, a table of the partial molar volumes of water at different acid concentrations are not suitable for repetitive, computer-based calculations. Since the system behaves almost linearly for sulfuric acid concentrations upto 12.17M and the experimental conditions of the EIL process deal with acid concentrations well below this value, it is reasonable to represent the data within the linear range by an equation obtained from regression analysis to relate the partial molar volumes of water to sulfuric acid concentrations and this is shown in equation [5.33]. The standard deviation for this equation is 0.99, which is sufficiently within the limits of experimental error.

$$\hat{V}_w = 18.23 - 4.39X_a \qquad [5.33]$$

Equation [5.5] may now be combined with equations [5.7] and [5.10] to calculate the osmotic head of water developed when two sulfuric acid solutions are separated by a

membrane or even a charged bilayer. The model requires input parameters of the bulk acid concentration, the surface charge on the solid particles creating the double layer and a length parameter corresponding to the pore diameter in the most general case. As shown in Figure 26, the charged bilayer surrounding two adjacent surfaces cannot exhibit any ion-exclusionary properties unless the surfaces are close enough for the double layers to overlap. When applied to a coal crevice, for example, the width of the crevice must be such that the double layer thicknesses on the walls of the pore are comparable with the pore radius in magnitude. Assuming this criterion is satisfied, it is possible to compute values of the osmotic pressure as functions of the pore size and the surface charge for known values of the bulk sulfuric acid concentration.

5.3.5 Surface Potential of Coal

A value for the surface potential of coal, appearing in equation [5.20] is required for the calculation of the osmotic pressure. It is well known that most coals possess a positive charge at pH < 2.0 as indicated by zeta-potential measurements. Different seams of coal have different zeta-potentials at a given pH. This type of behavior is partially attributed to the mineral matter present in the coal. These minerals are invariably charged in aqueous environments and the measured zeta-potential of a coal reflects a contribution from the charge aquired by the minerals present in the coal. The zeta-potential of coal is therefore related to its elemental composition which includes its ash and sulfur weight percent and has been quantified by semi-empirical equations (Mori et al., 1984).

5.3.5.1 Charging Mechanisms of Coal

The surface charges of solids originate through processes that involve the components of the solids themselves or in which the solids serve as hosts to other adsorbed species. For particles dispersed in liquids, the two most common are the ionization of chemical groups at the particle surface and the differential adsorption of ions from solution. Simple oxide minerals such as silica and alumina are usually charged by the adsorption of H^+ or OH^- ions on to amphoteric sites on the mineral surface. The surface charge of complex oxides can originate by the adsorption of charged hydroxo-complexes through different adsorption mechanisms (Parks, 1965). The charging mechanisms of coal macerals are not well understood due to the heterogeneous nature of their surfaces that contain complex organic substances and finely disseminated inorganic compounds. However, some striking similarities observed between the electrokinetic results of coal and oxide minerals suggest that hydronium and hydroxyl ions may be the potential determining ions for the coal surface, as in the case of oxides (Campbell and Sun, 1970). The organic and inorganic portion of the coal surface may have an outer oxide layer or an outer layer that has oxide-like characteristics. A surface charge may be established by the adsorption of hydronium or hydroxyl ions or by a dissociation of surface sites to form either a positive or negative charge (Parks, 1965). Although coal is a complex combination of organic macerals and inorganic minerals, it may therefore be assumed to behave as a pseudo-oxide where the potential determining ions are the hydroxyl and hydronium ions. Equation [5.34] is an equation for calculating the surface potentials of oxide minerals which may now be applied to coal (Parks, 1967).

$$\psi_0 = \frac{RT}{F}(pH_{pzc} - pH) \qquad [5.34]$$

in which pH_{pzc} is the pH (point-of-zero charge) at which the mineral or coal aquires no net surface charge, R is the gas constant, T is the temperature and F the Faraday's constant.

5.4 *Predictions from the Model*

5.4.1 Pore Size and Surface Porosity

The values of the osmotic pressures calculated by the EIL model are shown as functions of the pore radius in Figure 28. The osmotic pressure decreases exponentially with pore radius and are larger than the tensile stresses of most coals (Jaeger and Cook, 1979), and are therefore sufficient to cause fracture. At very small pore radii (<10 Å), it is unlikely that the high osmotic pressures predicted will be realized as other short-range surface forces will become operative. However, the values of the osmotic pressure predicted by the EIL model are within range of the osmotic pressures predicted by other models found in the literature, although these models utilized different approaches and computational techniques (see Sec.2.3.4). Coal is a heterogeneous organic solid with complex structure and composition. Thus any behavior predicted by the EIL model when applied to coal may not always prove consistent with experimental behavior. In most cases however, the correlation between actual behavior and theoretical expectations was sufficient to provide a significant degree of confidence in the EIL model.

When the pore spacing is extremely small, ionic diffusion will be severely impeded and it is unlikely that a double layer will be formed inside the pore. If the pore spacing is too large, the double layers surrounding the pore walls will not overlap and no ion-exclusionary properties will be exhibited by the pore (see Figure 26 on page 153). In either case, no osmotic pressure will develop inside the coal pore. Further, a coal surface that does not have many pores or cracks will develop only a planar distribution

of charges along its surface. In this situation, there will be a dearth of surfaces facing each other (as in a pore or crevice, for example). This reduces the opportunities normally available on rough surfaces for the double layers present on these surfaces to overlap and produce the desired osmotic effects. According to the model, therefore, for a given set of physical conditions, ***only*** those coals whose pore diameters fall within a certain range will exhibit double layer interaction and permit the build up of an osmotic pressure inside them to cause fracture. In addition, coals with a relatively smooth surface (on a microscopic scale), devoid of any cracks or crevices may be expected to respond poorly to the EIL process.

5.4.2 Surface Potential Changes

The coal surface may be expected to increase its positive charge when ferric ions are present in the system due to the electron abstraction mechanism discussed earlier. The zeta potential of coal increases with cations of increasing charge while the anions of these salts act as indifferent electrolytes (Campbell and Sun, 1970). With increasing concentrations of cations, the charge on the coal surface becomes more positive and hence, the surface potential of the coal and its pzc are increased. This has been experimentally shown for the effect of calcium ions added to coal over a wide pH range (Dawei et al., 1986). However, it is not possible to conduct similar measurements with ferric ions at the operating pH ranges of the EIL process which is ≤ 0.5. Most instruments for measuring zeta potentials are inaccurate at pH values ≤ 2.0, and ferric ions precipitate out at pH ≥ 4.0. Nevertheless, from the zeta potential changes in coal in the presence of other cations, it is reasonable to assume that ferric ions would cause similar, if not greater, changes due to the chemical oxidation of the coal by the ferric

ions. To examine the effect of surface potential increases on the osmotic pressure, it was assumed that the surface potential of the coal is not affected by changes in the sulfuric acid concentration. This assumption is reasonable, since the pH of sulfuric acid of concentration $\geq$ 1.0M is below 1.0, and most coals do not show a significant change in zeta potential at a pH$\leq$1.0. Figure 28 shows the change in the osmotic pressure developed inside a coal pore during the EIL process at different values of the surface potential. The increase in surface potential at a given sulfuric acid concentration increases the osmotic pressure developed inside the pore. The osmotic pressure increase becomes marginal for increases in the surface potential beyond 200mV. Increases in the surface potential within the 50-150mV range result in the largest increases in the osmotic pressure.

5.4.3 Sulfuric Acid Concentration

The changes in the sulfuric acid concentration will affect the aqueous activities and the partial molar volumes of water and hence, the osmotic pressure developed inside the coal pore. The pH's of the sulfuric acid solutions at varying concentrations were previously determined and the pzc of the coal used (Elkhorn seam) was determined to be 6.1. The surface potential on the coal for each acid concentration was obtained by using equation [5.34]. Figure 29 shows that the osmotic pressure increases with increasing sulfuric acid concentration at a given pore size. Thus the use of higher acid concentrations in the EIL process should result in improved ash rejection. This is exemplified in the experimental results discussed from Table 5 on page 72 and Table 10 on page 78.

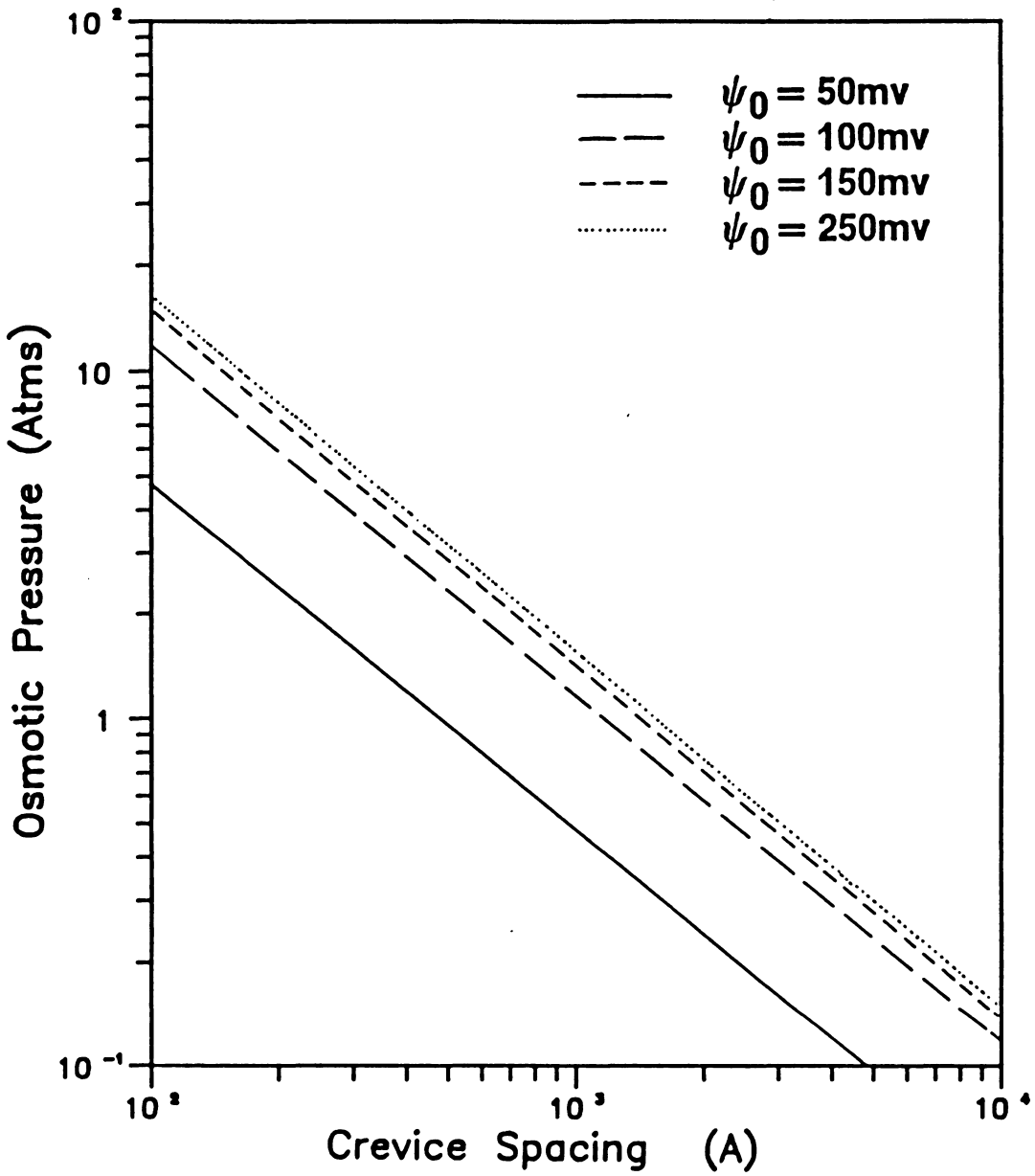

Figure 28. Osmotic Pressure Changes with Surface Potential During the EIL Process: Osmotic pressure changes inside a coal pore as a result of the increase in the surface potential of coal in a 1.0mol/ℓ sulfuric acid solution. This may be intensified by the oxidation of the surface of coal by ferric ions.

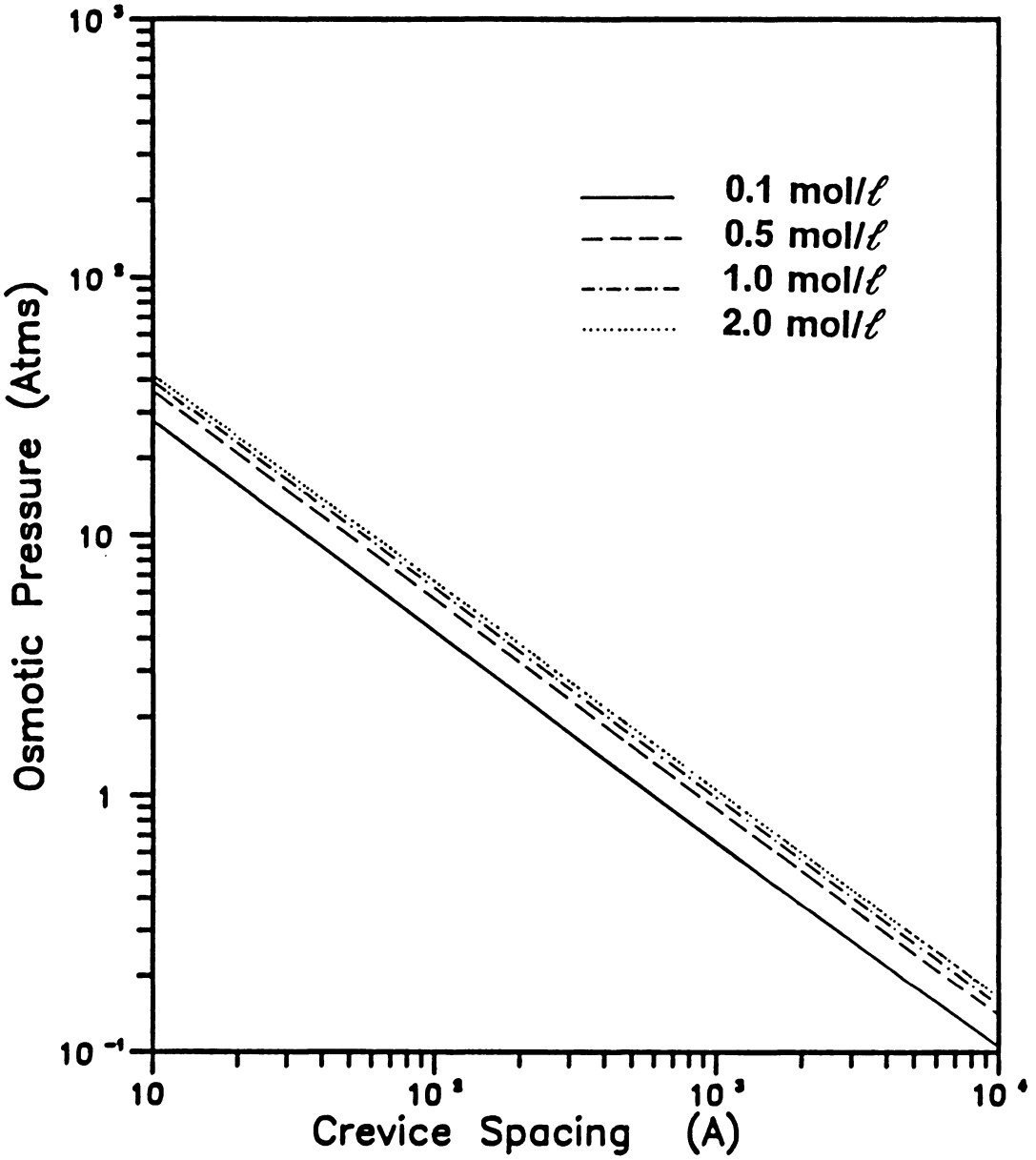

Figure 29. Theoretical Osmotic Pressure Developed Inside a Coal Pore During the EIL Process

5.5 *Limitations of the Model*

As with any mathematical description of a physical process, there will always be a point after which the mathematical results obtained will not make sensible physical correlations. With the osmotic pressure model, there are certain input values of parameters that do not produce any physically meaningful output data. In particular, for values of the crevice spacing or double layer separation below 10Å, the model predicts values for the sulfuric acid concentration inside the crevices larger than any physically obtainable concentration of sulfuric acid. As a result of this, the model predicts osmotic pressures in the order of a few hundred atmospheres for crevice separations <10Å. Owing to this limitation, Figure 28 on page 169 and Figure 29 on page 170 show only values of the osmotic pressure obtained only when all intrinsic values calculated by the model were physically feasible.

Secondly, the osmotic pressure model is based on classical double layer theories that have proven to be sufficiently accurate for most purposes. However, the model will break down whenever it is applied in situations where the double layer equations themselves are not valid. Furthermore, the validity of the classical double layer equations have been challenged on many occasions, particularly when double layer overlap is involved (Hogg et al., 1966). When the overlap is such that the co-ions are completely expelled and counter-ions are squeezed into a smaller volume (which may well occur during the EIL process), the classical equations need to be modified or new approaches developed to account for the increased repulsive force caused by the overlap (Spitzer, 1984). Thus the validity of the present model is also limited by the validity of the equations on which it was developed.

5.6 *Verification of the Model*

Most models involving short-range hydration forces described in the literature have not been directly verified. Although some have been indirectly verified (Israelachvili and Adams, 1978, Viani et al., 1983), the evidence is insufficient to dispel all degrees of uncertainty (Franks, 1981). However, some attempts were made to verify the osmotic pressure model, which showed some degree of correlation between the measured and theoretical values of the osmotic pressure.

The osmotic pressure model predicts the osmotic pressure developed when a charged surface separating two solutions of different concentrations behaves as a semi-permiable membrane. To predict the theoretical osmotic pressure, the model requires values for the surface potential, sulfuric acid concentration and pore spacing. To avoid problems caused by the heterogeneous nature of coal, the verification was attempted using a material with homogeneous properties, such as quartz. The first apparatus used for the verification of the model was a modified thistle tube with a stretched membrane at its open end. The bell-shaped compartment of the thistle tube was filled with quartz whose zeta potential behavior with pH was known. The tube was next filled with sulfuric acid solution while its mouth was contacted with a less dilute solution via the stretched membrane. However, several problems were encountered with this apparatus. Firstly, since the membrane itself had semi-permiable properties, it was not certain whether the rise in level of the liquid in the thistle tube was caused by the membrane or by the quartz inside the tube. Although this could have been circumvented by running blank runs with and without the quartz, a second more important design defect became apparent. In order for any mineral to exhibit semipermiable properties and behave as an osmotic membrane, it needs to be compressed such that the ionic double layers surrounding

adjacent particles overlap (Marine and Fritz, 1981). If this criterion was not satisfied, ions could pass freely through the quartz particles and hence, the quartz would not exercise any ion-exclusionary (*i.e.*, semi-permiable) characteristics.

It was therefore necessary to compress the mineral powder to allow the double layers on the particles to overlap. In reality, this would simulate the situation inside a crevice of a coal particle, where the width of the crevice would be small enough to permit the double layers on both walls of the crevice to overlap. A different design was employed in an attempt to provide this situation. Figure 30 shows a line diagram of the apparatus used which consisted of a cylinder whose base was closed off by a porous cap. A polypropylene pad was inserted between the end of the cylinder and its cap to support the mineral powder. The piston at the other end could move freely through the cylinder via a screw mechanism, by which the mineral contained inside the cylinder could be compressed to the desired extent. The mineral particles are shown greatly enlarged in relation to the cylinder in the Figure. The piston also had a narrow tube running concentric with its axis which extended much higher above the piston than shown in the Figure. Water flowing up into the cylinder by osmosis would rise up along this tube until the hydrostatic pressure became equal to the osmotic pressure.

A sample of very fine quartz (mean particle size $\leq 5\mu$) was selected as a suitable material for verifying the model. The electrokinetic properties of quartz are well documented in the literature or may be easily measured and are homogeneous and reproducible, unlike coal. Firstly, the zeta potentials of quartz were determined in sulfuric acid solutions of concentrations 10^{-4} to 10^{-1}mol/ℓ. A slurry of quartz and 10^{-4}mol/ℓ sulfuric acid was placed in the cylinder and left for several hours to ensure that every particle was wetted by the acid and formed double layers. The piston was rotated downwards to compress the slurry and cause overlap of the double layers surrounding the quartz particles. The porous base of the cylinder was placed in distilled

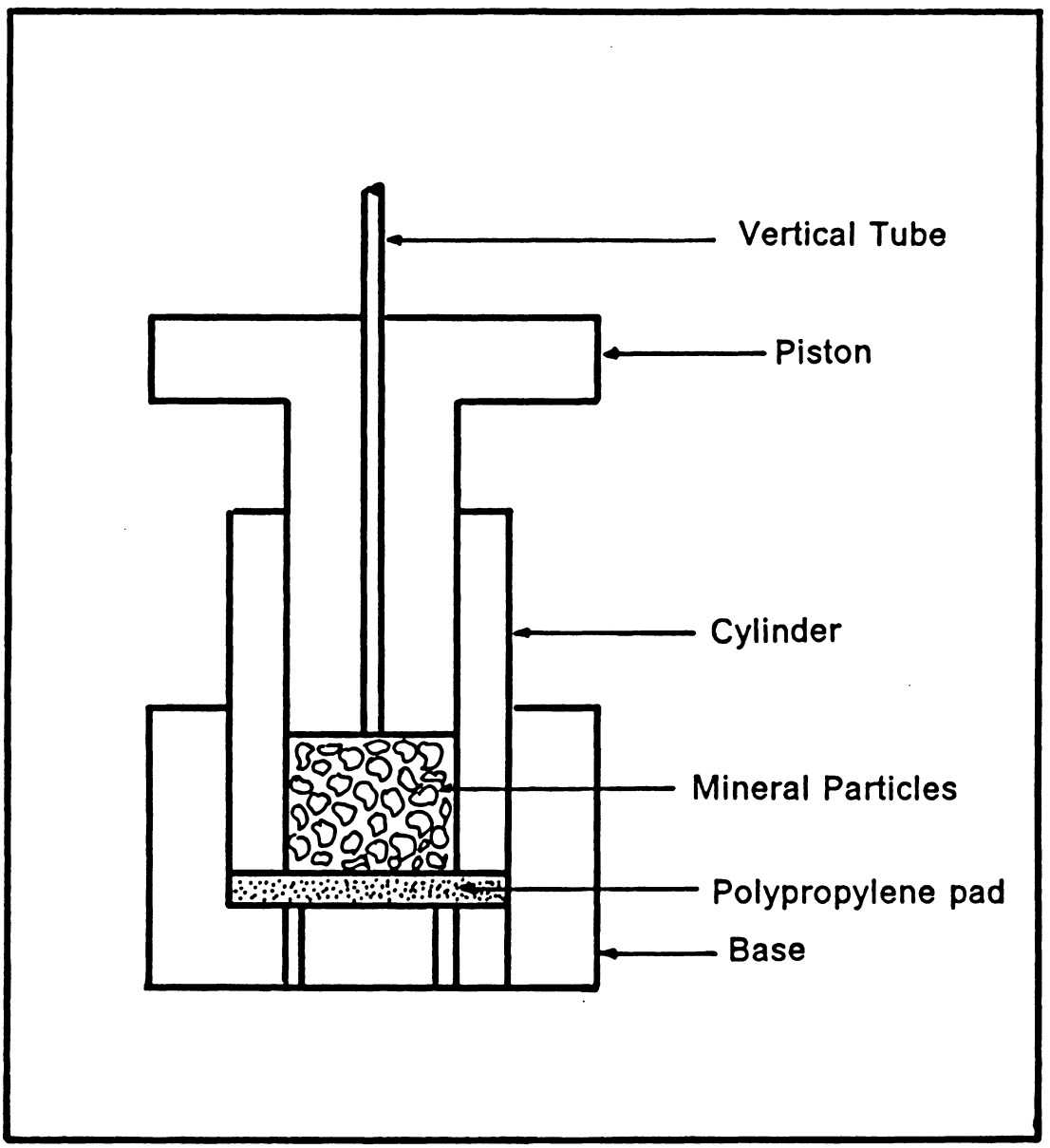

Figure 30. Apparatus for Measuring Osmotic Pressure Induced by Charged Particles

water and the rise in the level in the vertical tube was recorded after equilibration, which took 3-10 hours, depending on the degree of compression of the slurry. A highly compressed slurry took longer to equilibrate, although the rise in level of water in the vertical tube was higher. While increased compression increases double layer overlap (and hence, the osmotic behavior of the quartz), the diffusion of water through the quartz bed is severely affected by the decreased porosity.

The theoretical osmotic pressure for the quartz-sulfuric acid system may be calculated by applying the osmotic pressure model discussed earlier in this section. The first input parameter for the model, *i.e.*, the surface potential of quartz in sulfuric acid solutions, may be obtained by using Equation [5.34] since quartz, being an oxide, follows the surface-charging mechanisms for oxides (Yoon, 1977). There is no direct or indirect method available at present to obtain the second input parameter, the interparticle spacing in the compressed quartz bed. It was therefore obtained by back-calculating a value for it using the model in the following manner; a theoretical plot of the osmotic pressure variation with the interparticle spacing of quartz in 10^{-4}M/ℓ sulfuric acid was prepared using the model and this is shown in Figure 31. The experimentally observed rise in level of the water in the apparatus was measured and from this value, the corresponding interparticle spacing was read off. For the osmotic head of 5.5 inches water observed in the apparatus, the value of the interparticle spacing was 70Å. This value for the interparticle spacings was used to calculate the theoretical osmotic pressure at higher sulfuric acid concentrations.

Figure 32 shows the values of the theoretical osmotic pressures calculated using the model for the quartz-sulfuric acid system. The corresponding measured values are shown alongside for comparison. As the acid concentration increases, the values predicted by the model become less accurate, as shown by the divergence between the

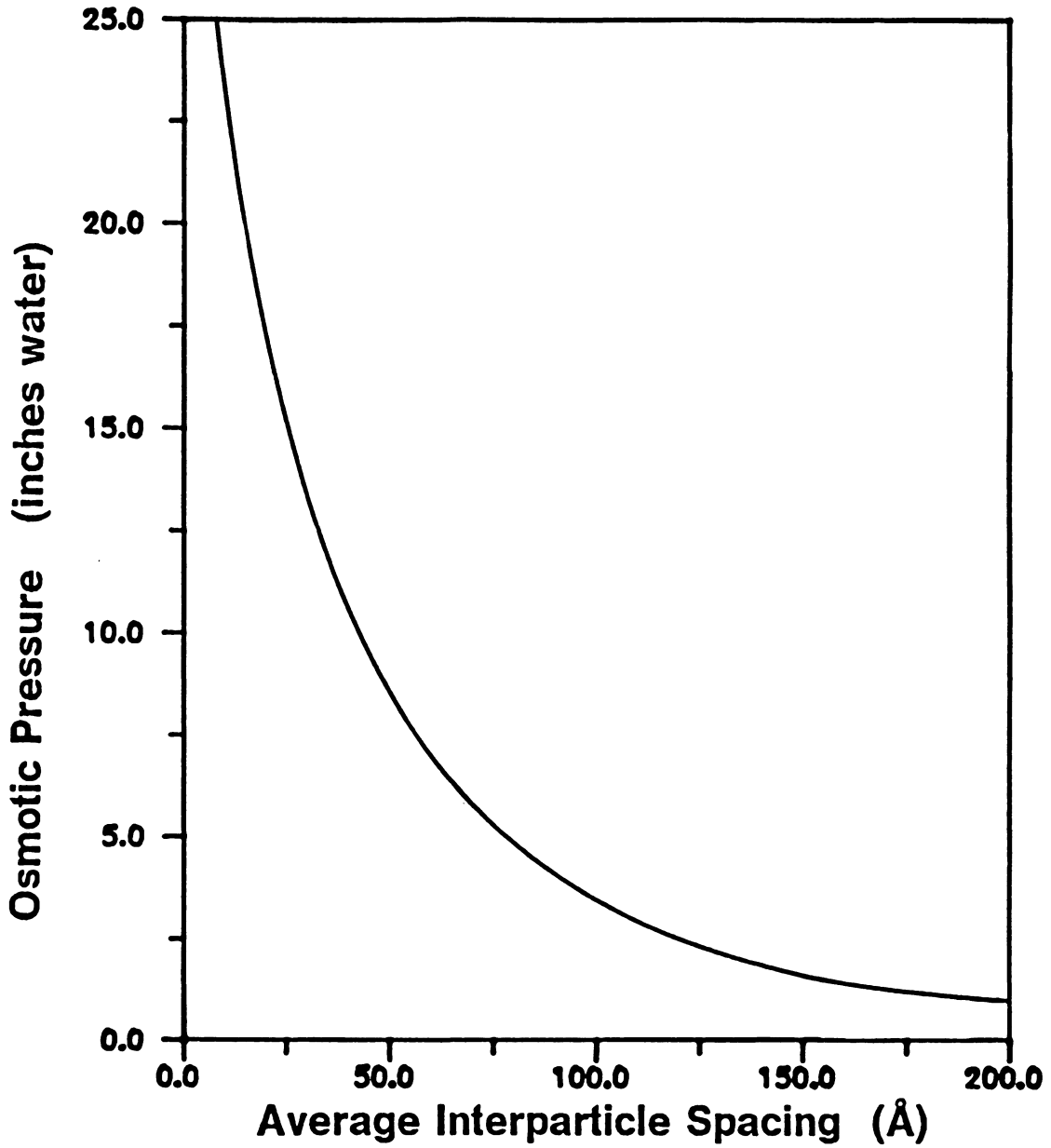

Figure 31. Theoretical Osmotic Pressure Developed Inside a Fine Quartz Bed Immersed in Sulfuric Acid.

graphs. This is due to both the inaccuracies of the model as well as the experimental apparatus.

In conclusion, it is not easy to verify a microscopic quantity using simple apparatus. Some possible measurements may be carried out using a specialized instrument developed solely for the purpose of measuring short-range, interparticle forces such as that manufactured by ANU Tech. PTY., Ltd., Australia. The measurements would then be more reliable and would assist in improving the present osmotic pressure model.

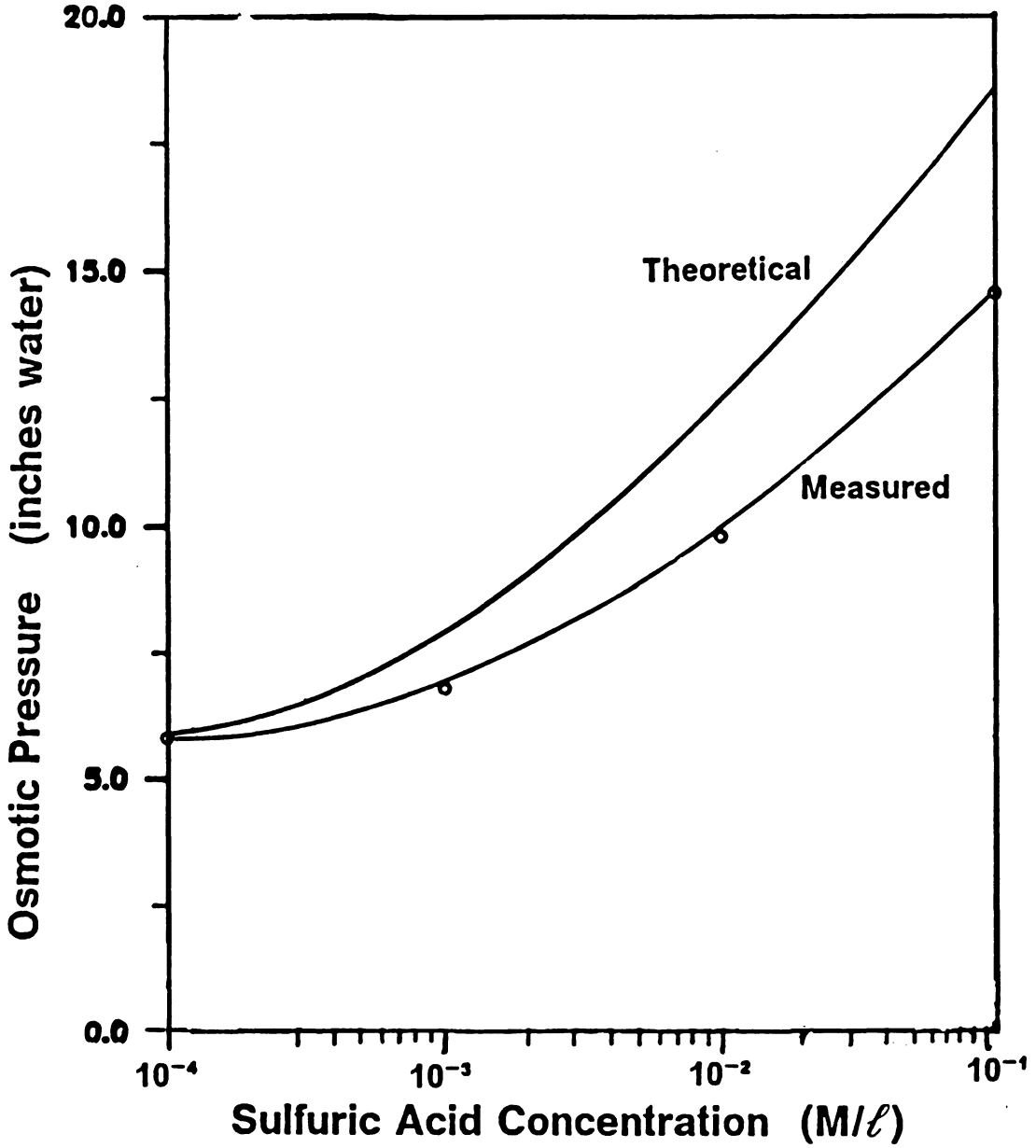

Figure 32. Theoretical and Measured Values of the Osmotic Pressures Developed Inside a Fine Quartz Bed in Sulfuric Acid

6.0 SUMMARY AND CONCLUSIONS

6.1 The EIL Process

1. The hydrostatic repulsive pressure present during the interaction of two double layers may be effectively utilized to improve the liberation of mineral matter from certain coals. This pressure is the result of the Donnan equilibrium of ions between the interior and the exterior of a pore (or crevice) present in a coal particle suspended in an electrolyte. When a coal surface is oxidized by ferric ions, it loses electrons and becomes positively charged, which in turn establishes an electrical double layer. When these double layers overlap, the chemical potential of water inside the crevices decreases due to the increased concentration of counter ions, which creates an osmotic pressure. The mineral matter contained within these crevices is pushed out by the osmotic pressure, thereby demineralizing the coal.

2. The ingress of water into the pores and crevices of coal during the EIL process causes the formation and propagation of cracks near the coal surface. The removal

of mineral matter is associated with these cracks. The propagation of these cracks by the osmotic pressure mechanism facilitates the flow of acid into the pore structure of coal to dissolve soluble mineral matter (if any).

3. The variety of coals of different ranks and origin tested by the EIL process responded favorably to demineralization, although some coals appeared to be more suitable than others. The percent removal of mineral matter from coals was as high as 89% or as low as 4%. The performance of a given coal may be influenced by the nature of the mineral matter present in the coal, relative amounts and the type of coal maceral in which they are entrapped. This in turn would depend upon the rank, petrographic composition, pore size distribution and the geological origin of the coal itself.

4. Mass balance studies indicate that over 90% of the mineral matter removed from a Wyodak coal by the EIL process is due to liberation. Coals that were pre-cleaned to remove all free mineral matter showed a substantial reduction in their ash content after EIL treatment, indicating that the process caused some degree of mineral liberation to take place from the coals.

5. The EIL treatment enhances the removal of mineral matter from coal over simple acid treatment. The extent of the improvement is dependent on the coal type and size as well as the acid type and concentration. Ferric ions used for the EIL process, may be regenerated by a variety of methods, such as electrolysis, oxygenation, etc. Since most coals contain ferrugenous impurites, these ions are self-generated during the EIL process. In the present work, ferric ions have been regenerated from the spent ferrous ions, under applied potential conditions, but the open circuit potential of the system is usually high enough for the oxidation. The application of a

potential, however, increases the rate of regeneration and ultimately, the rate of demineralization of the coal.

6. Scanning electron photomicrographs of the processed coals confirm the opening of pores and hairline fractures across some coal particles. These cracks do not extend across the entire particle as there is no significant size reduction of the coal when subjected to the EIL process. Vacant sites where mineral matter resided are visible in the coals treated by the EIL process, unlike those coals treated solely by an acid.

7. The osmotic pressure model developed for the EIL process predicts pressures ranging from 1-30 atm for crevice spacings of 50-1000Å. Below 10Å, the model is not applicable. The values of the osmotic pressure predicted by the model cannot be easily or accurately measured owing to their microscopic nature. However, they are numerically consistent with other models found in the literature that used different approaches to calculate osmotic forces between charged surfaces.

6.2 Industrial Applications

Of the many advanced physical coal cleaning processes that are being developed, a common denominator is that the ash-forming mineral matter has to be liberated by an appropriate technique such as attrition grinding, which constitutes a costly step. Furthermore, due to the increased surface area of the micronized coal, reagent consumption is high and the cost of dewatering the coal can be prohibitive.

The EIL treatment of coal can remove ash and sulfur without pulverisation and this immediately entails a saving in comminution costs, dewatering costs and provides ease of materials handling. The operating costs of this process will be relatively low because the spent acid can be recirculated and the spent ferric ions can be regenerated by electrolysis or other means. Apart from producing superclean coal, the EIL treatment may also be effectively used to obtain saleable products from coal refuse which is presently discarded due to a lack of appropriate processing technology.

If electrolysis is used for the regeneration of the spent ferric ions, a part of the operating cost can be estimated by measuring the total charge passed during the batch experiments. Typically, the electrical energy consumption ranged between 1.5 and 4 kwh/ton of coal. On a pilot plant for example, most of the energy will be consumed in heating the slurry to 40-80°C and agitating the slurry at low rpm. Considering that the cost of micronization is several hundred kwh/ton, the EIL process can substantially reduce processing costs.

Technically, the advantage of the process is its simplicity. Essentially, it requires a reactor in which a coal is contacted with an electrocatalyst, such as Fe^{3+} ions, and then separated from the liberated mineral matter by simple screening or an advanced coal cleaning process such as microbubble flotation.

The fact that coals processed by this method have large pores and cracks could prove beneficial for other unit operations. The breakage parameters of these coals may well be much lower due to the presence of the cracks and empty pores. The removal of organic sulfur from such coals by reagents may be improved since organic sulfur is an integral part of the coal maceral itself and its exposure to reagents is essential for more complete removal. The novel application of surface-chemical forces to liberate mineral matter from coal will open several new avenues for further investigation.

6.3 Future Work

The focus of the future work may be broadly classified into two categories. The first is devoted to fundamental studies with the objective of attaining a better understanding of the mechanisms by which the EIL process removes pyritic sulfur and mineral matter from coal and to learn more about the operating parameters of the process. The second concentrates on collecting engineering information for a scale-up of the EIL process and to test it on a bench-scale continuous operation.

6.3.1 Characterization

6.3.1.1 Petrography

Detailed petrographic characterization of coal is a vital step in understanding coal processing. The characterization identifies and defines the species, sizes and shapes of the different mineral and maceral grains present and determines the distribution of grains and pore spaces in absolute and relative proportions. It also reveals the degree to which important mineral grains are associated with, or included within, other mineral species. The feed coal selected should be completely and systematically characterized for petrographic composition, mineral matter size distributions as well as proximate, ultimate, BET surface and pore size analysis. The petrographic analysis may be effectively carried out using both optical and scanning electron microscopes equipped with quantitative image analysis capabilities. Characterization should be conducted on both the feed and the product coals so that changes may be related to the removal of

mineral matter and to the process variables. In addition, pore size distribution, surface area changes and size distribution of the mineral matter in the coal may also be studied in a similar manner on both feed and product coals.

6.3.1.2 FTIR Spectroscopy and X-Ray Diffraction

The characterization work should include FTIR spectroscopy for coal surface functional group analysis. The change in the infrared spectra of the product coal with time may be used as a tool for studying the kinetics of the EIL process provided that the low-temperature ash of the feed coal is used to standardize the FTIR. By comparing the spectra obtained with time, it is possible to follow the kinetics of demineralization. This should be supplemented by isolating the low-temperature ash of the coal and determining its composition by X-ray diffraction. This may then be compared with the composition of the low-temperature ash from the product coal to determine the type and extent of the minerals removed by the EIL process.

6.3.2 Determination of Optimum Conditions

6.3.2.1 Parametric Testing

The EIL process employs a number of variables and a voluminous number of experiments will need to be conducted to optimize the effects of all these variables for the EIL process. However, a statistical experimental design program may be constructed to reduce the number of experiments. Such a test matrix will provide values for key test variables and allow for a statistically sound evaluation of the data collected.

Based on information collected in this study, the more critical variables for testing include acid concentration, acid types, reaction time and ferric ion concentration and accordingly, the statistical experimental design need only incorporate these variables for testing. The products collected from the parametric tests should be subjected to sulfur, ash, major elements, and proximate analyses. This data should be analysed in comparison with the feed coal and used to determine the optimum conditions for operating the process.

6.3.2.2 Liberation Analysis

Since the EIL process liberates the mineral matter from coal by the osmotic pressure built up inside the coal pores or crevices, it may be regarded as a liberation process and its efficiency may therefore be correlated with the degree of liberation commonly used in coal comminution studies. By plotting the mass fraction of the mineral matter liberated as a function of time, the overall rate constant for the liberation may be determined. To calculate the mass fraction, the amount of mineral matter originally present in the feed coal will be determined by low-temperature ashing. Rate constants may determined under optimum operating conditions and the results normalized with respect to some of the key variables such as acid strength, E_A, stirring speed, pulp density, reaction time, contact time, etc.

At present, the extent of mineral liberation occuring by discrete change (size reduction) and continuous change (heterogenous chemical reaction) is uncertain. This may be investigated by treating a monosized feed coal with the EIL process under the optimum conditions obtained from the tests described above. Samples should be taken as a function of time and analyzed for size distribution pertaining to free coal, free mineral matter and various locked classes of coal-mineral types.

6.3.2.3 Kinetics of Pyrite Leaching

The rate of dissolution of pyritic sulfur from coal by the EIL process may be determined by monitoring the concentration of the ferric/ferrous redox potential with time. This may be accomplished by monitoring the redox potential of the system using an E_h-electrode. The kinetic information obtained as such may be correlated with the results obtained from the liberation analysis. Batch tests may also be carried out to study the kinetics of pyrite leaching. Important operating variables such as coal concentration, acid concentration, temperature, ferric ion concentration may be combined utilizing a central composite experimental design.

The spent acids after the EIL treatment shows a dark coloration only if the coals were not wet-screened prior to treatment. A complete analysis of the spent acid will indicate the nature and extent of the mineral species extracted from the coal which may have acted as electrocatalysts in the EIL process. Experiments such as those conducted above should therefore include the withdrawal of aliquots of the electrolyte to be analyzed for the chemical species present and their concentration changes with time. Based on the data collected in these tests, optimum conditions can be found using the principles of response surface methodology.

6.3.2.4 Ferric Ion Regeneration

In the present study, ferric ions were regenerated using electrodes and an applied potential. However, ferric ions may be regenerated by other means such as bacteria and air oxidation. The time constraints of each of these processes should be weighed against costs to determine optimal operating conditions for each of the processes.

6.3.3 Design and Construction of a Continuous EIL Treatment Unit.

The data collected from the batch test work may now be evaluated in determining the design of the continuous reactor for the coal-cleaning circuit. Allowance should be made for any reactor or circuit modifications that may be required when the initial continuous tests are conducted. The reactor design may be the traditional stirred-tank type reactor or a fluidized-bed type reactor incorporating a chemical engineering design similar to that used in fluidization columns. The discharge from the reactor is sent to a screen or a microbubble column, depending on the nature of the middlings present in the feed coal. If the product coal particles are smaller than the liberated mineral particles, screen separation will have to be done in several stages, each comprising a different size class, to collect the product containing the lowest ash. It may therefore be preferable to use a method of separation based on physico-chemical properties (such as flotation) rather than one based purely on size. Any peculiarities in the results due to the heterogeneties of coal will require retesting with a full set of analyses.

BIBLIOGRAPHY

1. Adamson, A.W., "Physical Chemistry of Surfaces," 4th edition, John Wiley and Sons Inc., New York, (1982)

2. Aldrich, R.G., Keller, D.V. Jr., Sawyer, R.G., U.S. Patent 3,815,826. and 3,850,477, (1974)

3. Alkire, R.C. and Reiser, D. B., *J. Electrochem. Soc.*, 131, (12), pp.2795-2800, (1984)

4. Anthony, K.E., and Linge, H.G., *J. Electrochem. Soc.*, 130, (11), pp.2217, (1983)

5. Baldwin, R.P., Jones, K.F., Joseph, J.T., and Wong, J.I., *Fuel*, 60, pp.739, (1981)

6. Bard, A.J. and Faulkner, L.R., "Electrochemical Methods", John Wiley and Sons, Inc., New York, (1980)

7. Bartoli, A., and Papasogli, G., *Nature*, 14, pp.122-123, (1881)

8. Beall, H., *Fuel*, 58, pp.319, (1979)

9. Beall, H., *Fuel*, 59, pp.140, (1980)

10. Beall, H., Savage, L.A., and Curry, M., *Fuel*, 62, pp.289, (1983)

11. Beersohne, C.F., Deutsch Rep. Patent #380387, (1923)

12. Belcher, R.J., *Soc. Chem. Indus.*, 67, pp.213-218, 265-267, (1948)

13. Berkowitz, N., "An Introduction to Coal Technology", Academic Press, New York, (1979)

14. Beyer, M., Ebner, H.G., and Klein, J., *Chemical Industry*, 6, pp.526-528, (1986)

15. Biegler, T., and Swift, D.A., *Electrochem. Acta*, 24, pp.415-420, (1979)

16. Bratcko, D., *Chem. Phys. Lett*, 96, (2), pp.263-265, (1983)

17. Brown, R.L., Caldwell, R.L., Fereday, F., *Fuel*, 31, pp.261, (1952)

18. Bryers, R.W., (ed). "Ash deposits and corrosion due to impurities in combustion gases", Hemisphere Publishing Co., Washington D.C.

19. Campbell, J.A.L., and Sun, S.C., *Trans. AIME*, 247, (2), pp.111-114, (1970)

20. Chang, R. and Kaplan, L. J., *J. Chem. Ed.*, 54, (4), pp.218-219, (1977)

21. Chi, C.Y., Fan, C.W., Markuszewski, R., Wheelock, T.D., *American Chemical Society Symposium Ser., (Fossil Fuel Div.)*, 319, pp.30-41, (1986)

22. Cochrane, T.T., *Medical Physics*, 10, (1), pp.29-34, (1983)

23. Coplen, T.B. and Hanshaw, B.B., *Geochim. Cosmochim. Acta*, 37, pp.2295-2310, (1973)

24. Coughlin, R.W., *Ind. Eng. Chem. Prod*, R.4D, pp.8, (1969)

25. Coughlin, R.W. and Farooque, M., *Nature*, 279, pp.301-303, (1979a)

26. Coughlin, R.W. and Farooque, M., *I&EC Process Design & Development*, 19, pp.211-218, (1980)

27. Coughlin, R.W., Lalvani, S.,Dorris, A., and Pata, M., *2nd World Congress of Chemical Engineering*, 3, pp.203-205, (1981)

28. Datta, R.S., Howard, P.H., Hanchett, A., "Pre-Combustion Coal Cleaning Using Chemical Communition," NCA/BCR Coal Conference and Expo III. Coal: Energy for Independence, Louisville, (1976)

29. Dawei, W., Kewu, W. and Jicun, Q., *Intl. J. Mineral Proc.*, 17, pp.261-271, (1986)

30. Debye, P. and Huckel, E., *Physik Z*, 24, pp.185, 305, (1923)

31. Dhar, H.P., Christner, L.G. and Kush, A.K., *J. Electroanal. Chem*, 213, pp.161-167, (1986)

32. Dhooge, P.M., Stilwell, D.E., and Park, S.M., *J. Elec. Soc.*, 129, (8), pp.1719-1724, (1982)

33. Dhooge, P.M. and Park, S.M., *J. Elec. Soc.*, 130, (5), pp.1029-1036, (1983a)

34. Dhooge, P.M. and Park, S.M., *J. Elec. Soc.*, 130, (7), pp.1539-1542, (1983b)

35. Dutrizac, J.E. and MacDonald, R.J.C., *Minerals Science & Engineering*, 6 (2), pp.59-100, (1974)

36. Eddinger, R.T., and Demorset, D.J., *Fuel*, 26, pp.157-159, (1947)

37. Fan, C.W., Markuszewski, R., and Wheelock, T.D., *Am. Chem. Soc. Div. Fuel Chem. Preprints*, 29, (1), pp.114-119, (1984a)

38. Fan, C.W., Markuszewski, R., and Wheelock, T.D., *Am. Chem. Soc. Div. Fuel Chem. Preprints*, 29, (4), pp.319-325, (1984b)

39. Farooque, M. and Coughlin, R.W., *Fuel*, 58, pp.705-712, (1979c)

40. Farooque, M. and Coughlin, R.W., *Nature*, 280, pp.666-668, (1979b)

41. Fritz, S.J., *Clay and Clay Minerals*, 34, (2), pp.214-223, (1986)

42. Fritz, S.J., and Marine, I.W., *Geochim. Cosmochim. Acta*, 47, pp.1515-1522, (1983)

43. Fuchs, W., Veiser, O. and Kishio, W., *Erdol Kohle*, 12, pp.223-228, 973-976, (1959)

44. Fuerstenau D.W. and Raghavan, S., "Some Aspects of the Thermodynamics of Flotation", A.M. Gaudin Memorial Flotation Symposium, AIME Publications, Port City Press, MD., (1976)

45. Garrels, R.M. and Christ, C.L., *Solutions, Minerals and Equilibria*, Harper and Row., New York, (1965)

46. Given, P.H., *J. Chem. Soc. (London)*, 548, pp.2684-2687, (1958)

47. Given, P.H., *Fuel*, 39, pp.147, (1960)

48. Given, P.H., and Schoen, J.M., *J. Chem. Soc.*, 548, pp.2680-2684, (1958)

49. Gleit., C.E., *Am. J. of Medical Electronics*, 2, pp.112-118, (1963)

50. Gluskoter, H.J., "Ash Deposits and Corrosion Due to Impurities in Combustion Gases", Bryers, R.W. (ed), pp.3-19, Hemisphere Publishing Co., Washington D.C., (1977)

51. Goldberg, R.N., *J. Res. National Bureau of Standards*, 89, (3), pp.251-263, (1984)

52. Grahame, D.C. and Soderberg, B.A., *J. of Chem. Phys.*, 22, (3), pp.449-460, (1954)

53. Grigera, J.R. and Blum, L., *Chem. Phys. Lett.*, 38, pp.486-497, (1976)

54. Grim, R.E., "Clay Mineralogy", pp.596, McGraw-Hill, New York, (1968)

55. Guruswamy, V. and Alexander, S. "Pretreatment of Coal Slurries by Electrolysis to Remove Ash and Modify the Coal" 56th Colloid & Surface Science Symp., Blacksburg, Virginia, (1982)

56. Hanshaw, B.B., and Zen, E., *Geol. Soc. Am. Bull.* 76, pp.1379-1387, (1965)

57. Harned, H.S. and Owen, B.B., "The Physical Chemistry of Solutions", Reinhold, New York, (1958)

58. Heinz, E., *Ger. Offen.*, DE 3,417,272, (1985)

59. Hemwall, J.B. and Low, P.F., *Soil Science*, 82, pp.135-145, (1956)

60. Herbst, J.A. and Sepulveda, J.L., *Proc. of the Technical program*, International Powder and Bulk Solids Handling, pp.452, (1978)

61. Hogg, R., Healy, T.W. and Fuerstenau, D.W., *Trans. Farad. Soc.*, 62, pp.1638

62. Howard, P.H. and Datta, R.S., "Coal Desulfurization", Wheelock, T.D., (ed.) ACS Symposium Series, Americal Chemical Society, Washington D.C., (1977)

63. Howard, P.H., Datta, R.S., Hanchett, A., *Fuel*, 56, pp.346, (1977)

64. Hudec, P.P., *Proc. 3rd. Intl. Symp. Water-Rock Interactions*, pp.153-154, Edmonton, Alberta, (1980)

65. Huggins, F.E., Huffman, G.P., and Lee, R.J., "Coal and Coal products", Comstock, M. J., (ed.) pp.239-258, American Chemical Society, Washington D.C., (1982)

66. Ialenti, R. and Caramazza, R. *J. Chem. Soc., Faraday Trans.*, 80, (55), (1984)

67. Israelachvili, J.N., "Intermolecular and Surface Forces" Academic Press, U.K., (1985)

68. Jaeger, J.C. and Cook, N.G.W., "Fundamentals of Rock Mechanics", 3rd edition, Chapman and Hall, London, (1979)

69. Johnson, P.H., *Mining Engineering*, 17, (8), pp.64-68, (1965)

70. Kedem, O. and Katchalsky, A. *Trans. Farad. Soc.*, 59, pp.1918-1930, (1962)

71. Keller, D.V., Jr. and Smith, C.D., *Fuel*, 55, pp.273, (1976)

72. Kharaka, Y.K. and Berry, F.A.F., *Geochim. Cosmochim. Acta*, 37, pp.2577-2603, (1973)

73. Kharaka, Y.K., and Smalley, W.C., *Am. Assoc. Pet. Geol. Bull.*, 60, pp.973-980, (1976)

74. Kreysa, G., and Kochanek, W., *J. Electrochem. Soc.*, 132, (9), pp.2084-2089, (1985)

75. Krevelan, D.W. Van, "Coal", Elsevior Publishing Co., New York, (1961)

76. Lalvani, S.B., *DOE Report # DOE/FE/60339-T-18*, (1985)

77. Lalvani, S.B., *Coal Science Technology*, 10, pp.265-288, (1987)

78. Lalvani, S.B., Pata, M. and Coughlin, R.W., *Fuel*, 62, pp.427-437, (1983)

79. Lalvani, S.B., Pata, M., and Coughlin, R.W., *Fuel* 65, pp.122-128, (1986)

80. Lalvani, S.B., and Shami, M., *J. Electrochem. Soc.*, pp.1364-1368, (1986)

81. Lee, C.K. and Tavlarides, L.L., *Polyhedron*, 4, (1), pp.47-51, (1985)

82. Levenspiel, O. "Chemical Reaction Engineering", John Wiley & Sons, Inc., New York, (1975)

83. Low, P.F., *Soil Science Soc. Am.* , 44, (4), pp.667-676, (1980)

84. Low, P.F. and Anderson, D.M., *Soil Science*, 86, pp.251, (1958)

85. Lowry, H.H., *Chemistry of Coal Utilization*, Vol.I, John Wiley & Sons, New York, (1963)

86. Lowson, R.T., *Chemical Reviews*, 82, (5), pp.461-497, (1982)

87. Lynch, C. and Collett, A., *Fuel*, 11, pp.408-415, (1932)

88. Mahajan, O.P. and Walker, P.L. Jr., "Analytical Methods for Coal and Coal Products", Karr, C.(ed), Vol.I, pp.125-162, Academic Press, New York, (1978)

89. Mankosa, M.J., "Investigation of Operating Conditions in Stirred Ball Milling of Coal", M.S.Thesis, Virginia Tech, (1986)

90. Marcus, H.J., *J. Geophys. Res.*, 67, pp.5215-5225, (1962)

91. Mathews, C.T., Robins, R.G., *Proc.Aust.Inst.Min.Met.*, 242, pp.47, (1972)

92. Marine, I.W., *Am. Assoc. Pet. Geol. Bull.*, 58, pp.1825-1837, (1974)

93. Marine, I.W. and Fritz, S.J., *Water Resources Research*, 17, (1), pp.73-82, (1981)

94. Markby, R.E., Sternburg, H.W. and Wender, I., *Nature* 199, (4897), pp.997, (1963)

95. Markuszewski, R., Mroch, D.R., Norton, G.A., Straszheim, W.E., *American Chemical Society Symposium Ser., (Fossil Fuel Div.)*, 319, pp.42-50, (1986)

96. McCready, R.G.L., and Zentilli, M., *C.I.M. Bulletin*, 78, (876), pp.67-68, (1985)

97. Meyers, R.A., "Coal Desulfurization", Marcel Dekker Inc., New York, (1977)

98. Mori, S., Hara, T., Aso, K. and Okamoto, H. *Powder Technology*, 40, pp.161-165, (1984)

99. Morooka, S., Murakami, A., Kusakabe, K., Kato, Y., and Kusunoki, K., *Fuel*, 63, (7), pp.947-951, (1984)

100. Myerson, A.S. and Kline, P.C., *Biotechnology and Bioengineering*, 26, pp.92-99, (1984)

101. Nordholm, S., *J. Chem. Phys.*, 78, (9), pp.5759-5763, (1983)

102. Ogunsola, O.M., and Osseo-Asare, K., *Fuel*, 66, (1987)

103. Okada, G., Guruswamy, V. and Bockris, J.O'M., *J.Electrohhem. Soc.*, 128, pp.2097-2102, (1981)

104. Outhwaite, C.W., *Statistical Mechanics*, 2, (Specialist Periodical Reports) Singer, K. (ed.), (1975)

105. Panzer, R.E. and Elving P.J., *Electrochim. Acta*, 20, pp.635, (1975)

106. Parks, G.A., *Chem. Review*, 65, 177, (1965)

107. Parks, G.A., *J. Geophys. Res.*, 89, (B6), pp.3997-4008, (1984)

108. Parks, G.A., "For His Fundamental Contribution to the Electrochemical Properties of Oxide Minerals in Aqueous Systems", A.M. Gaudin Memorial Lecture, 115th AIME Annual Meeting, New Orleans, Louisiana, (1986)

109. Park, S.M., *J. Elec. Soc.*, 131, pp.363C-373C, (1984)

110. Paul, A.D., "Pretreatment of Coal by Anodic Electrolysis of Acidified Coal-Water Slurries" Brookhaven National Labs., Report No. BNL 35429, (1984)

111. Peters, E. and Majima, H., *Canadian Metallurgy*, Q 7, pp.111-??., (1968)

112. Pitzer, K.S., *J.Chem. Soc. Farad. Trans.*, 80, pp.3451-3454, (1984)

113. Pitzer, K.S. and Kim, J.J., *J. Am. Chem. Soc.*, 96, pp.5701, (1979)

114. Pitzer, K.S., Roy, R.N. and Silvester, L.F., *J. Am. Chem. Soc., Farad. T*, 99, (15), pp.4930-4936, (1977)

115. Pytkowicz, R.M. (ed.) "Activity Coefficients in Electrolyte Solutions", 1, pp.65-156, CRC Press, Boca Raton, Florida, (1979)

116. Raask, E., *Progress in Energy and Combustion Science*, 8, pp.261-276, (1982)

117. Rard, J.A., *J. Chem. Eng. Data*, 28, #4, pp.384-387, (1983)

118. Rard, J.A., Habenschuss, A. and Spedding, F.H., *J. Chem. Eng. Data*, 21, (3), pp.374-379, (1976)

119. Rard, J.A. and Miller, D.G., *J. Chem. Eng. Data*, 26, (1), pp.33-43, (1981)

120. Rasaiah, J.C., *J. Solution Chemistry*, 2, pp.301, (1973)

121. Rasaiah, J.C. and Friedman, H.L., *J. Chem. Phys.*, 50, pp.3965-98, (1969)

122. Reggel, L., Raymond, R., Friedman, S., Friedel, R.A., and Wender, I., *Fuel*, 37, pp.126-128, (1958)

123. Renton, J.J., "Mineral Matter in Coal", Coal Structure, Meyers, R.A. (ed.) Academic Press, New York, (1982)

124. Reucroft, P.J., Patel, K.B. and Chiou, C.T., *Carbon*, 22, (1), pp.100-102, (1984)

125. Schofield, R.K., *Trans. Faraday Soc.*, 42B, pp.219-228, (1946)

126. Senftle, F.E., Patton, K.M., and Heard, I., *Fuel*, 60, pp.1131-1136, (1981)

127. Shimada, K., Hara, H. and Jomoto, Y. *Chemical Engineering (Japan)*, 10, #3, pp.395-399 (1984)

128. Smith, J.M. and Van Ness, S., "Introduction to Chemical Engineering Thermodynamics", McGraw-Hill Book Co., New York, (1987)

129. Spitzer, J.J., *Nature*, 310, 5976, pp.396-397, (1984)

130. Spitzer, Z., Biba, V., Bohac, F. and Malkova, E., *Fuel*, 56, pp.313-318, (1977)

131. Srivastava, R.C., and Avasthi, P.K., *Journal of Hydrology*, 24, pp.111-120, (1975)

132. Stach, E., Mackowsky, M.T., Teichmuller, M., Taylor, G.H., Chandra, D., and Teichmuller, R., *Stach's Handbook of Coal Petrology*, Gebruder Borntraeger, Berlin, West Germany, (1982)

133. Stanczyk, M.H. and Feld, I.L., "Ultrafine Grinding of Several Industrial Minerals by the Attrition Grinding Process", U.S. Dept. of Interior, Bureau of Mines, RI-7641, (1972)

134. Staverman, A.J., *Trans. Farad. Soc.*, 48, pp.176-185, (1952)

135. Sternburg, H.W., *Coal Science & Technology Symp*, Dept. of Energy, Mines & Resources, Ottawa, Canada, pp.168-174, (1967)

136. Sternberg, H.W., Delle Donne, C.L., Markby, R.E., and Wender, I., *Fuel*, 45, pp.469, (1966)

137. Sternberg, H.W. and Wender, I., U.S. Bureau of Mines Investigative Report #5943. (1962)

138. Sun, Y., Lin, H. and Low, P.F., *J. Colloid and Surface Chem.*, 112, (2), pp.556-564, (1986)

139. Taylor, N., Gibson, C., Bartle, K.D., Mills, D.G., Richards, D.G., *Fuel*, 64,(3), pp.415-419, (1985)

140. Thomlinson, M.M. and Outhwaite, C.W., *Molecular Physics*, 47, (5), pp.1113-1128, (1982)

141. Tomat, R. and Rigo, A., *J. Appl. Electrochem.*, 9, pp.301-305, (1979)

142. Usui, S. and Hachisu, S. "Electrical Phenomena at Interfaces" Kitara A. and Watanabe, A. (eds.), Marcel Dekker Inc., New York, (1984)

143. Vaseen, V.A., U. S. Patent 4,226,683 (1979)

144. Vasilakos, N.P., and Clinton, C.S., *Fuel*, 63, pp.1562, (1984)

145. Vetter, K.J., "Electrochemical Kinetics", pp.381, (1961)

146. Walker, P.L. Jr., *Phil. Trans.Royal Soc. London*, A-300, pp.65-81, (1981)

147. Wapner, P.G. and Lalvani, S.B., *Fuel Processing Technology*, 18, pp.25-26, (1988)

148. Waugh, A.B. and Bowling, K. Mc.G., *Fuel Processing Technology*, 9, pp.217-233, (1984)

149. Wen, W.W., Ph.D. Thesis, Penn. State University, (1979).

150. Whitehurst, D.C., Farcasiu, M., Mitchell, T.O. and Dickert, J. J., Electric Power Research Institute Report # EPRI-AF-480, (1977)

151. Widyani, E. and Wightman. J.P., *Colloids and Surfaces*, 4, pp.209-212, (1982)

152. Wiersma. C.L., and Rimstidt, J.D., *Geochim. Cosmochim. Acta*, 48, pp.85-92, (1984)

153. Wilson, C.L., "Coal: Bridge to the Future", Report of the World Coal Study, Nimrod Press, Boston, Mass., (1980)

154. Yoon, R.H., "The Role of Crystal Structure in the Surface Chemistry of Flotation" , Ph.D. Thesis, McGill University, Canada, (1977)

155. Yuroskii, A.Z., "Sulfur in Coals", pp.385-408, Indian National Scientific Documentation Center, New Delhi, (1974)

156. Zaitsev, I.D. and Aseev, G.G., *Russ. J. Phys. Chem. ecit., 56, (2), pp.239-241, (1982)*

Appendix A. COMPUTER PROGRAM FOR OSMOTIC PRESSURE CALCULATIONS

```
C ***********************************************************************
C     THIS PROGRAM CALCULATES THE OSMOTIC PRESSURE
C     INSIDE COAL CAVITIES DURING THE EIL PROCESS. THE
C     VALUES OF THE OSMOTIC PRESSURE ARE DETERMINED FOR
C     LOGARITHMICALLY INCREASING VALUES OF THE PORE SPACING
C ***********************************************************************
      IMPLICIT REAL*8(A-H,O-Z)
      REAL*8 KAPA,MOLAL,MOLAR,INCRE
C  ***********************************
C   INPUT OF VARIABLES
C ************THE UNITS OF PORAD ARE IN ANGSTROMS*******************
C ***************THE UNITS OF SFPOT IS IN VOLTS**********************
      MOLAR = 1.0D0
      PH = 0.24D0
      PZC = 6.1D0
      PORAD = 1.0D0
      INCRE = 1.0D0
      N = 1000
      ICOUNT = 1
      SFPOT = 0.059D0*(PZC-PH)
      Z = -1.0D0
      KAPA = 3.29D7*SQRT(MOLAR)
      B1 = 9.73534D0*SFPOT
      B = (DEXP(B1)-DEXP(-B1))/(DEXP(B1)+DEXP(-B1))
      WRITE(6,*)'
      WRITE(6,*)'BULK MOLAR CONCENTRATION = ',MOLAR
```

```
      WRITE(6,*)'PH AT THIS CONCENTRATION=',PH
      WRITE(6,*)'SURFACE POTENTIAL=', SFPOT
C     ************************************
      CALL CONVERT (MOLAR,MOLAL)
      CALL RARD (MOLAL,FYE,ALN)
      WRITE(6,*)'                    '
      WRITE(6,*)'                    '
      WRITE(6,*)'                    '
      ALNOT=ALN
      XOUT=MOLAL/(MOLAL+55.5087D0)
      PMOUT=18.23D0-4.39D0*XOUT
      DO 10 I=1,50
      CALL GYCH(KAPA,PORAD,B,MOLAR,POT,SMOLAR)
      WRITE(6,*)'POTENTIAL AT PORAD=',PORAD,'IS=',POT,'VOLTS'
      WRITE(6,*)'CONCENTRATION AT PORAD=',PORAD,'IS',SMOLAR
      IF(SMOLAR.GE.11.0D0) THEN
      WRITE(6,*)'CONCENTRATION TOO LARGE AND OUT OF RANGE    '
      BASE=PORAD
      GOTO 43
      X=0.0D0
      DX=PORAD/N
      IF(DX.EQ.0.0D0) THEN
      AVREA=11.0
      GO TO 67
      TAREA=0.0D0
      DO 30 L=1,N
      CALL GYCH(KAPA,X,B,MOLAR,POT,SMOLAR)
      DAREA=SMOLAR*DX
      TAREA=TAREA+DAREA
      X=X+DX
30    CONTINUE
      AVREA=TAREA/PORAD
      TEST=AVREA-0.1D0
      IF(TEST.LE.10D-5) THEN
      WRITE(6,*)'NO MORE DOUBLE LAYER AFTER PORAD=',PORAD
      GO TO 54
      END IF
      CALL CONVERT (AVREA,SMOLAL)
      IF(ICOUNT.GE.10) THEN
      INCRE=10.0D0
      N=5000
      END IF
      IF(ICOUNT.GE.19) THEN
      INCRE=100.0D0
      N=10000
      END IF
      IF(ICOUNT.GE.28) THEN
      INCRE=1000.0D0
      N=50000
      END IF
      IF(ICOUNT.GE.37) THEN
```

```
      INCRE=10000.0D0
      N=100000
      END IF
      WRITE(6,*)'AVERAGE MOLAR CONC. INSIDE PORE =',AVREA
      XIN=SMOLAL/(SMOLAL+55.5087D0)
      PMIN=18.23D0-4.39D0*XIN
      PMVM=(PMOUT+PMIN)*0.5D0
      WRITE(6,*)'PMVM=',PMVM
      CALL RARD (SMOLAL,FYE,ALN)
      ALNIN=ALN
      WRITE(6,*)'LOG ACTIVITY OF SOLUTION INSIDE=', ALNIN
      OPRESS=(ALNOT-ALNIN)*82.05D0*298.0D0/PMVM
      OPH2O=1033.26D0*OPRESS
      WRITE(6,*)'OSMOTIC PRESSURE IN CMS.WATER=', OPH2O
      WRITE(6,*)'OSMOTIC PRESSURE IN ATMOSPHERES=', OPRESS
      WRITE(6,*)'                '
   43 PORAD=PORAD+INCRE
      ICOUNT=ICOUNT+1
   10 CONTINUE
   54 STOP
      END
      SUBROUTINE CONVERT (MOLAR,MOLAL)
      REAL*8 VOLACD,MOLAR,MOLAL
      IF (MOLAR.GT.11.0D0) MOLAR=11.0D0
      VOLACD=100.0D0*98.08D0*MOLAR/(97.0D0*1.8337D0)
      MOLAL=1000.0D0*MOLAR/(1000.0D0-VOLACD)
      RETURN
      END
      SUBROUTINE RARD (MOLAL,FYE,ALN)
      REAL*8 FYE,ALN,MOLAL,MOLAR
      DIMENSION A(7), R(7), SUM(7)
      DATA A/-55.4552D0,208.7446D0,-288.7967D0,177.7105D0,
     & -41.1274D0,0.002D0,-0.0006D0/
      DATA R/0.750D0,0.875D0,1.0D0,1.125D0,1.25D0,3.125D0,3.375D0/
      DO 15 J=1,7
      SUM(J)=0.0
   15 CONTINUE
      SUMT=0.0
      DO 20 K=1,7
      SUM(K)=A(K)*MOLAL**R(K)
      SUMT=SUMT+SUM(K)
   20 CONTINUE
      FYE=1.0D0-1.3581D0*(MOLAL**0.5D0)+SUMT
      ALN=-FYE*2.0D0*MOLAL*18.0D0/1000.0D0
      RETURN
      END
      SUBROUTINE GYCH(KAPA,X,B,MOLAR,POT,SMOLAR)
      IMPLICIT REAL*8(A-H,O-Z)
      REAL*8 KAPA,MOLAR
      C=DEXP(-KAPA*X*1.0D-8)
      D=0.5D0*DLOG((1.0D0+B*C)/(1.0D0-B*C))
```

```
POT = D/(9.73534D0)
SMOLAR = MOLAR*DEXP(38.94135D0*POT)
IF(SMOLAR.GE.11.0D0) SMOLAR = 11.0D0
RETURN
END
```

Appendix B. MINERALS IN COAL

Mineral	Chemical Formula[1]
Sulfide Minerals	
Pyrite	FeS_2
Marcasite	FeS_2
Sphalerite	ZnS
Galena	PbS
Chalcopyrite	$CuFeS_2$
Arsenopyrite	FeAsS
Millerite	NiS
Carbonate Minerals	
Calcite	$CaCO_3$
Dolomite	$CaMg(CO_3)_2$
Siderite	$FeCO_3$
Ankerite	$(Ca, Mg, Fe)CO_3$

[1] Gluskoter, 1977

Witherite	$BaCO_3$

Sulfate Minerals

Barite	$BaSO_4$
Gypsum	$CaSO_4.2H_2O$
Anhydrite	$CaSO_4$
Bassanite	$CaSO_4.½H_2O$
Jarosite	$(Na,K)Fe_3(SO_4)_2(OH)_6$
Szomolnokite	$FeSO_4.2H_2O$
Rozenite	$FeSO_4.4H_2O$
Melanterite	$FeSO_4.7H_2O$
Coquimbite	$Fe_2(SO_4)_3.9H_2O$
Roemerite	$FeSO_4.Fe_3(SO_4)_2.12H_2O$
Mirabilite	$Na_2SO_4.10H_2O$
Kiesserite	$MgSO_4.H_2O$
Sideronatrite	$2Na_2O.Fe_2O_3.4SO_3.7H_2O$

Chloride Minerals

Halite	NaCl
Sylvite	KCl
Bischofite	$MgCL_2.6H_2O$

Silicate Minerals (Clays)

Montmorillonite	$Al_2Si_4O_{10}(OH)_2.xH_2O$
Illite-sericite	$KAl_2(AlSi_3O_{10})(OH)_2$
Kaolinite	$Al_4Si_4O_{10}(OH)_8$
Halloysite	$Al_4Si_4O_{10}(OH)_8.4H_2O$
Chlorite	$Mg_5Al(AlSi_3O_{10})(OH)_8$

Silicate Minerals (non-clay)

Quartz	SiO_2

Biotite	$K(Mg,Fe)_3(AlSi_3O_{10})(OH)_2$
Zircon	$ZrSiO_4$
Tourmaline	$Na(Mg,Fe)_3Al_6(BO_3)_3(Si_6O_{18})(OH)_4$
Garnet	$(Fe,Ca,Mg,)_3(Al,Fe)_2(SiO_4)_3$
Kyanite	Al_2SiO_5
Staurolite	$Al_4FeSi_2O_{10}(OH)_2$
Epidote	$Ca_2(Al,Fe)_3Si_3O_{12}(OH)$
Albite	$NaAlSi_3O_8$
Sanidine	$KAlSi_3O_8$
Orthoclase	$KAlSi_3O_8$
Augite	$Ca(Mg,Fe,Al)(Al,Si)_2O_6$
Hornblende	$NaCa_2(Mg,Fe,Al)_5(SiAl)_8O_{22}(OH)_2$
Topaz	$Al_2SiO_4(OH,F)_2$

Oxide and Hydroxide Minerals

Hematite	Fe_2O_3
Magnetite	Fe_2O_3
Rutile	TiO_2
Limonite	$FeO.OH.nH_2O$
Goethite	$FeO.OH$
Lepidocrocite	$FeO.OH$
Diaspore	$AlO.OH$

Phosphate Minerals

Apatite (Fluorapatite)	$Ca_5(PO_4)_3(F,Cl,OH)$

Appendix C. LIST OF COAL SUPPLIERS

Coal Seam	Supplier
Blair	Glamorgan Coal Co., VA
Elkhorn	United Coal Company, VA
Elkhorn #3	Consolidation Coal Co., PA
Glamorgan	Glamorgan Coal Co., VA
Jacob Ranch	Kerr McGee Coal Corp., WY
Pittsburg #8	Consol Coal Co., PA
Powell Mountain	Powell Mountain Coal Co., VA 24219
Sahara	Sahara Coal Co., IL
Splashdam	United Coal Co., Grundy, VA
Taggart	Westmoreland Coal Co., VA
Upper Freeport	Department of Energy, PA
Widow Kennedy	Wellmore Coal Corp., VA
Wyodak	Kerr McGee Coal Corp., WY

Appendix D. COAL ANALYSES

Coal Seam	Moisture	Volatiles	Carbon	Ash	Sulfur	BTU (MAF)
Blair	1.5-11.0	35.82	60.82	3.36	0.56	15,116
Glamorgan		32.74	65.62	1.64	0.59	15,356
Graphitic Anthracite		3.58	70.70		0.53	12,746
Middle Wyodak		49.34	46.57	4.09	0.33	9,424
Norton	2.1-4.1	28.70	53.73	17.57	1.66	15,344
Powell Mountain		39.37	52.44	8.19	2.56	14,889
Sahara		39.76	53.63	6.61	2.57	14,436
Splashdem	4.4-17.6	32.6	63.60	8.9	1.6	15,588
Taggart	1.5-4.3	36.46	61.88	1.66	0.6	15,192
Upper Freeport		24.79	52.49	22.72	1.38	15,050
Upper Wyodak		57.36	35.25	7.39	1.3	10,494

The vita has been removed from the scanned document